SOY PROTEIN BASED GREEN NANOFIBERS BY ELECTROSPINNING

A Thesis
Presented to the Faculty of the Graduate School
Of Cornell University
In Partial Fulfillment of the Requirements for the Degree of
Master of Science

By
Sunayna Jain
January 2013

ABSTRACT

Green nanofiber membranes were fabricated from blends of soy protein using electrospinning method. Soy flour was purified using a lab-scale filtration process to obtain purified soy flour (PSF) with higher protein content, which was blended with Polyvinyl alcohol (PVA) and Polyethylene oxide (PEO) to electrospin nanofibers.

The composition of polymer solution was varied by varying the molecular weights of PVA and PEO and their concentrations, using various forms of soy protein (SPI, SPC and PSF) over a range of concentrations, varying the type and amounts of surfactants, and using various additives to reduce gelling in soy protein/PVA blends. The process parameters applied voltage, needle tip-collector distance and solution flow rate were also varied to determine their effect on fiber diameter and distribution. The individual and interaction effects of solution concentration, PVA molecular weight, applied voltage and needle tip-collector distance were determined using statistical analysis. Concentration, molecular weight and needle tip-collector distance were found to have a significant effect on fiber diameter, whereas effect of applied voltage was insignificant. Solution flow rate was observed to affect the size and uniformity of fibers. Beads and flat fibers were observed at low and high flow rates.

The mechanical properties of electrospun membranes were measured to determine the effect of increasing soy protein content and PEO content on the strength and modulus of the membranes. The strength and modulus were found to increase with increasing membrane cohesion and protein content, while the strain at break increased with increasing PEO content.

The biodegradability of electrospun membranes was studied by composting films of SPC/PVA and SPC/PEO over five weeks. It was observed that the loss in weight of the membranes was only about 3-4%, even though soy protein is known to degrade fast.

BIOGRAPHICAL SKETCH

Sunayna Jain was born in Agra, India on June 13th, 1985. She graduated from the Indian Institute of Technology (I.I.T), Delhi with a Bachelor of Technology degree in Textile Technology, in 2008. After graduating from I.I.T., she worked in an insurance firm and in a non-profit organization in India for one year each.

In fall 2010, she enrolled in the Fiber Science program at Cornell University. In January 2013, she received a Master of Science degree under the guidance of Professor Anil N. Netravali.

To my parents and my friends, for their love and support

ACKNOWLEDGMENTS

I thank my advisor, Prof. Anil Netravali, for his guidance and suggestions. I also thank my minor advisor, Prof. Joo, for his support in my thesis work.

I wish to thank Sam Zeng for training and technical assistance with a variety of instruments. I also thank the department of Chemical Engineering and Cornell Center for Materials Research (CCMR) for allowing me to use various instruments.

I am also thankful to my department colleagues Daniela, Kaiyan and Trina, and my friends Sachin, Sonika and Ishani for their help and guidance in my research work.

TABLE OF CONTENTS

LIST OF FIGURES

LIST OF TABLES

1. INTRODUCTION

1.1. Soybean production

Soybean is an important global crop, and a major source of oil and protein. The U.S., Brazil, Argentina, China and India are the world's largest soybean producers and represent more than 90% of global soybean production. In 2011, the worldwide production of soybean was 251.5 million metric tons with the United States alone accounting for 33% of the total produce. Figure 1.1 shows the major producers of soybean in 2011, and their percent contribution to the total. Brazil was the largest exporter of soybean in 2011, accounting for 41% of the total exports.

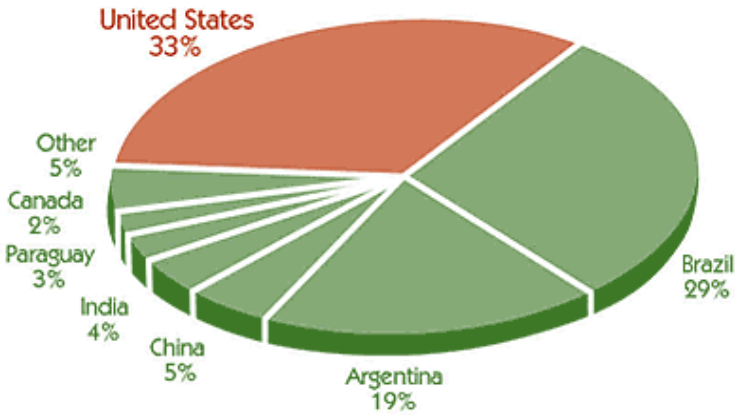

Figure 1.1: Major producers of soybean in 2011

(Source: Soystats by the American Soybean Association)

Soybean is commercially available as Soy Protein Isolate (SPI), Soy Protein Concentrate (SPC) and Soy Flour (SF). In the United States, the bulk of the harvest of soybean is solvent extracted with hexane to produce soybean products with high protein content. The remaining defatted soymeal is used to raise farm animals on an industrial scale. A small portion of the crop is consumed directly by humans or used in a large variety of processed foods. The use

of SPI for making edible films and coatings has been investigated by Brandenburg and co-workers (Brandenburg et al., 2006). Composite films of SPI with gelatin have also been fabricated for potential use in food and drugs packaging (Cao et al., 2007).

In a 2011 study by the American Soybean Association, soybean was found to constitute 68% of the total protein meal consumption worldwide, and was the second largest source of vegetable oil consumption. Soybean being a yearly renewable crop, it is being used increasingly in the industry to develop biodegradable, 'green' materials.

1.2. Electrospinning

Electrospinning is a technology for nanofiber formation, which utilizes electrical forces to produce polymer fibers with diameters ranging from 2 nm to a few microns (Bhardwaj and Kundu, 2010). The first patent that described electrospinning appeared in 1934, when Formhals disclosed an apparatus for producing polymer filaments by taking advantage of electrostatic repulsion between surface charges (Li and Xia, 2004). Since then electrospinning has been utilized in a number of applications because of the unique advantages offered by electrospun membranes as discussed later in section 1.3. However, the process has certain limitations too. The throughput of nanofibers has been a limitation in their widespread use in the industry (Bhardwaj and Kundu, 2010).

1.3. Applications of electrospinning

Electrospinning is being put to use in a number of applications such as in tissue engineering, filtration, protective clothing, energy generation applications etc. (Bhardwaj and Kundu, 2010). Electrospun fibers and mats offer several advantages such as high surface to volume ratio, high aspect ratio, tunable porosity etc. Fiber diameter and cross section can be tuned as per requirement by varying the process and solution parameters. Fiber diameter in

turn controls the porosity of electrospun membranes. A mesh of fine nanofibers has lower porosity than a mesh of thick fibers as can be expected. The adjustable porosity of electrospun membranes makes them valuable in filtration applications.

Another advantage of electrospinning is that it can be used to spin a wide range of polymers, both synthetic and natural. By varying the solution and process parameters, water soluble polymers, biopolymers and liquid crystalline polymers can be electrospun. Also, fibers with a variety of cross sectional shapes and variations along their length can be produced (Doshi and Reneker, 1995).

The high surface area to volume ratio of electrospun membranes makes them suitable for application as scaffolds in tissue engineering, dressings for wound healing, in drug delivery, in artificial blood vessels, filtration and as biosensors (Bhardwaj and Kundu, 2010).

Electrospinning is being used extensively for preparation of nanofibrous scaffolds. It offers the flexibility to engineer scaffolds with micro to nanoscale topography and high porosity similar to the natural extra cellular matrix (ECM) (Sill and Recum, 2008). Electrospun fibers can be oriented or arranged randomly, giving control over the mechanical properties and biological response of the scaffold.

Materials ranging from proteins to drugs such as antibiotics and anticancer agents can be incorporated into electrospun scaffolds (Sill and Recum, 2008). Drug delivery systems work on the principle that dissolution rate of a certain drug increases with increase in surface area of both the drug and the corresponding carrier (Bhardwaj and Kundu, 2010).

The high surface area to volume ratio and the resultant high surface cohesion makes electrospun nanofiber membranes attractive for filtration applications. Particles of the order of less than 0.5 μm can be easily trapped in the membranes (Bhardwaj and Kundu, 2010).

Nanofiber membranes are also being used in fabrication of antimicrobial filters (Burger et al., 2006).

1.4. Soy based electrospun membranes

Electrospun membranes composed of blends of soy have been found to have potential applications in the packaging industry (Vega-Lugo and Lim, 2009). Naturally occurring antimicrobial compounds can be encapsulated in electrospun membranes for use in active packaging. Active packaging is a form of packaging in which subsidiary constituents such as antimicrobial agents are added to the packaging material and allowed to diffuse into the product to inhibit the proliferation of microorganisms during storage (Robertson, 2006).

Vega-Lugo and Lim studied the controlled release of naturally occurring antimicrobial compound, allyl isothiocyanate (AITC), from electrospun fibers of soy protein isolate (SPI)/ poly (ethylene oxide) (PEO) blend and PLA (Vega-Lugo and Lim, 2009). Because of their submicron to nanoscale diameters and large surface areas, electrospun fibers offer a number of additional advantages compared to film and sheet carriers, such as being more responsive to changes in the surrounding atmosphere. Moreover, electrospinning is usually carried out at room temperature, which makes it advantageous over other encapsulation methods such as spray drying, and helps preserve the efficacy of bioactive substances during fiber formation (Vega-Lugo and Lim, 2009).

2. LITERATURE REVIEW

2.1. Electrospinning

Fibers with diameters ranging from a few nanometers to a few micrometers (microns) can be produced using electrospinning method. This method uses electric field to produce fine fibers from a liquid. Solutions of both natural as well as synthetic polymers can be electrospun to get membranes consisting of nanofibers (Ahn et al., 2006); (Lannutti, 2007); (Hunley and Long, 2008); (Reneker and Yarin, 2008).

The electrospinning setup commonly consists of a high voltage DC supply, a grounded metal collector plate, and a digitally controlled syringe pump to supply polymer solution at a fixed rate. The high voltage DC supply generates a potential difference between the polymer solution and the collector. One electrode of the high voltage supply is connected to a blunt-ended metal needle, as shown in Figure 2.1. The polymer solution is fed from the syringe mounted on the metering pump. The collector is kept grounded.

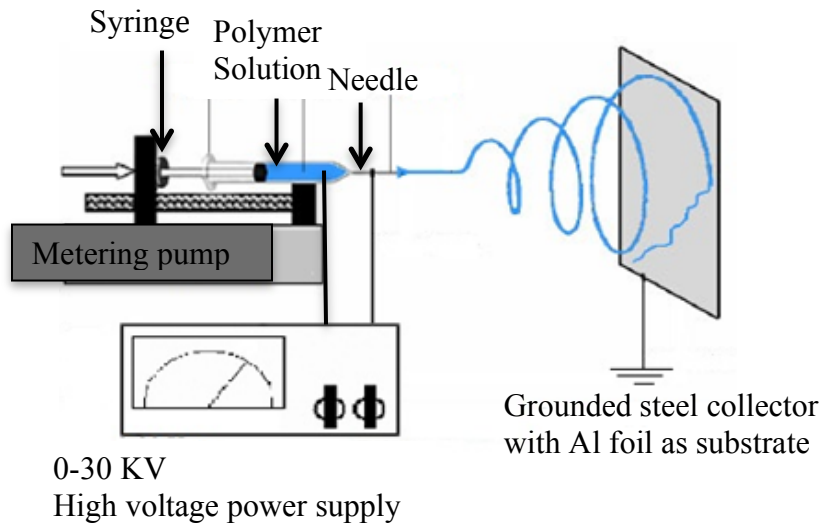

Figure 2.1 A laboratory electrospinning setup

The process involves application of electric field on a polymer droplet suspended from the needle. As the polymer droplet gets charged, mutual repulsion between like charges on the surface forces a fluid jet to be ejected from the surface. The fluid jet dries up during its flight and accumulates as a dry fiber web on the collector (Gupta et al., 2005).

Electrospinning offers several advantages over conventional spinning, including the ability to manipulate nanofiber composition by controlling solution and process related parameters. A wide range of nanofiber diameters can be obtained using this process. Moreover, electrospun nanofibers have a very large length to diameter (aspect) ratio and a small mass to volume ratio, which makes them suitable for a wide array of industrial applications (Chowdhury and Stylios, 2010). The pore size of electrospun membranes can also be controlled by varying the diameter of the constituent nanofibers (Zussman et al., 2003); (He et al., 2005). As the diameter of nanofibers decreases, the pore size also goes down proportionately.

Electrospun nanofibers have found applications in numerous fields, including tissue engineering scaffolds, protective clothing, filtration, biomedical, healthcare, defense and environmental engineering (Luu et al., 2003); (Subbiah et al., 2005); (Ramakrishna et al., 2006) as discussed earlier in sections 1.3 and 1.4. The process of electrospinning is briefly described below.

2.1.1. Formation of Taylor cone

The process of electrospinning begins with the formation of a Taylor cone, followed by ejection of the fluid jet from the polymer droplet.

The polymer solution coming out of the needle forms a droplet that is held together at the tip of the metal needle by surface tension forces. However, being connected to the high voltage supply, the droplet gets charged. Like charges accumulate on the surface of the droplet,

causing electrostatic repulsion to develop. The repulsion force acts in opposition to surface tension and viscous force, and favors formation of a conical shape of the droplet. Surface tension, on the other hand, favors a spherical shape of the droplet. As the electric potential of the surface increases, the droplet attains a conical shape, called a 'Taylor cone'. Electric field is more intense at the tip of the cone, and at some critical value, it overcomes the surface tension (Reneker and Chun, 1996). A charged jet of fluid then emanates from the tip of the cone. The formation of a Taylor cone is shown schematically in Figure 2.2.

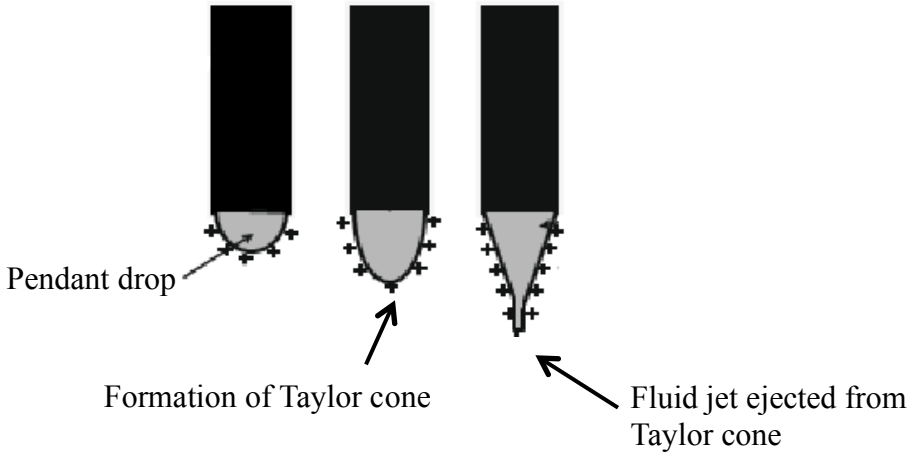

Figure 2.2: Formation of a Taylor cone

2.1.2. Bending instability

The fluid jet follows a straight path towards the collector plate initially. The diameter of the jet decreases monotonically in the straight segment as the Coulombic forces act in opposition to surface tension and viscoelastic forces, and elongate the jet (Reneker and Yarin, 2008).

The initial straight segment of the jet is followed by a region of bending instability during which the jet forms a three-dimensional coil. The jet undergoes lateral perturbations under the effect of electric field, as shown in Figure 2.3 (Reneker and Yarin, 2008). The charge carried with the perturbed segment is forced downward and outward by charges above the

perturbed region, due to repulsion between the like charges. Similarly, the perturbed segment is forced upward and outward by the charges below it creating a force that acts radially outward. This causes the perturbed segment to move perpendicular to its initial straight trajectory. The force grows exponentially with time as the radial displacement of the perturbed segment increases. At the same time, repulsion between adjacent charges on the jet causes it to elongate along its original axis. The elongation is higher in the bent segments. Thus, bending instability allows the jet to elongate by several factors, in a small region of space.

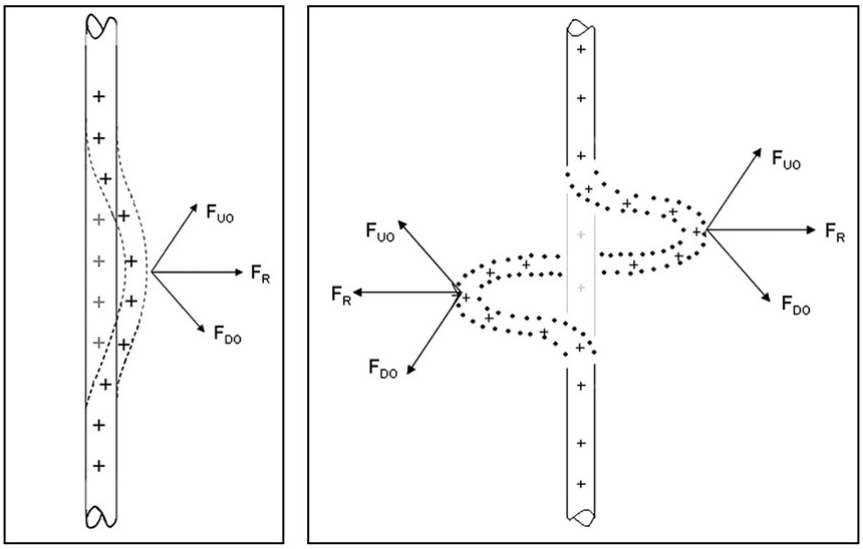

Figure 2.3 Lateral perturbations acting on a fluid jet

Bending instability causes the jet to form a three dimensional coil, whose diameter increases as the jet progresses towards the collector. The jet diameter reduces drastically in this region (Shin et al., 2001). Consequently, jet surface area increases, which accelerates evaporation of solvent from the jet. Hence, the bending instability serves two purposes; it reduces the jet diameter by several factors as well as allows rapid evaporation of the solvent from the jet.

2.2. Parameters associated with electrospinning

There are a number of parameters associated with electrospinning, which can be varied to control the diameter and properties of electrospun nanofibers (Ramakrishna, 2005). They can broadly be classified into three categories: a) Solution properties (Inai et al., 2005); (Lee et al., 2003); (Hohman et al., 2001) b) Process parameters and c) Ambient conditions (Shenoy et al., 2005). A number of researchers have studied the effect of electrospinning parameters on different polymers. In one such study, Zong and coworkers studied the effect of process parameters such as applied voltage, solution feed rate and salt addition on the structure and properties of PLLA nanofibers (Zong et al., 2002). They concluded that concentration and salt addition (increase in solution conductivity) had a relatively larger effect on the fiber diameter than other parameters (Zong et al., 2002). Demir and co-workers found that the average diameter of electrospun fibers from polyurethane-urea copolymer increased with the third power of the solution concentration (Demir et al., 2002). Buchko and co-workers found that the morphology and thickness of electrospun protein non-woven membranes depended on solution concentration, applied electric field strength, deposition distance and deposition time (Buchko et al., 1999). These factors are discussed below.

2.2.1. Solution properties

Solution parameters that affect electrospinning are viscosity, concentration, molecular weight, electrical conductivity and surface tension. However, these factors are not independent of each other. Viscosity is strongly correlated with solution concentration and the molecular weight of constituent polymers. Mit-uppatham and co-workers have studied the effect of solution properties on electrospun polyamide-6 fibers, and reported that

viscosity increases exponentially as solution concentration increases (Mit-uppatham et al., 2004). Also, surface tension and conductivity have also been reported to vary with concentration and molecular weight (Koski et al., 2004).

2.2.1.1. Concentration

Solution concentration is one of the most critical parameters during fiber formation. A certain minimum concentration is required for fiber formation to take place. This minimum concentration varies from one polymer composition to the other depending on the chemistry and structure. At low concentrations, a mixture of beads and fibers is obtained. This is because at low solution concentrations, the viscosity is also low. Therefore, surface tension dominates over the viscoelastic force, leading to formation of beads. As the concentration increases, the beads become spindle like and ultimately, uniform fibers are obtained. However, high concentrations are also detrimental to electrospinning. The formation of continuous fibers is inhibited because of difficulty in maintaining the flow of the solution at the needle tip, resulting in the formation of non-uniform fibers. Formation of branches from large diameter fibers has also been observed at high concentrations (Reneker and Yarin, 2008).

2.2.1.2. Molecular weight

Molecular weight of the polymer, or polymers in the case of blends, has a significant effect on solution properties such as viscosity, surface tension and conductivity. It has been shown to affect the diameter and properties of electrospun nanofibers (Frenot and Chronakis, 2003). The number of chain entanglements is a function of molecular weight, and determines the viscosity to a significant extent. A certain minimum number of chain entanglements are required for fiber formation to take place. At high molecular weights, and consequently high

viscosities, the viscoelastic force dominates over surface tension. This leads to a reduction in the number of beads formed during electrospinning (Tan et al., 2005). However, at very high molecular weights the viscosity is very high and the number of entanglements is high making it harder to spin, as explained later in section 2.2.1.3.

The fiber diameter has been shown to increase with an increase in the molecular weight. This is because increased chain entanglements produce a strong viscoelastic force, which resists elongation due to coulombic repulsion in the jet. Secondly, the fluid jet maintains a straight trajectory over a longer distance due to resistance to bending instability by the viscoelastic force. This restricts the reduction in jet diameter, majority of which takes place with the onset of bending instability.

2.2.1.3. Viscosity

Solution viscosity is also found to be an important factor in determining fiber diameter and morphology. At low viscosities, the viscoelastic force is insufficient to overcome the surface tension and hold the jet together. As a result, the jet breaks up into drops and solution spraying takes place instead. At high viscosities, the ejection of fluid jet from polymer solution becomes difficult. Therefore, an optimal viscosity is required for uniform fiber formation (Supaphol et al., 2005). To summarize, the fiber structure varies over the range of viscosities, from beaded fibers at low viscosities to uniform fibers at optimal viscosities, to flat ribbon-like fibers at high viscosities. The formation of flat fibers has been discussed in section 2.3.

2.2.1.4. Conductivity

Electrical conductivity of the solution also has a significant effect on the diameter of nanofibers and the range over which diameters are distributed (Khil et al., 2005); (Sun et al.,

2012). Solution conductivity depends mainly on polymer type, solvent used, and the availability of ionizable salts. The conductivity can be increased by addition of ionic salts such as sodium chloride (Qin et al., 2007). Demir et al. studied the electrospinning of polyurethane fibers, and observed that the addition of a small amount of salt increased the mass flow of polymer solution dramatically due to an increase in conductivity (Demir et al., 2002).

It is observed that there is a significant reduction in fiber diameter with an increase in solution conductivity. At low conductivities, non-uniform fibers with beads are formed because there is insufficient electrostatic repulsion to elongate the jet.

However, highly conductive solutions become unstable in the presence of strong electric fields, resulting in a broad diameter distribution. Moreover, continuous spinning could not be achieved at high conductivities because the voltage was short-circuited when the jet reached the collector (Jaeger et al., 1998).

2.2.1.5. Surface tension

Surface Tension is a critical parameter during Taylor cone formation and ejection of fluid jet from the cone. The surface tension holds the polymer droplet together, and has to be overcome by the electrostatic force for fiber formation to take place. At low viscosities, surface tension dominates over the viscoelastic force and promotes bead formation in fibers. Therefore, it is desired to have a low surface tension of polymer solution for electrospinning to take place. However, very low surface tension is also unfavorable because it leads to flattening of fibers. As a result, there exists a range of surface tension values over which a solution can be successfully electrospun into round fibers. The surface tension is also found to vary with concentration and molecular weight, though not significantly.

2.2.2. Process parameters

Process related parameters include applied voltage, feed rate, needle tip-collector distance, collector type and needle gauge. All these parameters can be varied with ease and are known to affect fiber formation to varying extents (Teo et al., 2011); (Bhardwaj and Kundu, 2010); (Chowdhury and Stylios, 2010).

2.2.2.1. Applied voltage

Applied voltage refers to the voltage supplied by the high voltage DC source during electrospinning. The DC source is connected to the needle, which supplies polymer solution. It generates a potential difference between the polymer solution and the grounded collector. It is also responsible for charge accumulation on the surface of the polymer droplet. As stated earlier, the charge accumulation causes repulsion between adjacent charges, which overcomes surface tension force, leading to jet formation. A certain threshold voltage is required for jet formation to take place. It increases as solution concentration or viscosity increases because stronger electrostatic forces are required to overcome surface tension and viscoelastic force acting on the jet (Demir et al., 2002).

Increasing the applied voltage has a twofold effect. As voltage increases, solution drawn from the needle reaches collector at a faster rate under the effect of a stronger electric field. This facilitates formation of larger diameter fibers (Zhang et al., 2005b). Bead formation is also favored at high voltages (Chowdhury and Stylios, 2010). On the other hand, coulombic repulsion between adjacent charges on the jet is stronger, which leads to greater jet elongation and hence smaller diameter fibers (Teo et al., 2011). These effects act in opposition to each other. Hence, the effect of applied voltage and its level of significance varies from one set of conditions to the other.

2.2.2.2. Feed rate

Feed rate refers to the rate at which polymer solution is fed into the syringe needle. In general, it is kept fixed at a desired level using a digitally controlled syringe pump. It is a measure of the amount of material drawn from the needle per minute. Rutledge et al. observed that more uniform fibers were produced when the flow rate was controlled, whereas broader diameter distributions were obtained when there was no control on flow rate (Rutledge et al., 2004).

An optimal value of feed rate is required for uniform fiber formation. An optimum feed rate should be the same as the rate at which material is drawn towards the collector, to avoid solution dripping. At low feed rates, solvent evaporation starts taking place at the needle tip, which hinders electrospinning. On the other hand, at high feed rates, solvent evaporation remains incomplete when the fibers hit the collector. This leads to flattened fibers with defects.

The fiber diameter and bead size has been shown to increase with an increase in feed rate (Homayoni et al., 2009). This is due to the greater amount of material drawn from the needle per unit time. Li et al. fabricated membranes for use as tissue engineered scaffolds, and reported that the shape and size of electrospun fibers could be optimized by varying the solution concentration and delivery rate of the polymers (Li et al., 2005).

2.2.2.3. Needle tip-collector distance

The needle tip-collector distance refers to the distance between the needle tip and the collector, measured perpendicular to the plane of the collector plate. Two critical phenomena, reduction in jet diameter and solvent evaporation, take place in this region. As the needle tip-collector distance increases, bending instability takes place over a longer

distance. This leads to a greater reduction in fiber diameter. Moreover, as the jet diameter decreases, solvent evaporation is accelerated because of the increasing jet surface area. Hence, fibers get more opportunity to dry up before depositing on the collector.

Fiber diameter and cross section can be controlled by varying the needle tip-collector distance. At small distances, flat fibers are obtained because of incomplete solvent evaporation from the fibers before they hit the collector (Buchko et al., 1999). At large distances, fibers with round cross sections are obtained (Buchko et al., 1999).

2.2.2.4. Needle gauge

The needle gauge is a measure of the diameter of the needle from which polymer solution is ejected during electrospinning. The internal diameter of the needle tip plays a role in electrospinning; a smaller internal diameter reduces clogging due to less exposure of the solution to the atmosphere during the process, and hence, lower evaporate of solvent (Homayoni et al., 2009). Due to exposure to the atmosphere, solvent evaporation starts at the needle tip, which increases the viscosity. The increase in viscosity leads to clogging when the internal diameter of the needle is large.

Zeng and co-workers have reported that higher voltage is required for higher needle diameters, because of the increased flow rate from a wider outlet (Zeng et al., 2003). They also observed an increase in fiber diameter with an increase in needle diameter (Zeng et al., 2003).

2.2.2.5. Type of collector

Most commonly a smooth surface e.g. aluminum foil, is used as collector. Liu and Hsieh have studied the effect of collectors during electrospinning of cellulose acetate, and report that the nature of the collector affects both fiber morphology as well as fiber packing (Liu

and Hsieh, 2002).

During electrospinning, the polymer jet carries a charge as it travels from the needle to the collector. The dissipation of this residual charge affects fiber arrangement as it deposits on the collector. Moreover, fibers getting deposited on the collector carry residual solvents. The diffusion and evaporation of residual solvents also affects the fiber structure. Both these factors depend on the type of collector being used.

Liu and Hsieh studied the effect of collector type by using different target materials, that is, copper mesh, aluminum foil and water, and paper. Fibers collected on paper were observed to have smooth surfaces and uniform diameters with fewer defects. Fibers collected on water had a broader size distribution and were more densely packed. Electrically conductive collectors, such as aluminum foil and water, favor a tightly packed membrane structure, whereas nonconductive collectors such as paper give a loosely packed fibrous network structure (Liu and Hsieh, 2002). This is because the electrically charged jet is attracted more towards a conductive collector than a non-conductive one. Kim et al. studied the deposition of poly (L-lactide) (PLLA) and poly(lactide-*co*-glycolide) (PLGA) nanofiber membranes on a metal collector, water reservoir and a methanol reservoir (Kim et al., 2005). Smooth membranes were obtained from the metal collector, whereas the membranes became rough due to shrinkage and slow charge dissipation when deposited on a water reservoir. The crystallization of the membranes was also affected by the choice of collector. When electrospun on the water reservoir, the PLLA membranes remained amorphous. However, crystalline PLLA was obtained by electrospinning on the methanol reservoir due to the swelling of nanofibers by methanol (Kim et al., 2005).

Collectors with different types of geometries have been tested (Pham et al., 2006). Fridrikh

and co-workers used two parallel plates when spinning their fibers in order to generate uniform electric fields (Fridrikh et al., 2003). Frame collectors were shown to yield aligned fibers with a conductive frame producing better alignment than a non-conductive one (Huang et al., 2003). Also, an array of electrospun fibers has been produced using two conductive, collection rings (Dalton et al., 2005). The fibers were suspended between the rings, and fibers up to 10 cm long were obtained. The rotation of one of the collection rings allowed for the production of a multi-filament yarn (Dalton et al., 2005). PEO was also spun using a multiple field method in which the polymer jet passed through three parallel rings, each connected to an independent power supply (Deitzel et al., 2001). This method produced smaller, bead-free fibers that collected in a more focused area (Deitzel et al., 2001).

2.2.3. Ambient conditions

Ambient conditions such as temperature and humidity also affect fiber diameter and morphology during electrospinning (Li and Xia, 2004). If the ambient temperature is high, it reduces the humidity. A decrease in humidity affects solvent evaporation, especially in cases where the solvent is non-volatile.

At high humidity, the rate of solvent evaporation is reduced, while at low humidity a volatile solvent might start evaporating from the needle tip before being ejected. As a result, electrospinning with a volatile solvent can be carried out for only a few minutes before the needle gets clogged (Baumgarten, 1971). The change in humidity in turn affects fiber morphology (Zeng et al., 2002).

2.3. Fiber morphology

Concentration and temperature are found to have a significant effect on fiber diameter distribution and morphology. Trimodal (Demir et al., 2002) and bimodal distributions

(Koombhongse et al., 2001) were reported at high concentrations for polyurethane and PEO solutions respectively. At lower concentrations, and consequently, at lower viscosities, fibers exhibited 'beads on string' type morphology (Fong and Reneker, 1999).

Solution temperature also plays a key role in determining fiber morphology and spinnability. It is possible to electrospin higher concentrations of polymer solution at higher temperatures because of a decrease in viscosity at higher temperatures. Demir et al. observed that 12.8 wt% of polyurethane solution was the highest concentration that could be electrospun at room temperature, whereas a 21.2 wt% solution could be electrospun at 70^0C (Demir et al., 2002). At a high temperature, several jets were formed from the polymer droplet at the needle tip, with a large angle between each other. The fibers electrospun at higher temperature were also found to have uniform diameters despite being electrospun from a higher concentration. Moreover, it was observed that the deposition rate increased as a function of temperature. The increase in solution temperature resulted in a reduction in fiber diameter for the same concentration of solution. The reduction in viscosity led to a stronger coulombic stretching force relative to the viscoelastic force, which caused a reduction in fiber diameter (Mit-uppatham et al., 2004).

Koombhongse and coworkers studied the formation of flat ribbons and other cross sectional shapes by electrospinning (Koombhongse et al., 2001). Ribbon-like jets of a synthetic polypeptide were also reported by Nagapudi et al. (Nagapudi et al., 2002). Similarly, jets of non-circular cross sections that split into loops were observed by Shkadov and Shutov (Shkadov and Shutov, 2002). Fibers in the form of ribbons resulted from a thin skin formed by the rapid evaporation of the solvent. Remaining solvent escaped by diffusion through the skin.

The phenomenon of branching from the primary jet was reported by Deitzel et al. (Deitzel et al., 2001). The elongation of the jet and the evaporation of the solvent both change the shape and the charge per unit area carried by the jet. The balance between the surface tension and electrical forces can shift so that the shape of a jet becomes unstable. Such an unstable jet has a tendency to reduce its local charge per unit surface area by ejecting a smaller jet from the surface of the primary jet or by splitting apart into two smaller jets (Koombhongse et al., 2001).

2.4. Soy protein

Soy protein is a protein that is derived from soybean. It is commercially available in the form of soy meal, soy flour (SF), soy protein concentrate (SPC) and soy protein isolate (SPI). These products differ in the amount of protein present. The composition of different soybean products is given in Table 2.1 (Endres, 2001); (Lusas and Rhee, 1995).

Table 2.1 Composition of various soybean products

	Soybean	Soy Meal	Soy Flour	SPC	SPI
Protein (%)	35-43	50-51	52-54	68-72	90-92
Carbohydrate (%)	32-38	40-48	30-32	19-21	3-4
Moisture (%)	10-12	12	6-8	4-6	4-6
Crude Free Lipid (%)	18-21	0.5-1.0	0.5-1.0	0.5-1.0	0.5-1.0
Crude Fiber (%)	4.0-5.5	5.0-6.9	2.5-3.5	3.4-4.8	0.1-0.2
Ash (%)	4.0-5.0	5.0-6.2	2.5-6.0	3.8-6.2	3.8-4.8

2.4.1. Structure of soy protein

Soy protein is globular, reactive and water soluble in most forms. It consists of 18 amino acids, both polar and non-polar. The polar and hydrophilic amino acids impart reactivity and water solubility to soy protein (Ly et al., 1998). Functional groups present in amino acids that impart chemical reactivity to them are the carboxylic, primary and secondary amine, aliphatic and aromatic hydroxyl, and sulfhydryl groups. The amino acids present in the

soybean protein, along with their content and structural units, are listed in Table 2.2 (Berg, 1992); (Creighton, 1993); (Liu 1997).

Table 2.2 Amount of amino acids present in soybean protein and their chemical formulae

Amino Acid	Amount (%)	Chemical Formula
Aspartic Acid*	12	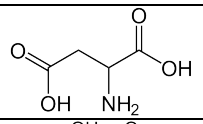
Threonine*	3.9	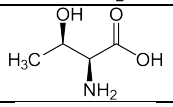
Serine*	5.3	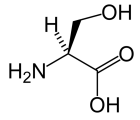
Glutamic Acid*	19.9	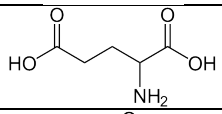
Proline	5.5	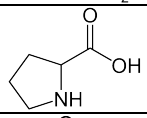
Glycine*	4.3	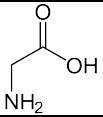
Alanine	4.3	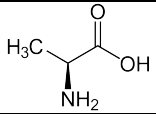
Cystine*	1.2	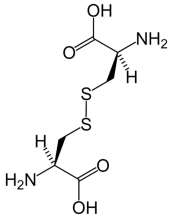
Valine	4.7	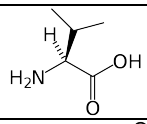
Methionine	1.4	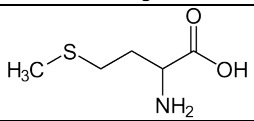
Isoleucine	4.7	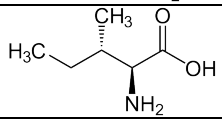

Leucine	8.3	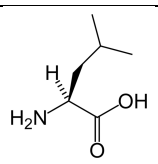
Tyrosine*	4.2	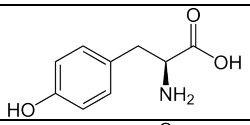
Phenylalanine	5.4	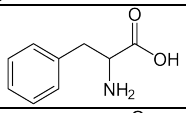
Histidine*	2.7	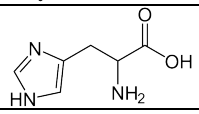
Lysine*	6.4	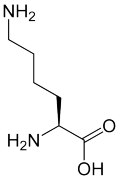
Arginine*	8.2	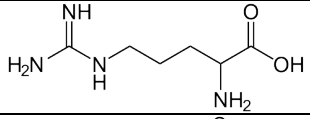
Tryptophan	1.1	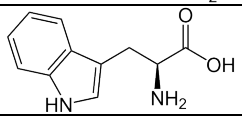

*Polar amino acids

Proteins have four levels of structural organization, as shown in Figure 2.4. The primary structure refers to the sequence of amino acids held together by amide linkages (peptide bonds) (Kielce, 2012). Secondary structure is the coiled conformation of the polypeptide chains. Tertiary structure refers to the way in which polypeptide chains are folded to form a compact globular structure. Quaternary structure is the spatial arrangement of the subunit polypeptides (Ly et al., 1998).

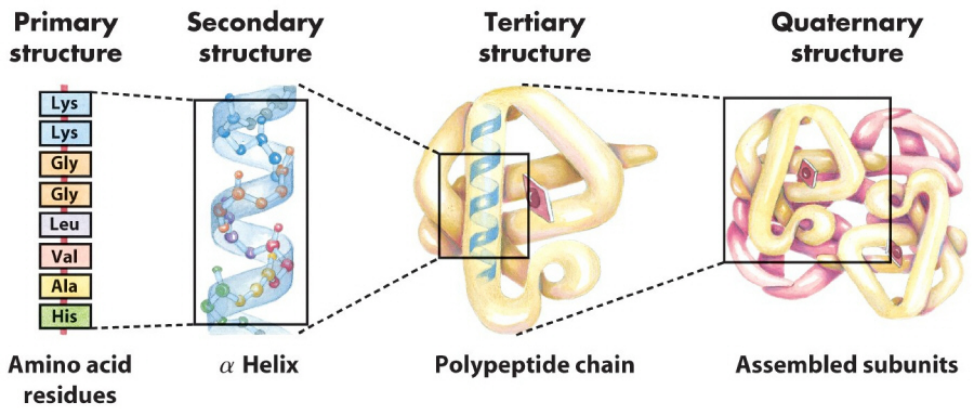

Figure 2.4: The four levels of structural organization in proteins

(Source: Science web portal of St. John's University)

Soy proteins are composed of a mixture of albumins and globulins, 90% of which are storage proteins with globular structure. They consist of groups of proteins of different molecular sizes, which lead to different ultracentrifugal sedimentation fractions. The ultracentrifugal pattern of soy protein has four fractions, namely 2S, 7S, 11S and 15S, where S stands for Svedberg units (Ly et al., 1998).

Soybean consists mainly of 7S and 11S globulins. The 7S globulin is a trimer composed of four subunits, of which the α (72 kDa), α' (68 kDa) and β (52 kDa) are the most important while the γ subunit (with a molecular mass similar to β) is a minor component. All of these subunits have similar amino-acid sequences and are poor in cysteine, methionine and tryptophan. By contrast, the 11S globulin is a hexamer whose six subunits are composed of an acidic polypeptide A and a basic polypeptide B covalently linked by a disulfide bond. It has a cysteine, methionine and tryptophan content higher than that of 7S globulin. The 7S fraction is also known as "conglycinin", while the 11S fraction is also called "glycinin". The molecular weights of the 7S and 11S fractions are roughly 180 and 350 kDa (Denavi et al., 2009).

2.4.2. Manufacture of commercial soybean products

Soy flour is obtained by grinding defatted soybean, and is the starting material for production of SPC and SPI. After soybeans are dehulled and the oil is extracted, the remaining protein and carbohydrate meal is ground into soy flour.

SPC can be produced using one of the three methods, the aqueous alcohol wash process, the acid wash process and the hot water leaching process. In the aqueous alcohol wash process, the sugars are dissolved with alcohols such as methanol, ethanol etc. The alcohols do not dissolve soy proteins. Alcohols are used in 50% to 80% concentrations by weight. Soy proteins are found to be least soluble at alcohol concentrations around 60%, and the solubility increases on either side of this concentration. After the extraction of sugars, the alcohol is recovered and re-used (Ly et al., 1998).

The acid wash process utilizes the principle of minimum protein solubility at its isoelectric point. The isoelectric point of a protein is the pH at which the protein has no net charge. At pH values lower than the isoelectric point, the basic functional groups of amino acids become protonated to give the protein a net positive charge. Similarly, at pH values higher than the isoelectric point, the acidic side chains get deprotonated, giving the protein a net negative charge.

The solubility of protein is minimum at its isoelectric point. This is because the absence of a net charge on the surface of a protein molecule reduces protein-water interactions and favors protein-protein interactions. The protein-protein interactions make the molecules clump together into globular units and thus precipitate.

The isoelectric point of soy protein is between 4 and 5 (Ly et al., 1998). Soy protein has relatively high amounts of glutamic and aspartic acid, which contain carboxylic acid, which is why soy protein is soluble in alkali but precipitates at pH around 4.5 (Ly et al., 1998).

In the acid wash process, a solution of soy flour in water is made acidic to its isoelectric point. The soluble sugars are separated from the protein that precipitates out. Because some proteins remain soluble at pH between 4 and 5, there is a reduction in the protein yield.

The hot water leaching process involves denaturation of protein by heat, rendering it insoluble in water. Denaturation of proteins is the disruption of tertiary and secondary structures in their native state. The loss of tertiary structure implies a disruption in covalent interactions between amino acid side chains, non-covalent dipole-dipole interactions, and Van der Waals interactions between non-polar amino acid side chains. The loss of secondary structure is the disruption in the alpha-helix and beta sheets in a protein, and formation of a random coil. The primary structure, that is, the sequence of amino acids held together by peptide bonds, however, remains intact during denaturation.

A number of methods such as application of heat, addition of acids and bases etc. can bring about protein denaturation (Ophardt, 2003). In this study, heat together with treatment with a base, has been used to bring about denaturation of soy protein. Heat acts by disrupting the hydrogen bonds and non-polar hydrophobic interactions. It imparts kinetic energy to the molecules and increases their motion, because of which bonds get disrupted. Bases act by disrupting salt bridges that form between acidic and basic functional groups in amino acids (Ophardt, 2003).

SPI is the purest and most expensive type of commercially available soybean protein. It is composed of over 90% protein. The protein is extracted from defatted soybean flakes with water or mild alkali in a pH range of 8-9, followed by centrifuging to remove insoluble fibrous residue, while the protein remains in solution. The solution pH is then brought down to 4.5, which causes most of the protein to precipitate out. The precipitated protein is again separated from soluble

sugars by centrifugation (Endres, 2001); (Ly et al., 1998).

2.5. Poly vinyl alcohol (PVA)

PVA is a synthetic, water-soluble polymer that is non-toxic and highly biocompatible (Koski et al., 2004). The excellent chemical stability, processability and film forming properties of PVA have led to the development of many commercial products based on this polymer (Krumova et al., 2000). PVA is used as an emulsifier and as a stabilizer for colloid suspensions, as a sizing agent and coating in the textile and paper industries, and as an adhesive (Shao et al., 2003). PVA is also biodegradable, with the degradation products being water and carbon dioxide. Hence, it is used in many biomedical and pharmaceutical applications (Cai and Gupta, 2002).

The chemical structure of poly vinyl alcohol (partially hydrolyzed) is shown in Figure 2.5.

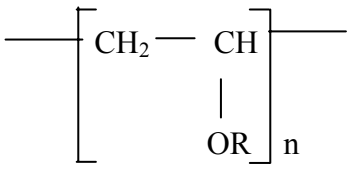

where R = H or $COCH_3$

Figure 2.5: Chemical structure of PVA

PVA is commercially manufactured by the hydrolysis of poly (vinyl acetate). The process takes place in two steps. The first step is polymerization of vinyl acetate monomer to produce poly vinyl acetate. Saponification or hydrolysis is based on the partial replacement of ester group in vinyl acetate with the hydroxyl group, and is completed in the presence of aqueous sodium hydroxide. Polyvinyl alcohol is precipitated, washed and dried. The degree of hydrolysis is determined by the duration of the saponification reaction (Hodge et al., 1996).

The percentage hydrolysis of PVA refers to the amount of the acetate groups replaced by the hydroxyl groups, and is given by the ratio of hydroxyl groups to the total number of hydroxyl

and acetate groups in the polymer.

2.5.1. Effect of degree of hydrolysis (DH) on PVA solubility

The degree of hydrolysis of PVA affects its behavior in solutions. When PVA is dissolved in water, hydrogen bonds form between the PVA chains and water molecules, in addition to the existing PVA-PVA hydrogen bonds. The extent of inter-chain and intra-chain hydrogen bonding, and the PVA-solvent hydrogen bonding is determined by the DH (Briscoe et al., 2000). Thus, the solubility of PVA in water is affected by its DH, for the same degree of polymerization and solution temperature.

Very high degrees of hydrolysis, 98% or higher, make the solution highly crystalline with strong inter and intra chain hydrogen bonds. This leads to a significant reduction in PVA solubility, especially in the range of 98% DH. For such high DH values, a solution temperature of 80^0C or higher is required for complete dissolution. The increase in temperature imparts increased mobility to PVA chains, which leads to a disruption in inter and intra chain hydrogen bonds within PVA. PVA solutions with DH values below 88% dissolve readily in water at room temperature. The increase in the number of hydrophobic acetate groups disrupts the hydrogen bonds within PVA and consequently increases its solubility. A further increase in the number of acetate groups starts disrupting PVA-solvent interactions as well. As a result, PVA becomes insoluble in water when the DH value falls below 70% (Briscoe et al., 2000).

2.5.2. Effect of DH on electrospinning

Zhang and coworkers have investigated the effect of PVA degrees of hydrolysis on the morphology of electrospun fibers (Zhang et al., 2005). They compared electrospun fibers from three PVA solutions of the same degree of polymerization, but different DH values. Flat ribbon shaped fibers with agglomerations at their junctions were obtained from PVA of 80% DH. This

indicates that the fibers were still wet at the time of deposition on the collector. Moreover, the conductivity of PVA with 80% DH was found to be an order of magnitude lower than that of PVA with 99% DH. The increase in conductivity with increase in DH could be attributed to the increased number of polar hydroxyl groups in higher degrees of hydrolysis.

The stretching of liquid jet was limited due to low solution conductivity, and consequently solvent evaporation from the fluid jet was incomplete at the time of deposition. Fibers electrospun from 88% degree of hydrolysis PVA gave the most uniform fibers with smallest diameters. Beaded fibers were obtained from PVA with 99% DH. The solution conductivity was found to increase with DH, which led to instability of the liquid jet.

2.6. Polyethylene oxide (PEO)

Polyethylene oxide is a water soluble, synthetic polymer, which is also widely used in electrospinning. It has the advantage of being low cost, and offers ease of processing. Being non-toxic, it finds application in a number of clinical products such as laxatives and skin creams (Khan, 2007). It is known to be biocompatible, and has been successfully blended with soy protein and collagen by researchers (Jin et al., 2002). The chemical structure of PEO is shown in Figure 2.6.

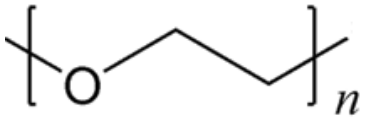

Figure 2.6: Chemical structure of PEO

While PEO is soluble in water, its homologues poly (methylene oxide) and poly (propylene oxide), are not. The matching of oxygen-oxygen inter distance on the PEO chain with oxygen-oxygen inter distance in water, has been used to explain is solubility in water (Vega-Lugo and Lim, 2008).

2.6.1. Effect of PEO on electrospinning of SPI

The addition of PEO to biopolymers such as chitosan and soy protein has been found to increase their spinnability substantially (Kriegel et al., 2009). Vega-Lugo and Lim have reported the effect of adding PEO to SPI solutions for electrospinning (Vega-Lugo and Lim, 2008). They observed that solutions of SPI in water could not be electrospun. However, SPI solutions could be readily electrospun when small amounts of PEO were added. The addition of PEO increased polymer chain entanglements and prevented the fluid jet from breaking down into droplets. Moreover, the presence of PEO brought down the electrical conductivity of the polymer solution. The fluid jet has been found to become unstable at high solution conductivities. Since the PEO chain is flexible and has both the hydrophilic ether oxygen and hydrophobic methylene segments, it has the ability to interact with amino acids in protein through both ionic as well as hydrophobic interactions. These interactions are believed to bring down the electrical conductivity of SPI solutions (Vega-Lugo and Lim, 2008).

2.6.2. Interaction of PEO with sodium dodecyl sulfate

Sodium Dodecyl Sulfate (SDS) is an anionic surfactant used commonly in sodium dodecyl sulfate polyacrylamide gel electrophoresis (SDS-PAGE) for unraveling proteins (Wikipedia). The technique works by disrupting non-covalent bonds in the proteins, denaturing them, and causing the molecules to lose their native conformation.

SDS is an organosulfate consisting of a 12-carbon chain attached to a sulfate group, giving the material the amphiphilic properties required of a detergent (Wikipedia). Figure 2.7 shows the chemical structure of the SDS molecule.

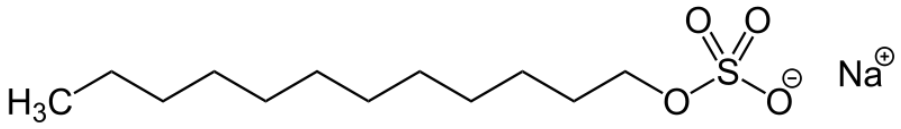

Figure 2.7: Chemical structure of SDS

In the present study, SDS has been used in combination with Triton X-100 to reduce the surface tension of electrospinning solutions. Proteins under treatment with SDS become completely blanketed by negatively charged dodecyl sulfate anions. This causes them to unwind and attain an extended conformation.

Many researchers have studied the interaction of PEO with SDS (Gjerde et al., 1998); (Jones, 1967). At a constant concentration of PEO and increasing amounts of SDS, two critical concentrations, the critical aggregate concentration (cac) and c_2 of the surfactant appear. The cac is the concentration at which interaction between the surfactant and polymer starts, and c_2 is the concentration at which polymer becomes saturated with surfactant. At the cac, the surfactant forms micelle-like aggregates and clusters on the polymer (Gjerde et al., 1998). Jones has reported that the cac is weakly dependent on the amount of polymer in solution (Jones, 1967). The formation of aggregate in surfactant is a function of surfactant concentration for a particular polymer. The values of c_2, however, are directly proportional to polymer concentration.

3. EXPERIMENTAL PROCEDURES

3.1. Materials

Soy Flour (SF), 7B, Soy Protein Concentrate (SPC) and Soy Protein Isolate (SPI), PRO-FAM 974, were obtained in powder form from Archer Daniels Midland Co., Decatur, IL. SF has been reported to contain approximately 50% protein, whereas SPC and SPI have 70% and 90% protein content, respectively (Endres, 2001).

Analytical grade sodium hydroxide (NaOH) was purchased from Mallinckrodt Chemicals, Capitol Scientific, Inc., Austin, TX. Polyvinyl Alcohol (PVA), Polyethylene oxide (PEO), Sodium Dodecyl Sulfate (SDS) and Tween 80 were purchased from Sigma Aldrich, St. Louis, MO. Triton X-100 was purchased from Acros, Hampton, NH.

3.2. Purification of soy flour

Soy flour originally contains approximately 50-52% protein (Endres, 2001). The remainder is composed of carbohydrates, ash, fiber, fat and other impurities, as reported earlier. The SF was purified to obtain higher protein content. Sugars in SF are small molecules and cannot be electrospun. Hence, the removal of sugars facilitates electrospinning. Removal of sugars also increases the protein content of soy, because the majority of protein is retained during the purification process. Protein exists as long coiled up chains, which when opened, can be electrospun.

3.2.1. Removal of particulate impurities

SF solution in water was observed under an optical microscope to determine the size of impurities present in the powder. SF was found to contain large particulate impurities of size greater than 400 micron.

Sieving was done to remove these large particulate impurities present in SF. Three sieves of

pore sizes (500, 300 and 250 μm), compliant with ASTM E-11 specification, were used in a Sieve Shaker (model # SS-15, Gilson Company, Inc.). SF was kept on the 500 μm sieve and the shaker was run for 30 minutes. However, the process was found to be inefficient because most of the material agglomerated to form small balls, which could not pass through all the sieves.

Filter papers of pore sizes varying from 2.5 μm to 11 μm were also used to remove impurities from soy flour solutions. Before carrying out the filtration, the SF solutions in deionized (DI) water, concentrations ranging from 15% to 5%, were made basic (solution pH from 10 to 12) by adding 10% NaOH solution. Soy protein exhibits minimum solubility at an acidic pH between 4-5, its isoelectric point, and the solubility increases as the solution becomes more basic or acidic (Endres, 2001). Hence, protein was first dissolved in solution so that filtration removed only the undesired material and not the protein.

3.2.2. Removal of soluble sugars

The soluble sugars were removed from SF using the acid wash separation process (Lusas 1995). The process involves making a 10% solution (by weight) of soy flour in DI water. The solution pH is made acidic using concentrated hydrochloric acid (HCl). The isoelectric point of soy flour is close to pH 4.5 (Ly et al., 1998). Isoelectric point is the pH at which a particular molecule or surface carries no net charge. For an amino acid, isoelectric point is the pH at which it exhibits minimum solubility (Ly et al., 1998). SF is composed of 18 amino acids, each of which has a distinct acid dissociation constant (pK) (Kielce, 2012).

The isoelectric point of SF can be determined theoretically from the pK values of amino acids using the following Henderson-Hasselbach equations:

For negatively charged macromolecules:

$$\sum_{i=1}^{n} \frac{-1}{1 + 10^{pKn-pH}}$$

where pKn is the acid dissociation constant of negatively charged amino acid.

For positively charged macromolecules:

$$\sum_{i=1}^{n} \frac{1}{1 + 10^{pH-pKp}}$$

where pKp is the acid dissociation constant of positively charged amino acid.

After addition of HCl, the solution is heated in a water bath at 50^0C for one hour, post which filtration is done. Microfiber based fabrics were used as filters in the present work. The advantage of using fabric filters is that they can be used repeatedly unlike the paper filters, which are suitable for one-time use only. A water aspirator was used as vacuum source to increase the rate of filtration. The filtrate containing sugars was discarded and the retentate, which consists of purified soy flour, was used for electrospinning experiments.

During the process of filtration, two process parameters, namely fabric filter type and solution pH, were varied to get the combination of fabric and pH that gives the highest protein content in retentate. Two types of microfiber fabrics (Yellow and Blue) were compared for their filtration efficiency. The solution pH was kept at 4, 4.5 and 5. The retentate, termed as purified soy protein (PSF) because of its higher protein content, obtained from all combinations of the above parameters was analyzed for nitrogen content.

3.2.2.1. Nitrogen content analysis

Nitrogen content analysis is commonly performed to determine the amount of protein present in a material (McClements and Julian, 2007). Nitrogen is a measure of the protein content, and a conversion factor of 6.25 is used to determine the protein content from nitrogen present in the sample (McClements and Julian, 2007). A CN-2000 Carbon and Nitrogen Analyzer (Leco Corporation, St. Joseph, MI) was used to carry out the analysis.

For the analysis, the PSF obtained from filtration was first heated at 100^0C for about 6 hours to remove all the water. It was then ground into a fine powder. Four microfiber fabrics were tested and the results of nitrogen content (and protein content) in various PSF specimens were compared. Several specimens were tested under the same conditions to ensure that the results were consistent and reproducible over time.

Nitrogen content in the filtrate was also determined. Attenuated total reflectance-Fourier transform infrared spectroscopy (ATR-FTIR) was first performed to confirm the presence of nitrogen in the solution. The presence of amide linkages was an indicator of the presence of nitrogen, and hence protein. The results showed an amide peak, confirming the presence of protein in the solution. The solution was then dried at 100^0C for a prolonged period until all the water evaporated and a solid mass was left behind. The solid mass was then ground similarly into a fine powder.

3.2.2.2. Porosity measurement of filter fabrics

The average pore size of the four microfiber based filter fabrics was tested on a Capillary Flow Porometer (model # CFP-1100AEHXL, Porous Materials Inc., Ithaca, NY) to determine the co-relation between pore size and the protein content obtained after filtration.

3.3. Electrospinning of soy with PVA and PEO

All three commercial forms of soy protein, SPI, SPC and SF were blended with PVA or PEO and electrospun. SPI was electrospun first, followed by SPC and SF, because it has the highest protein content and hence, is easier to electrospin than SPC and SF. SF was first purified using the filtration process as discussed in section 3.2.2 to give PSF, and then electrospun.

3.3.1. Electrospinning of SPI/PVA

PVA of molecular weight 78,000 g/mol and a DH value of 99.7% was used to make blends with SPI for electrospinning. Three compositions of SPI/PVA, 25/75, 50/50 and 75/25, were prepared to observe the effect of increasing soy content on electrospinning performance. The electrospinning set up is described later in section 3.6.

The solutions (10% concentration by weight) were prepared by mixing SPI, PVA and deionized (DI) water together, followed by stirring at RT for 30 minutes. In order to prepare a solution of 10% concentration of 25/75 SPI/PVA, 0.25gm of SPI and 0.75gm of PVA was dissolved together in 9 gm of DI water. The solutions were heated at 95^0C for 2 hours, and then stirred at RT for 30 minutes. 10% NaOH solution was added to make the pH of the solution 12. The addition of NaOH and heating together bring about protein denaturation. The final step in the solution preparation process was addition of 0.5% Triton X-100, which is a non-ionic surfactant (Tong Lin, 2004). The addition of Triton X-100 reduces solution surface tension and facilitates jet formation during electrospinning.

3.3.2. Effect of DH and solution pH on electrospinning of PVA

Before electrospinning SPC and PSF with PVA, it was necessary to compare the electrospinning performance of different degrees of hydrolysis of pure PVA. Hence, electrospinning was done with 100% PVA solutions of 88% and 99.7% DH values, to determine the effect of DH on

electrospinnability of PVA. Solutions of PVA of 10% concentration (molecular weight 78,000 g/mol) and DH values of 88% and 99.7% were prepared. The 88% DH PVA solution was prepared by stirring at RT for 30 minutes, followed by heating at 95^0C for 2 hours. The PVA solution of 99.7% DH was prepared by stirring at RT overnight, since it is difficult to dissolve in water (Zhang et al., 2005). The two solutions were electrospun using the same electrospinning parameters, in order to compare their efficacy in forming nanofibers. It was observed that the 99.7% DH solution doesn't form a Taylor cone due to high surface tension. The surfactant Triton X-100 (0.5% by weight) was thus added to the 99.7% DH solution to reduce its surface tension and improve its electrospinnability.

Electrospinning was done over a range of parameters to determine the optimum spinning conditions. The solution flow rate was varied from 5 µl/min to 10 µl/min. The voltage applied was varied between 15 KV and 20 KV and the needle tip-collector distance was varied between 15 cm and 20 cm. It was observed that the optimum spinning conditions were obtained at a needle tip-collector distance of 15 cm, voltage of 15 KV and a flow rate of 5 µl/min, for the PVA solutions of 10% concentration. At a flow rate higher than 5 µl/min, solution dripping was observed from the needle because the rate at which solution was drawn towards the collector was lower than the rate at which it reached the needle tip. When the voltage was increased to 20 KV and the needle tip-collector distance was maintained at 15 cm, 10 µl/min could be used. This is because at higher voltages, the electrostatic force that drives the fluid jet towards the collector is higher.

While electrospinning both 88% and 99.7% DH PVA, the flow rate was 10 µl/min, voltage was 20 KV, distance between the needle tip and collector was 15 cm and the deposition time was 5 minutes. The solution pH was maintained between 5 and 6.

Pure PVA solutions were also spun at pH values of 8, 10 and 12, to observe the effect of pH on fiber formation during electrospinning. Pure PVA solution was found to be slightly acidic with pH values between 5 and 6.5. The hydroxyl group in PVA has the ability to donate an H^+ ion when reacted with bases, making PVA solution mildly acidic. It is made basic by adding 10% sodium hydroxide solution. PVA solutions at pH 8, 10 and 12 were electrospun, keeping all other electrospinning conditions constant. Electrospinning was done at a flow rate of 10 µl/min with an applied voltage of 15 KV, and the needle tip-collector distance was maintained at 15 cm.

3.3.3. Electrospinning of SPC/PVA

Blends of SPC with PVA were prepared using the process detailed in section 3.3.1 for SPI/PVA. Similar to SPI, 25/75, 50/50 and 75/25 blends by weight of SPC/PVA were electrospun. PVA of both 88% and 99.7% DH values was used in preparing blends. The other electrospinning parameters were kept constant. The solution flow rate was 10 µl/min, voltage was maintained at 20 KV, the needle tip-collector distance was 15 cm and the deposition time was 15 minutes in all cases.

3.4. Solution preparation for electrospinning

Blends of soy protein with PVA and PEO were prepared for electrospinning. Soy protein in the form of PSF, prepared in laboratory by purifying SF, was used for majority of the experiments. However, PSF was later replaced by SPC for preparing solutions as its performance was found to be similar to SPC. Also, it avoided the time consuming process of preparation of PSF. The dry weight of PSF had to be determined by heating a portion of the freshly prepared PSF at 100^0C for about 6 hours. Meanwhile, the dry weight was roughly estimated as 35% and used in calculations while preparing PSF solution of a specific concentration. However, this method was not as effective as expected because the dry weight varied between 30 and 40%. This implied

that the PSF solution concentration was actually different from the desired value, and interfered with the subsequent electrospinning experiments. Since SPC and PSF were found to have similar protein content of about 65% and their electrospinning performance was equivalent, SPC was used in place of PSF, as is discussed later in section 4.1.2.

3.4.1 Solution preparation procedure

The first step in solution preparation was to make solutions of PSF or SPC, and PVA or PEO. The solutions were prepared separately by dissolving the polymer in DI water. Both PVA and PEO solutions were kept under mechanical stirring at RT overnight to dissolve the polymer. It should be noted that solutions at higher concentrations, or made from high molecular weights of polymer are difficult to dissolve, and may require heating along with stirring.

SPC was dissolved in 1% sodium dodecyl sulfate (SDS) solution. SDS is an anionic surfactant, which helps reduce the solution surface tension as well as increase protein solubility in water by blanketing the protein chains with negative charge and opening them up (National diagnostics, 2012). It was used to improve protein solubility in water, and overcome the problem of solution gelling at high concentrations of soy. The function of SDS is discussed in greater detail in section 3.5.6. The solution was stirred for ½ hour, followed by addition of 10% NaOH solution to make solution pH 12. The solution is heated in a water bath at 60^0C for 1 hour. The addition of NaOH and heating together bring about protein denaturation, which opens up the protein chains further and facilitates electrospinning of the solution (Endres, 2001) ; (Ly et al., 1998).

The solution of SPC was blended with PVA in the desired ratio, and nonionic surfactant Triton X-100 was added to make the concentration of SDS and Triton-X 100 together at 0.75%. In the case of PEO, the total surfactant concentration was made 1%. The blended solution was stirred at RT for 2 hours to bring about uniform mixing of the polymers.

3.5. Effect of solution composition on electrospinning

It was aimed to prepare solution blends from the highest possible concentrations of the constituent polymer solutions of soy, PVA and PEO. An increase in solution concentration leads to greater material deposition on the collector per unit time, and hence increases the production efficiency of the process. However, increasing the concentration beyond a certain level leads to gelling, and makes electrospinning difficult. Moreover, branching, formation of large beads, and a broad distribution of diameters, is observed at high concentrations. Therefore, it is desired to have an optimal concentration at which uniform fibers can be electrospun. The maximum concentration that can be electrospun varies from one polymer to another. It also depends on the molecular weight and the solution temperature. Heating the solution breaks the polymer-polymer and polymer-solvent interactions that cause gelling at high concentrations. For polymers with low molecular weights, electrospinning is possible at high concentrations.

Both soy protein and PVA/PEO were used over a range of concentrations for making solution blends.

3.5.1. Effect of molecular weight of PVA and PEO on electrospinning

PVA of DH value 88% and molecular weights ranging from 67,000 to 205,000 g/mol was tested over a range of concentrations to determine the optimum combination of concentration and molecular weight which gave the best results when electrospun with soy protein. PVA of molecular weight 67,000 g/mol was prepared in 10% and 12% concentrations, and blended with PSF solution. Similarly, PVA of average molecular weight 115,500 g/mol was used in 10% concentration with PSF.

PVA with molecular weights of 130,000 and 205,000 g/mol were later used for experiments because it was observed that a higher molecular weight of polymer favored formation of uniform

fibers during electrospinning. Moreover, a lower proportion of polymer was required to be blended with soy protein to obtain fibers, which was one of the goals of the present research.

PEO of molecular weights of 300,000 g/mol, 600,000 g/mol and 900,000 g/mol were also electrospun after forming blends with soy. Concentrations ranging from 0.5 to 8% were tested for each case to determine the optimum combination of molecular weight and concentration that gives uniform, low diameter nanofibers.

3.5.2. Effect of surfactant type on electrospinning

Two types of surfactants, Triton X-100 and Tween 80, were used while preparing electrospinning solutions. The function of a surfactant is to reduce surface tension, which has to be overcome by the electrostatic force during electrospinning. Therefore, lowering the surface tension facilitates Taylor cone formation and subsequent ejection of jet from the polymer droplet. Triton X-100 is a nonionic surfactant that has a hydrophilic polyethylene oxide and a hydrophobic aromatic hydrocarbon group. Apart from reducing surface tension of aqueous solutions, Triton X-100 serves as detergent and cleaning compound (Wikipedia).

Tween (polysorbate 80) is another nonionic surfactant and emulsifier that is derived from polyethoxylated sorbitan and oleic acid. It is a viscous, water-soluble yellow liquid, used commonly in foods (Wikipedia).

Both Triton X-100 and Tween 80 were used in electrospinning solutions to compare their efficacy in reducing solution surface tension. Tween 80 was used in 1% and 2% concentrations in blends of PEO, whereas 0.5% and 1% was added to blends to PVA. Triton X-100 was tested under the same conditions.

3.5.3. Comparison of electrospinning performance of SPI, SPC and PSF

SPI, SPC and PSF were each electrospun with PVA and PEO using the solution preparation procedure described in section 3.4.1. All three forms of soy were prepared in 7% concentrations, and blended with 10% PVA (avg. mol. wt. 115,500 g/mol) or 5% PEO (600,000 g/mol).

3.5.4. Electrospinning of PSF/PVA/PEO blends

The problems of gelling at high concentrations were more acute in PSF/PVA solutions because of hydrogen bonding between PSF and PVA, which acts as a crosslinking network and leads to gelling. As mentioned earlier, gel formation is detrimental to electrospinning. Hence, PEO was also added in small amounts to PSF/PVA blends in order to disrupt the hydrogen bonding between PSF and PVA. PSF/PVA/PEO blends were prepared by mixing the 3 solutions in the ratio 70/25/5.

3.5.5. Use of stearic acid to reduce gelling in PSF blends

Use of stearic acid to overcome the problem of gelling at high concentrations of PSF/PVA solutions was assessed. Stearic acid is a saturated fatty acid with an eighteen-carbon chain. The carboxylic group acts as the polar head whereas the carbon chain acts as the non-polar tail. Stearic acid functions by forming amide linkages with PSF, and thus disrupts or reduces the hydrogen bonding between PSF and PVA.

Stearic acid is available in the form of chips. Its meting point is close to 70^0C. Hence, it was required to heat the solutions to above 70^0C to melt and dissolve the acid. Two methods of solution preparation with stearic acid were tested and electrospun. In one of the methods tried, stearic acid was added directly while blending the PSF with PVA and PEO. The blends were heated above 70^0C for 1 hour to completely melt and dissolve the stearic acid. Blends of PSF/PEO and PSF/PVA/PEO were electrospun. Stearic acid (1.05% by wt.) was added to a 10

gm solution, while the PSF/PVA and PEO were mixed in the ratio 66:32:2. PSF (11% concentration)/PEO 900,000 g/mol (5% concentration) blends, mixed in the ratio 93:7, were also electrospun.

In the second method, stearic acid was added in 2.5% concentration to PSF solution, followed by addition of NaOH to the solution, and stirring above 70^0C to melt and dissolve the stearic acid. This solution was later used to prepare same PVA/PVA/PEO and PSF/PEO blends as described above.

3.5.6. Effect of SDS addition to electrospinning solutions

Sodium dodecyl Sulfate (SDS) was also tested as an additive to reduce the problem of gelling at high concentrations of electrospinning solutions. It is an anionic surfactant used commonly in SDS-PAGE for unraveling protein molecules. It works by disrupting non-covalent bonds in the proteins, denaturing them, and causing the molecules to lose their native conformation.

Proteins blended with SDS become completely blanketed by negatively charged dodecyl sulfate anions. This causes them to unwind and attain an extended conformation, as shown in Figure 3.1 (National Diagnostics 2012).

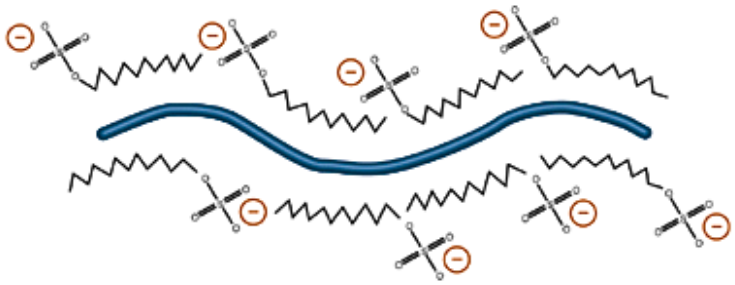

Figure 3.1: Protein chain blanketed by negative charge from SDS

(Source: Nation Diagnostics, Buffer Additives-Surfactants)

The motivation for using SDS was to improve the solubility of protein in water and also to increase the charge on the protein chains. PSF solutions were prepared in approximately 11%

concentrations and 1% solid SDS powder was added to the solutions. The solutions were then treated with NaOH and heated, as described in section 3.4.1.

The PSF solution was blended with PEO (5% conc., mol wt. 900,000 g/mol) in the ratio 93:7 (solids content of the blend – approx. 10%). Triton X-100 was added to make the total concentration of SDS and Triton X-100 equal to 1%.

Similarly, PSF/PVA/PEO blends were prepared in the ratio 69:29:2, the solids content being 11.75%. Triton X-100 was added to make the total surfactant concentration equal to 1%. These solutions were electrospun and the results were compared with similarly prepared solutions, but without SDS. The control specimens were prepared using 12% PSF solutions. Triton-X 100 was added in 1% conc. to the PSF/PEO and PSF/PVA/PEO samples.

3.6. Fabrication of the electrospinning setup

The electrospinning setup consisted primarily of a high voltage supply, a grounded metal collector and a syringe pump.

A positive high voltage supply (model # ES30P-5W, unit rated at 0-30KV, 166uA, Input voltage: 90-240VAC) was purchased from Gamma High Voltage Research, Ormond Beach, FL. A PHD Ultra Syringe Pump (Infuse Only Standard) was bought from Harvard Apparatus, Holliston, MA. The polymer solution was filled in a 6 ml plastic syringe mounted on the syringe pump, which supplied polymer solution at a fixed rate through a blunt metal needle attached to it. Needles of gauges varying from 17 to 20 were bought from Hamilton Company, Reno, NV. A needle gauge of 17 corresponds to an inner diameter (ID) of 1.067 mm and an outer diameter (OD) of 1.476 mm. The needle gauge of 20 corresponds to an ID of 0.603 mm and OD of 0.9081 mm.

The region between the needle and collector was insulated from the surroundings by enclosing it

in a poly methyl methacrylate (PMMA, Plexiglas®) box. The PMMA rectangular box was constructed with one side open, as shown in Figure 3.2.

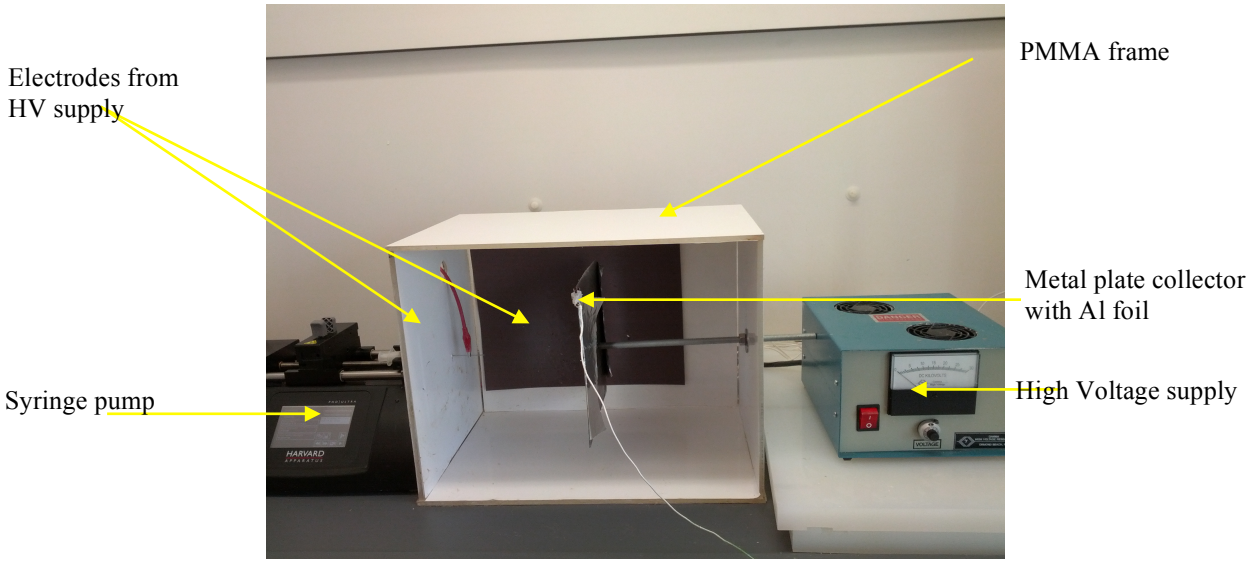

Figure 3.2: Laboratory electrospinning setup

A steel plate collector was screwed on to one side of the box. The collector, a 20x20 cm flat steel plate, was placed inside the PMMA box using a threaded metal rod attached to a stand. The collector was clamped in this way to ensure that the nanofibers do not get attracted to anything else and get deposited entirely on the collector. The distance between the syringe tip and collector was adjustable.

3.7. Effect of electrospinning parameters on fiber diameter

As discussed earlier in section 2.2, solution properties, process parameters and ambient conditions play a critical role in determining fiber diameter and their morphology. Solution properties include concentration, polymer molecular weight, viscosity, conductivity and surface tension.

Solution properties such as concentration and molecular weight were varied over a range of values to determine the optimal combination of concentration and molecular weight that would

give the desired solution viscosity for electrospinning. The viscosity increases both with an increase in concentration as well as the polymer molecular weight. Process parameters that can be varied during the process include applied voltage, solution flow rate and the needle tip-collector distance.

The high voltage source used in our electrospinning setup could supply a voltage of up to 30 KV. The solution flow rate, controlled through the syringe pump, was varied between 15 and 30 μl/min depending on the solution properties and other process parameters used. The needle tip-collector distance was varied between 10 cm and 25 cm, to control the diameter and morphology of nanofibers.

Ambient parameters such as temperature and humidity were varied by keeping a hot plate in the vicinity of the electrospinning setup. The hot plate has the dual effect of increasing the ambient temperature and reducing humidity. The effect of blowing hot air on the collector in conjunction with the hot plate as well as independently, was also tested. A commercial hair dryer was used for this purpose, and a metal wire mesh was used instead of a steel plate as collector, to allow passage of air through it. Figure 3.3 shows the wire mesh and hair dryer arrangement in the electrospinning setup. A number of substrates, such as filter paper and a plastic mesh, were taped to the metal wire mesh for collecting nanofibers.

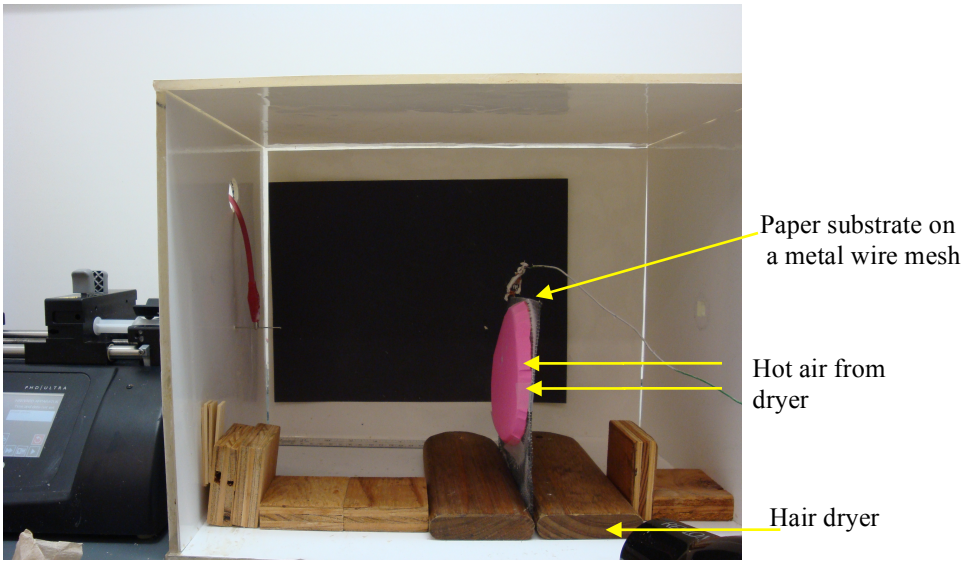

Figure 3.3: Wire mesh and hair dryer arrangement in the electrospinning setup

3.8. Characterization

3.8.1. Scanning electron microscopy

A Leica 440 Scanning Electron Microscope (SEM) was used at an accelerating voltage of 25 KV, to measure the diameter and morphology of electrospun nanofibers. The electrospun nanofiber membrane samples were first coated with Au-Pd, followed by imaging on SEM. Magnifications of up to 12,000X were used to determine the diameters of nanofibers in the range of 50-200 nm.

3.8.2. Measurement of fiber diameter and statistical analysis.

The diameter of electrospun nanofibers was measured using *ImageJ,* an image processing program developed by the National Institutes of Health, and available as open source software on the internet. Images obtained from scanning electron microscopy of the nanofibers were analyzed with the software, and the diameter was measured at 60 points on a single image.

Statistical software *JMP* (developed by SAS Institute, Cary, NC) was used to carry out statistical analysis of the effect of electrospinning parameters on fiber diameter. The electrospinning

parameters such as solution concentration (C), molecular weight (M), applied voltage (V), and needle tip-collector distance (D) were chosen as independent parameters, and their effect on average fiber diameter and distribution was determined using *JMP*. Electric field (E), which is given by the applied voltage over needle tip-collector distance, was used as an independent parameter initially. Hence, analysis was done with solution concentration, molecular weight and electric field as the three independent variables.

From the initial analysis with the three independent parameters, the effect of electric field was found to be insignificant. Hence, analysis was done again keeping the four parameters separate from each other. The needle tip-collector distance was found to affect the fiber morphology, that is, fiber had flat cross sections because of incomplete solvent evaporation when the needle tip-collector distance was low. For non-volatile solvents such as water, incomplete evaporation of solvent before deposition was often observed. Hence, it was expected that the effect of needle tip-collector distance on fiber diameter would be significant.

A factorial experiment was designed to test the individual and combined effect of the parameters, that is, data were collected for all possible combinations of the input parameters. A 60/40 blend of SPC/PVA was used to carry out the experiment. Two values of concentration of SPC, 10% and 12.5%, were used. The same concentration of PVA, 10%, was used in all solutions. It was attempted to electrospin SPC/PVA blends using 7.5% SPC solution concentration. However, the nanofibers, when observed under SEM, were found to consist predominantly of beads. Similarly, any concentration of SPC above 12.5% could not be electrospun with PVA because it formed a gel on mixing the two polymers.

The molecular weight used consisted of two values of PVA, 130,000 g/mol and 205,000 g/mol. The molecular weight of SPC was the same in all cases. Three values, 22, 26 and 30 KV, were

chosen for applied voltage. The needle tip-collector distances used were 15, 18 and 21 cm. Thus, a total of 36 electrospinning conditions were obtained. Electrospinning was done at each of the 36 conditions, followed by scanning electron microscopy to determine the fiber diameter and distribution.

3.8.3. Measurement of solution viscosity

The viscosity of SPC, PVA and PEO solutions, and their blends, was determined with an AR-2000 Advanced Rheometer (TA Instruments, New Castle, DE) using the cone and plate geometry. The rate of shear was varied from 0 to 500 sec^{-1}, and stress was plotted as a function of shear. The rheological behavior of SPC and the effect of SDS on solution solubility were determined with the help of viscosity measurements. An increase in solution solubility implies a corresponding increase in viscosity due to the opening up of protein chains.

3.8.4. Strength of nanofiber membranes

The tensile strength of electrospun nanofiber membranes was measured using Instron, model 5566 (Instron Co., Canton, MA) using a 100 N load cell. A gauge length of 10 mm and a strain rate of 50% per minute were used for all specimens. At least 10 specimens were tested to obtain the average strength values.

3.8.4.1. Preparation of samples for strength measurement

Various membranes of SF/PEO, SPC/PEO and SPI/PEO were electrospun in order to characterize the effect of protein content on the strength of membranes. PEO, molecular weight 600,000 g/mol, was used in 5 wt% concentration. SF, SPC, and SPI solutions were prepared at 12% concentrations using the method outlined in 3.4.1. The ratio of soy and PEO in the blend can also affect its mechanical properties. Hence, 51/49 and 70/30 (by wt.) blends of soy protein/PEO were prepared for all the three forms of soy. Pure PEO (molecular weight 600,000

g/mol, concentration 4 wt%) was also electrospun, to determine the effect of adding soy on the strength of membranes.

In order to get membranes, a spun bond fabric was pasted on the aluminum foil, which was in turn taped to the collector plate. However, it was difficult to peel out the nanofiber membranes from the aluminum foil. Hence, the membranes were deposited on to a polypropylene (PP) spun bonded fabric and peeled off later for strength measurement. A 51/49 blend of SF/PEO is shown in Figure 3.4.

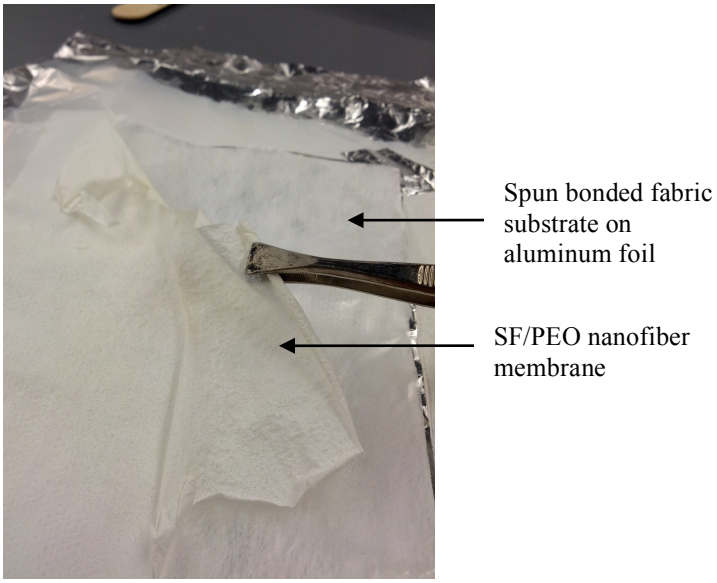

Figure 3.4: SF/PEO membrane on a spun bonded fabric

The deposition was done for 1.5 hours in each case, to obtain a significant thickness of membrane, and also to facilitate the process of peeling out the membrane from the spun bonded fabric. An applied voltage of 25 KV was used, and the needle tip-collector distance was maintained at 21 cm in all cases. A flow rate of 30 µl/min was used to electrospin the solutions of SPC, SPI and pure PEO. However, the flow rate was reduced to 20 µl/min to electrospin blends of SF, in order to avoid solution dripping.

Once the membranes were peeled from the spun bond fabric substrate, they were cut into 10x5

mm rectangular specimens, which were mounted on a paper window, as shown in Figure 3.5. The paper window was cut from both sides before starting the test.

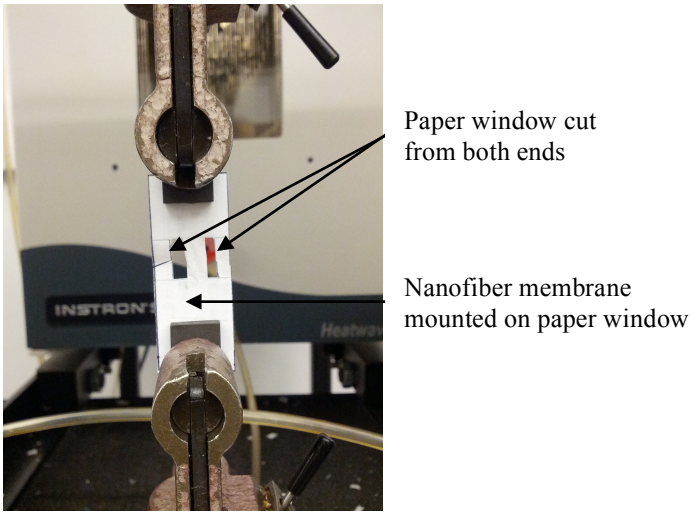

Figure 3.5: A paper window with nanofiber membrane

The paper window was used to facilitate the process of mounting the specimens between the clamps, and avoid breaking the specimens during the process of mounting them.

3.9. Composting study

Composting is defined as an exothermic bio-oxidative decomposition of organic materials by indigenous microorganisms in a controlled moist and warm aerobic environment leading to the production of 'compost', a mixture of carbon dioxide, water, minerals and a stabilized organic matter (Lodha and Netravali, 2005).

Composting technique has been utilized to characterize the biodegradation of blends of SPC with PVA and PEO (Cho et al., 2012). The solutions of SPC with PVA and PEO were used to electrospin nanofiber membranes. Films were made from the polymer solution blends and used as specimens for composting. The films were prepared by pouring polymer solutions on Teflon® coated glass plates, followed by heating in an oven at 40^0C until the films became dry.

The blends of SPC/PEO were prepared using 12% concentration of SPC and 5%

concentration of PEO of molecular weight 600,000 g/mol. The SPC/PVA blend consisted of 12% concentration of SPC and 14% concentration of PVA of molecular weight 130,000 g/mol. All the blends were mixed in the ratio 70:30 by weight, SPC being the 70% component in all cases.

The composting medium was prepared by blending sawdust and chicken manure (droppings) in the ratio 1:1 (w/w) to obtain a C/N ratio of 50/50. A small plastic container, which contained the prepared compost media, was placed inside another big plastic container. The inside container had circular holes on its wall for air circulation. The composting conditions such as moisture, temperature and pH were monitored periodically. The moisture content of the compost mix was maintained at 50% by adding water periodically.

The film specimen weights were measured after drying in a vacuum oven for 24 hours. Non-woven, non-degradable polypropylene (PP) bags with high porosity were used to place the specimens inside the composting medium. The PP bags, due to their porous structure, allowed moisture, air and micro- organisms to move in and out freely.

The composted specimens were successively retrieved from the media after desired time periods. Specimens were composted for up to 5 weeks. Two films of each blend were retrieved every week to analyze the degradation over time. The weight of the retrieved specimens was measured after drying them in a vacuum oven overnight.

The film specimens were observed under a Leica 440 SEM to observe any changes on the film surface due to degradation. All specimens were coated with Au-Pd to prevent charging during SEM imaging.

4. RESULTS AND DISCUSSION

4.1. Purification of soy flour (SF)

Purification of SF was carried out to remove carbohydrates (sugars) and other impurities. This leads to an increase in the net protein content. Moreover, sugars are small molecules that cannot be electrospun. Hence, removal of sugars from SF facilitates electrospinning. The removal of sugars was carried out using a lab-scale filtration system. But first it was attempted to remove the particulate impurities, which were large enough to interfere with the filtration process by clogging the filter pores.

4.1.1. Removal of particulate impurities

Sieving was done in order to remove the particulate impurities present in SF. SF solution was first observed under an optical microscope to determine the size and structure of these impurities. Figures 4.1 and 4.2 show images of SF solution under an optical microscope, and a black particulate impurity present in the solution, respectively. It was observed that black, irregular shaped impurities in the range of 400 micron, were present in SF powder.

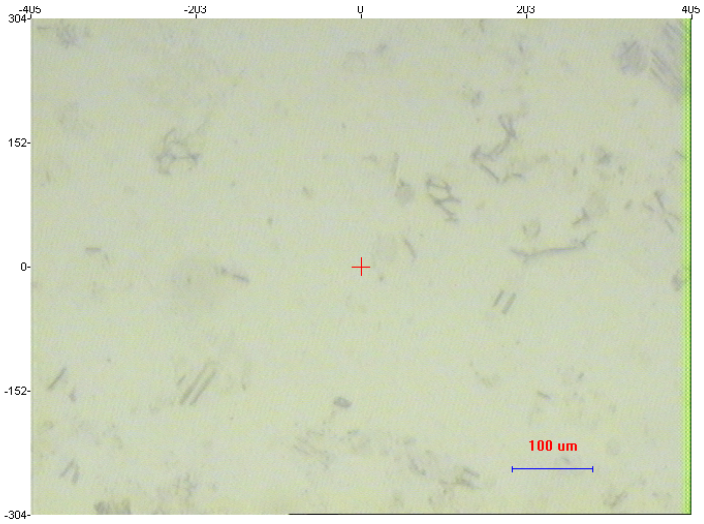

Figure 4.1: SF solution under an optical microscope

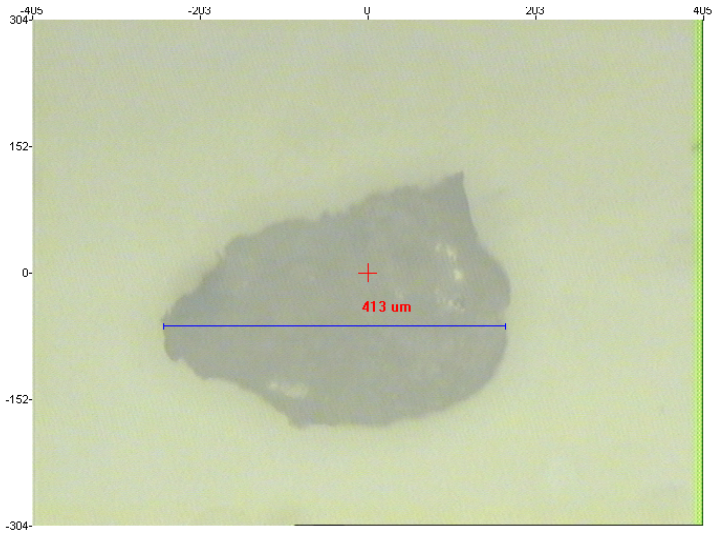

Figure 4.2: A black particulate impurity present in the solution

Sieving was done on a Sieve Shaker using three different sieves (pore sizes 500, 300 and 250 µm). The finest sieve had a pore size of 250 µm, which was lower than the size of the impurities observed. However, sieving was found to be inefficient since most of the SF was left behind on the sieves along with the impurities. Moreover, the process did not give consistent results each time sieving was done. Hence, it was not used for purifying SF.

In the next step, SF solutions, concentrations ranging from 15% to 5%, was made basic (pH ranging from 10 to 12) by adding 10% NaOH solution, and filtered using cellulose based filter papers of pore sizes varying from 2.5 µm to 11 µm. However, it was observed that the pores of filter paper got clogged and SF also got collected on the filter paper along with the impurities. As a result, this effort was also abandoned.

Since the preliminary purification processes for removing particulate impurities did not work satisfactorily, a microfiber based filtration process was employed directly for removing the soluble sugars from SF. This filtration process has been described in detail in section 3.2.2. It

utilizes the principle of minimum protein solubility at its isoelectric point to separate it from the soluble sugars. Two process parameters, filter type and solution pH, were varied to determine the combination of parameters that gave the highest protein content in the purified soy flour (PSF).

4.1.2. Nitrogen content analysis

The protein content of the PSF obtained from filtration was measured using a Nitrogen analyzer. The protein content was calculated by multiplying a Kjeldahl factor of 6.25 to the nitrogen content obtained (Watson and Galliher, 2001). The results are summarized in Table 4.1. Two types of microfiber based fabrics (Blue and Yellow) and three pH values (4, 4.5, 5) were tested during the filtration process, to determine the fabric and pH value which gave the highest protein content in PSF.

Table 4.1: Results from nitrogen analysis of dried PSF

Filtration Conditions	Protein Content (%)
Yellow, pH 5	62.9
Blue, pH 5	64.6
Yellow, pH 4.5	64.9
Blue, pH 4.5	65.6
Yellow, pH 4	65.4
Blue, pH 4	66.5

The average protein content in PSF was found to be 65%, which is similar to the protein content of SPC (Lusas and Rhee, 1995). As evident from the results of nitrogen content analysis, the protein content did not vary significantly from one specimen to another even though the filtration parameters varied. Hence, if the filtration conditions are kept constant, there should not be a high variability in the protein content between different specimens. However, the Blue fabric at pH 4 gave the highest protein content among all the samples tested.

4.1.3. Porosity measurement of filter fabrics

Further tests were done using pH 4 and two more microfiber based fabrics of higher pore sizes to determine the variation in protein content of PSF as a function of pore sizes of the fabrics. The average values of the results are summarized in Table 4.2. The average protein content in PSF across all four fabrics was found to be 66.27%. This is close to the protein content obtained by Kim and Netravali using a similar process for purification of SF (Kim and Netravali, 2010). They have reported a 67.5% content of protein in SF post filtration. Table 4.2 also gives the protein content of the filtrate. The 18% protein lost in the filtrate was assumed to be consisting of smaller molecular weight protein molecules that passed through the fabric pores.

Table 4.2: Protein content in PSF obtained from the four filter fabrics

Sample type	Protein Content (%)
Filtrate	18.32
Red	66.62
Grey	66.49
Yellow	65.43
Blue	66.53

Table 4.3 presents the mean pore diameter values for the four filter fabrics used. Since the protein content obtained from the four fabrics is almost similar, it cannot be said with certainty what effect the pore size has on filtration efficiency. However, it is likely that the globular protein size is larger than 9.22 μm, the largest pore size in this study.

Table 4.3: Mean pore diameters of the filtration fabrics

Fabric Type	Mean Pore Diameter (μm)
Blue	7.13
Grey	9.22
Red	7.64
Yellow	5.85

The PSF obtained from the filtration process contains a significant amount of water. The presence of water needs to be accounted for while preparing PSF blends with PVA and PEO. Hence, the filtration was carried out over five times to get an average value of the dry weight. PSF was heated at 100^0C for 6 hours until the weight stabilized. The dry weight of PSF was approximately 35% after 6 hours of heating.

4.2. Effect of solution composition on electrospinning

4.2.1. Electrospinning of SPI/PVA

Figures 4.3 a, b and c show SEM micrographs of electrospun fibers from SPI/PVA solutions blended in the ratios 25/75, 50/50 and 75/25, respectively.

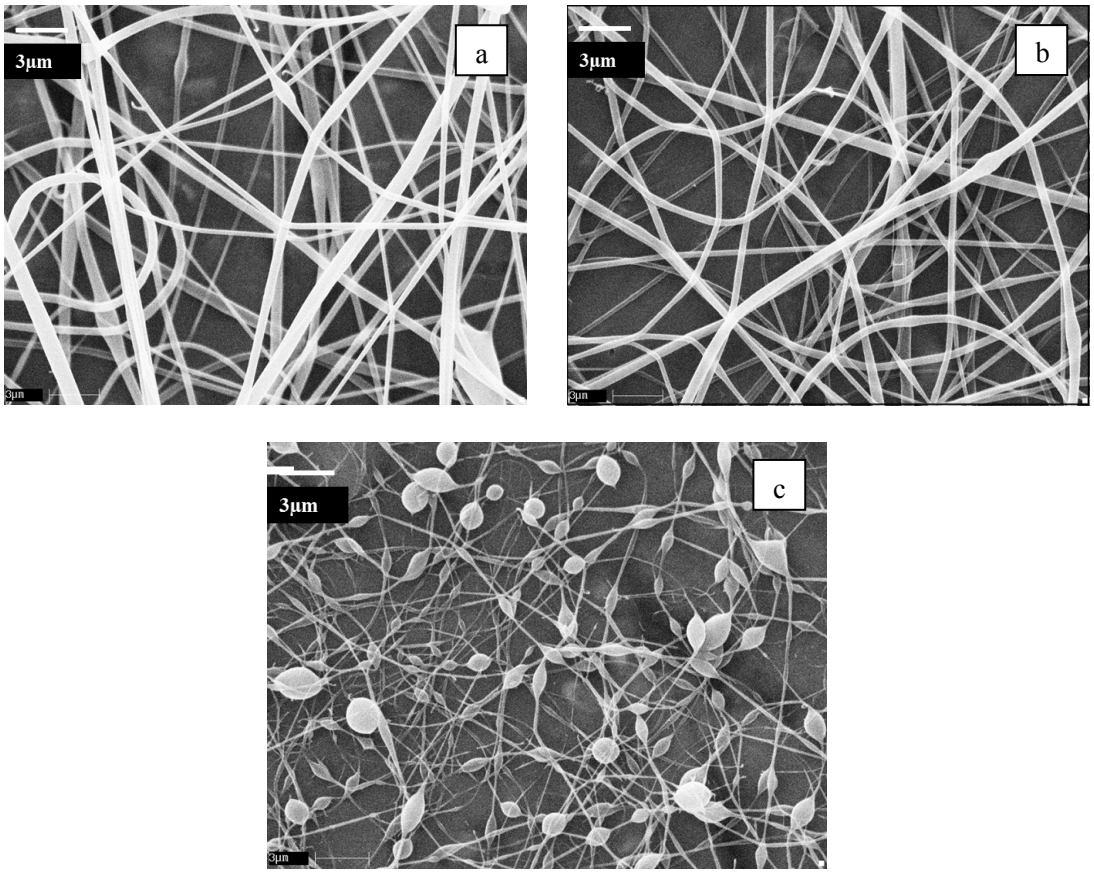

Figure 4.3: SEM micrographs of electrospun fibers from SPI/PVA solutions blended in the ratios (a) 25/75 (b) 50/50 (c) 75/25

PVA with molecular weight of 78,000 g/mol and DH value of 99.7% was used for preparing the blends. The same electrospinning conditions were used in all cases. The solution flow rate was 5 µl/min, applied voltage was 20 KV, the needle tip-collector distance was 15 cm, the needle gauge was 19, and the deposition time was 10 minutes in each case.

The fibers obtained from all the three compositions were non-uniform, especially for the 75/25 solution. The presence of a large number of beads in the 72/25 solution is due to high surface tension and low solution viscosity in comparison to the 25/75 and 50/50 cases (Fong et al., 1999). The non-uniformity of SPI/PVA nanofibers can be attributed to low voltage and the use of 99.7% degree of hydrolysis PVA, as will be determined in sections 4.3 and 4.2.2 (Zhang et al., 2005).

Pure PVA was electrospun next, to investigate the effect of degree of hydrolysis on electrospinning.

4.2.2. Effect of DH and solution pH on electrospinning of PVA

Figure 4.4 shows SEM micrographs of nanofibers electrospun from 88% and 99.7% DH solutions of PVA. A comparison of the SEM micrographs in Figure 4.4 shows that PVA with 88% DH is preferred over PVA with 99.7% DH. This is because the fibers are uniform, and with a smaller variation in diameters. Moreover, the average fiber diameter is lower in 88% PVA, which is also preferred in this study. A small average fiber diameter of an electrospun membrane gives a small pore size and increase surface area to volume ratio, which has several applications as discussed in section 1.3. The mean diameter of fibers electrospun from 88% DH was 336 nm, with a coefficient of variation (CV) 6.25%. For the 99.7% DH PVA, the mean fiber diameter was 395 nm, with a CV of 27.3%.

The formation of uniform fibers is explained by the relatively lower viscosity and conductivity of

the 88% DH solution of PVA than the 99.7% solution. Higher solution conductivity in the 99.7% DH PVA solution results in instability of the liquid jet, which in turn gives a wider distribution of fiber diameters (Zhang et al., 2005).

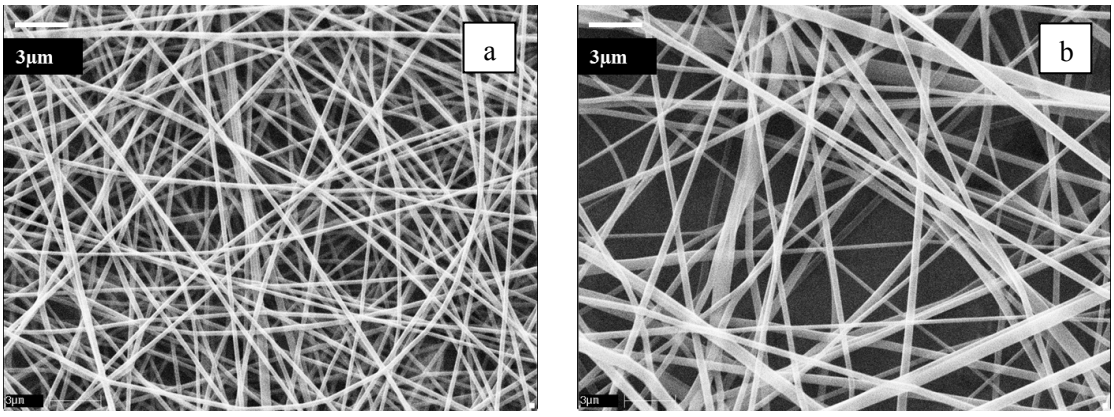

Figure 4.4: SEM micrographs of nanofibers electrospun from (a) 88% DH and (b) 99.7% DH solutions of PVA

Figure 4.5 shows SEM micrographs of nanofibers electrospun from 10% concentration of PVA solutions at pH (a) 8 (b) 10 and (c) 12. PVA with molecular weight of 78,000 g/mol and DH value of 88% was used for determining the effect of pH.

All the three pH values of solutions gave uniform nanofibers. However, the fibers became straighter and finer as the solution became more basic. The conductivity of PVA solutions has been found to vary significantly with pH, whereas the viscosity and surface tension do not change significantly (Son et al., 2005). The increased conductivity at basic pH exerts stronger elongational forces on the fluid jet, resulting in straighter and finer fibers at pH 12. In addition, it is known that as the pH moves away from the isoelectric point (about 4.5), the protein molecules open up from globular to a straighter conformation, making it easier to electrospin.

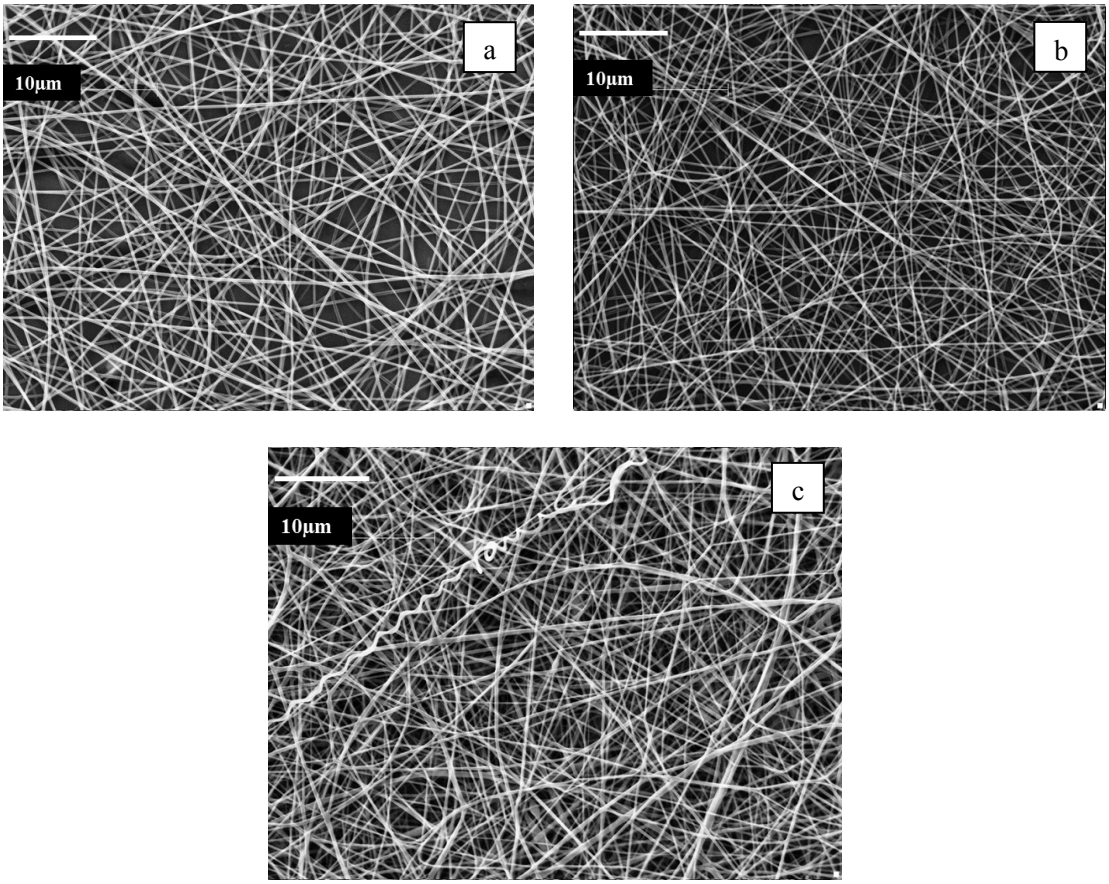

Figure 4.5: SEM micrographs of nanofibers electrospun from 10% concentration of PVA solutions at pH (a) 8 (b) 10 and (c) 12

The pH of PVA solution was increased to pH between 10-12 after blending with soy protein solutions. This is because the soy protein solution is denatured with NaOH prior to blending with PVA. As discussed above, the increase in pH of PVA solution favors formation of finer fibers, which is preferred in this study.

4.2.3. Electrospinning of SPC/PVA

Figure 4.6 shows SEM micrographs of fibers electrospun from SPC/PVA solutions in the ratios 25/75 and 50/50. PVA 99.7% DH used earlier in section 4.2.2 for electrospinning SPI/PVA blends, was replaced by PVA 88% DH in this case. A constant flow rate 10 µl/min was used in both cases. However, the applied voltage was increased from 15 KV to 20 KV for

electrospinning the 50/50 blend, and the deposition time was increased from 5 min. to 10 min. This is because it was expected that SPC/PVA blends would be more difficult to electrospun, due to the lower protein content (70%) in SPC compared to 90% in SPI. A higher voltage reduces bead formation by acting against the surface tension, resulting in easier stretching of the jet (Fong et al., 1999).

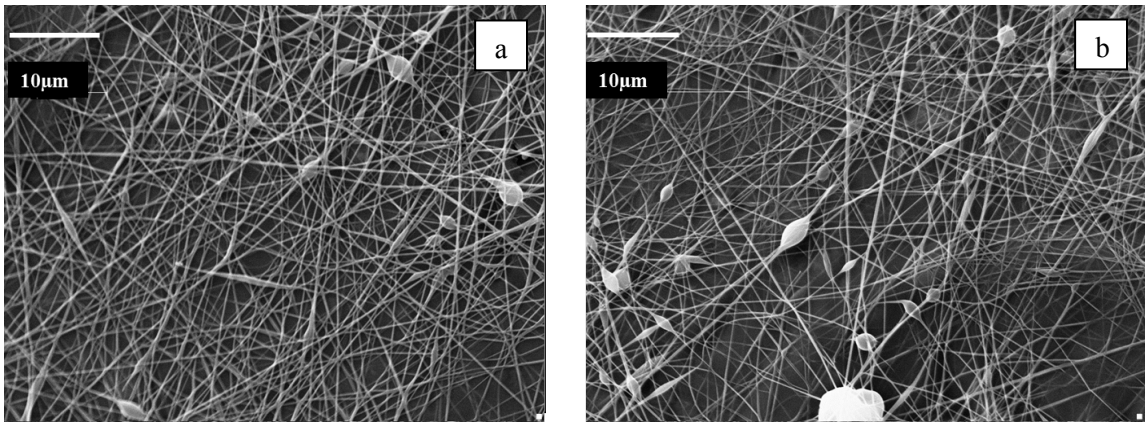

Figure 4.6: SEM micrographs of fibers electrospun from SPC/PVA solutions in the ratios (a) 25/75 and (b) 50/50

A comparison of the SPC/PVA nanofibers with SPI/PVA nanofibers shows that the SPC/PVA nanofibers have a smaller average diameter. This is because the SPC/PVA solution has a lower viscosity than SPI/PVA solution, for the same blend ratio. SPI forms a more viscous solution than SPC, because of the higher amount of protein in SPI. Protein exists in the form of long chains, which open up on denaturation and increase the solution viscosity significantly (Endres, 2001).

4.2.4. Effect of surfactant type on electrospinning

The efficiency of Triton X-100 and Tween 80 as surfactants was compared by electrospinning solutions with the two surfactants, keeping all other parameters constant. Blends (58/42 by wt.) of PSF (7% concentration) with PEO 600,000 g/mol (5% concentration) were prepared and 2%

Triton X-100 was added in one case, whereas 2% Tween 80 was added in the second. Similarly, blends (37/63 by wt.) of PSF (7% concentration) with PVA 115,000 g/mol (12% concentration) were prepared and 0.5% of the non-ionic surfactants were added to one each. Figure 4.7 shows SEM micrographs of PSF/PEO and PSF/PVA blends with Triton X-100 (a, c) and Tween 80 (b, d) respectively.

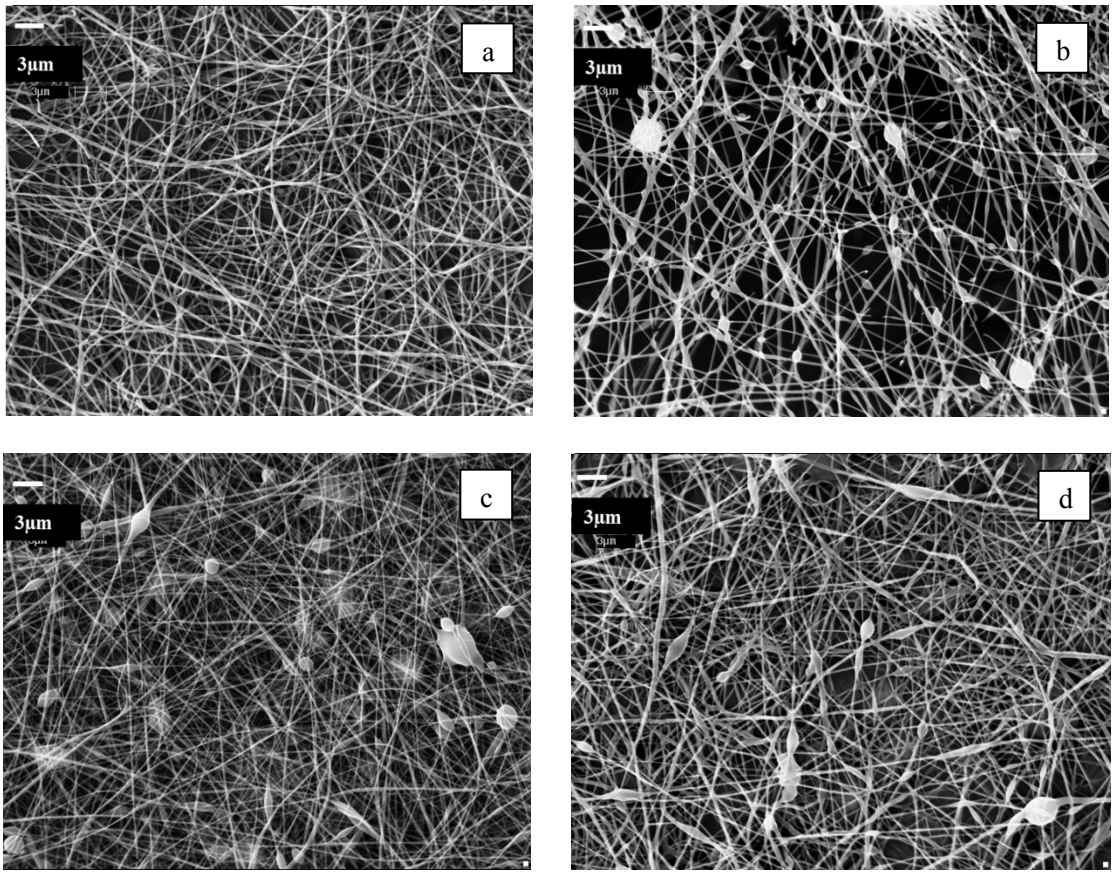

Figure 4.7: SEM micrographs of PSF/PEO and PSF/PVA blends with Triton X-100 (a, c) and Tween 80 (b, d), respectively

It was observed that the PSF/PEO nanofibers (Figure 4.7 b) were broken and scanty when Tween 80 was used as a surfactant. The PSF/PEO blend with Triton X-100, on the other hand, gave uniform fibers (Figure 4.7 a). For the PSF/PVA blends, the fibers were flat and had a fused appearance when Tween 80 was used (Figure 4.7 d). The PSF/PVA blend with Triton X-100,

however, produced fibers with circular cross-sections (Figure 4.7 c).

It was also observed that the number of beads was higher in the case of Tween 80 in both the blends of PSF. The presence of beads indicates that the solution being electrospun has high surface tension, which the electrostatic charge is unable to overcome fully. Surface tension tries to make the surface area per unit mass smaller by changing the jets into spheres jet (Fong et al., 1999). Solution viscosity also affects bead formation in nanofibers. Since the blends had the same composition other than surfactant type, the viscosities of the two PSF/PVA blends were similar. The viscosities of the two PSF/PEO blends were also comparable. Therefore, the effect of viscosity in bead formation can be ruled out.

Hence, it could be concluded that the efficiency of Triton X-100 in lowering solution surface was higher for both the blends of PSF. Triton X-100 was used in solution preparation in subsequent experiments.

4.2.5. Comparison of electrospinning performance of SPI, SPC and PSF

To compare the electrospinning performance of the two commercially available soy protein forms, SPC and SPI, and purified soy flour (PSF), they were electrospun by blending with PVA and PEO. All three forms of soy protein were prepared in 7% concentrations, and blended with 10% PVA (avg. mol. wt. 115,500 g/mol) or 5% PEO (600,000 g/mol). Figure 4.8 shows SEM micrographs of fibers spun using blends (58/42 by wt.) of (a) PSF/PEO (b) SPC/PEO (c) SPI/PEO. Electrospinning was done at a flow rate of 30 µl/min, an applied voltage of 25 KV and a needle tip-collector distance of 15 cm.

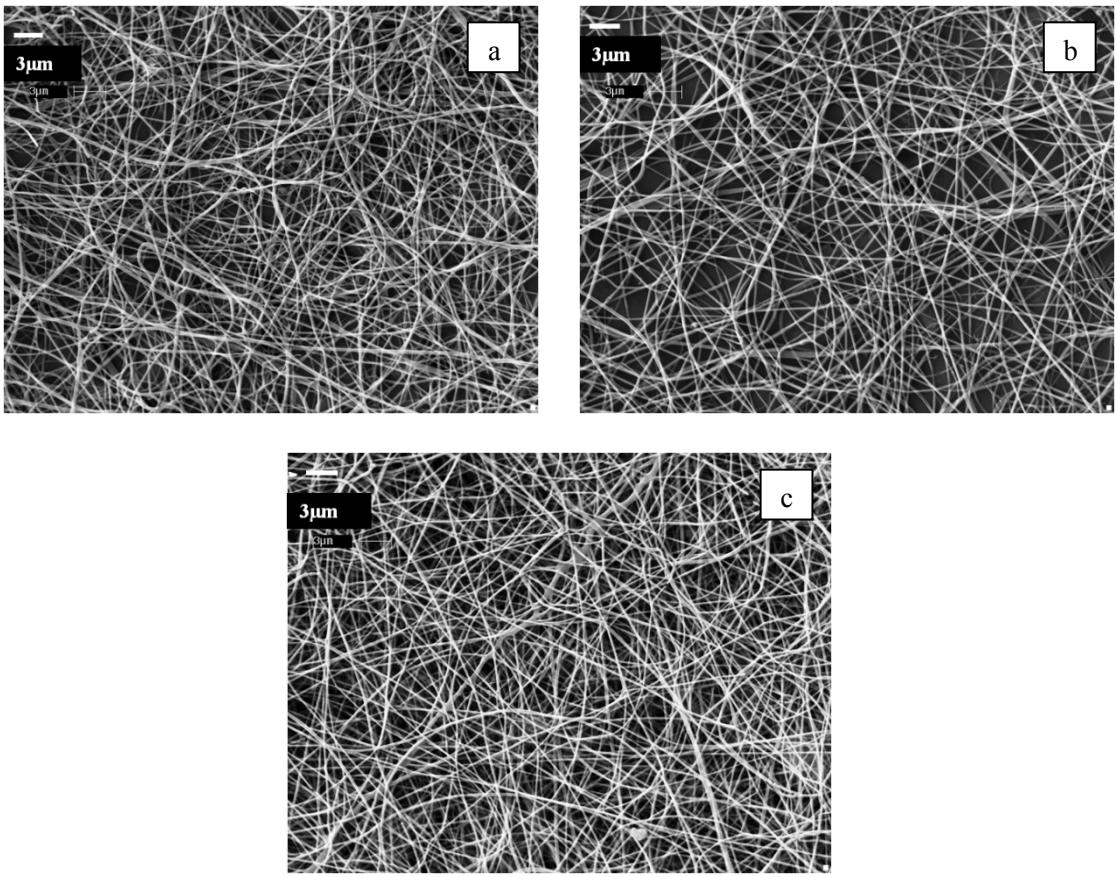

Figure 4.8: SEM micrographs of fibers spun using blends (58/42 by wt.) of (a) PSF/PEO (b) SPC/PEO (c) SPI/PEO

From Figure 4.8, it was seen that all three blends gave uniform nanofibers on electrospinning. The formation of uniform fibers in all cases, irrespective of protein content, can be attributed to the presence of high molecular weight PEO. The long polymer chains in high molecular weight PEO facilitate formation of uniform fibers on electrospinning.

PSF, SPC and SPI were also blended with PVA 115,500 g/mol in a 41/59 ratio by wt., and electrospun at a flow rate 15 µl/min, applied voltage of 25 KV and a needle tip-collector distance of 15 cm. It was observed that when 12% concentration of PVA is blended with PSF, the blend's electrospinning performance was better than in the case of 10% PVA. The formation of beads was significantly reduced with the use of a higher concentration of PVA. This is because

the blend with 10% concentration of PVA does not have adequate viscosity required for uniform fiber formation. However, SPC and SPI solutions give uniform fibers with some beads, when blended with 10% concentration of PVA. This is because the viscosity of SPI and SPC is greater than PSF, at the same concentration of each solution. Figure 4.9 shows SEM micrographs of fibers spun using 41/59 blends of (a) PSF/PVA (b) SPC/PVA (c) SPI/PVA. PVA was used in 10% concentration, whereas 7% solutions of PSF, SPC and SPI were used to prepare the blend.

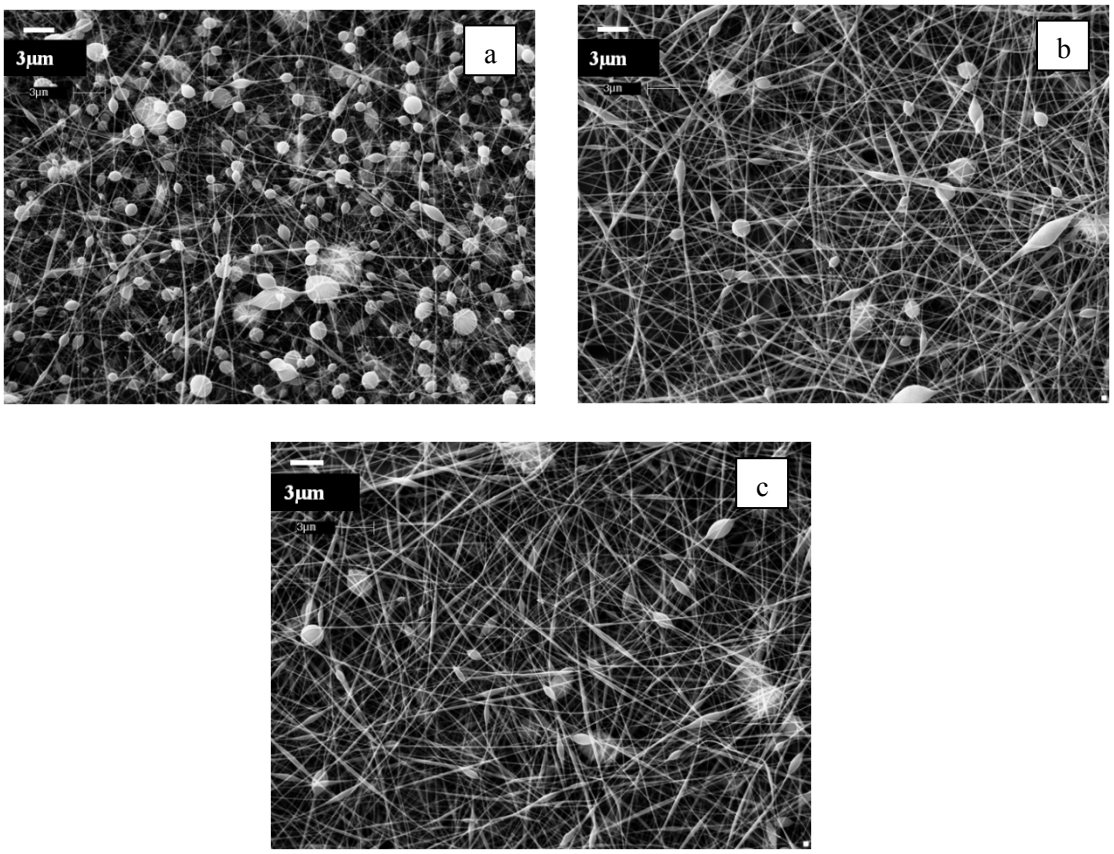

Figure 4.9: SEM micrographs of fibers spun using 41/59 blends of (a) PSF/PVA (b) SPC/PVA (c) SPI/PVA

4.2.6. Effect of molecular weight of PVA and PEO on electrospinning

Pure PVA was electrospun over a range of molecular weights, from 67,000 to 205,000 g/mol, to determine the molecular weight that gave the desired viscosity and solids content of the

electrospinning solution. As mentioned earlier, a high concentration of both soy and PVA/PEO were desired in order to maintain high solids content, and therefore, high production rate of the process. It was also desired to minimize the content of PEO/PVA in the blend as much as possible. A higher molecular weight of the polymer was preferred, since adding a small amount of the high molecular weight polymer was sufficient for uniform electrospinning of the blend.

PVA with molecular weights of 115,500 g/mol, 130,000 g/mol and 205,000 g/mol were blended with PSF and electrospun, to compare its electrospinning efficiency. It was observed that PVA 205,000 g/mol could not be used in more than 10% concentration, because the solution became very viscous. However, for PVA 130,000 g/mol, it was possible to use up to 14% concentration of the polymer. Hence, 14% of PVA 130,000 g/mol was chosen as the optimum combination of concentration and molecular weight for preparing blends with soy protein.

Similarly, PEO 300,000 g/mol, 600,000 g/mol and 900,000 g/mol were blended with PSF to determine the molecular weight most suitable for electrospinning with soy protein. It was observed that when PEO 300,000 g/mol was blended with PSF, it formed beaded fibers. However, PEO 600,000 and PEO 900,000 g/mol gave uniform fibers on electrospinning. PEO 900,000 g/mol could not be used at high concentrations because of its high viscosity. Hence, 5% concentration of PEO 600,000 was chosen as the optimum combination of concentration and molecular weight, for electrospinning with soy protein.

4.2.7. Electrospinning of PSF/PVA/PEO blends

It was attempted to overcome the problem of gelling in PSF/PVA blends at high solids content of solution, by adding PEO. Gelling was observed in PSF/PVA blends at high concentrations of PSF resulting from heavy hydrogen bonding between the two. PEO was added to the PSF/PVA blends in order to disrupt the hydrogen bonds between PSF and PVA.

It was observed that addition of PEO overcame the problem of gelling to some extent. However, it was still difficult to electrospin PSF of concentrations higher than 13% with PVA. As a result, other methods such as addition of stearic acid and SDS were tried.

4.2.8. Use of stearic acid to reduce gelling in PSF blends

Stearic acid, with long hydrocarbon chain, was used as an additive in an effort to reduce gelling in PSF blends with PVA and PEO, at high concentrations of PSF. However, stearic acid was successful only in the case of PSF/PEO blends. PSF/PVA/PEO and PSF/PVA blends could not be electrospun even with the help of stearic acid. Hence, this method was not used in subsequent experiments.

4.2.9. Effect of SDS addition to electrospinning solutions

SDS was added to solutions of SPC, in order to increase its solubility in water and increase the conductivity of the solutions by blanketing the protein chains with negative charge. It was observed that at concentration above 12%, SPC and SPI solution were difficult to blend and electrospun if SDS was not added. It was possible to electrospin a blend (88/12 by wt.) of SPC (5% concentration) with PEO 900,000 g/mol (5% concentration), by adding SDS to the SPC solution. SPC solution was prepared by dissolving it in 1% SDS solution in DI water, followed by heating and addition of NaOH to bring about protein denaturation. Figure 4.10 shows an SEM micrograph of nanofibers electrospun from 15% SPC/5% PEO600 blend. Electrospinning was done at a flow rate 30 µl/min, applied voltage 25 KV, and needle tip-collector distance of 18 cm.

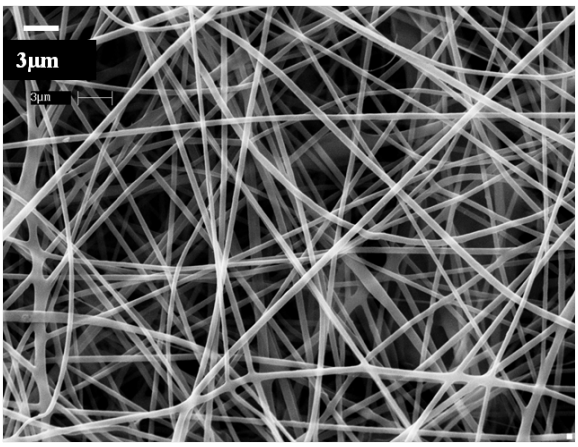

Figure 4.10: SEM micrograph of nanofibers electrospun from 15% SPC/5% PEO 600 blend

4.3. Effect of electrospinning parameters on fiber diameter

Statistical analysis was carried out using *JMP* to determine the effect of parameters concentration (C), molecular weight (M), applied voltage (V) and needle tip-collector distance (D), on fiber diameter and its distribution. A factorial experiment was designed with these parameters as factors or independent variables. Concentration and molecular weight had 2 levels each, whereas applied voltage and needle tip-collector distance had 3 levels.

The two levels of concentration of SPC solution were 10% and 12.5%. It was not possible to add a third level below 10% or above 12.5%, because SPC/PVA blends were found to give uniform fibers only in the range of 10% to 12.5% concentration of SPC solution. It was attempted to electrospin a blend (60/40 by wt.) of SPC/PVA using 8.5% concentration of SPC. However, the electrospun nanofibers consisted predominantly of beads in the 8.5% SPC/10% PVA130 blend, because of low solution viscosity. Polymer chain entanglements are necessary in order to produce uniform nanofibers. At low concentrations, chain entanglements are not sufficient to stabilize the fiber jet and the contraction of the jet driven by surface tension leads to beads or beaded fibers (Zhang et al., 2005). At SPC concentrations above 12.5%, SPC/PVA blends

cannot be electrospun because the high solution viscosity makes liquid jet formation difficult (Zhang et al., 2005).

The 2 levels of molecular weight were chosen as 130,000 g/mol and 205,000 g/mol of PVA, abbreviated as PVA130 and PVA205, respectively. The molecular weight of SPC was constant in the experiment. A concentration of 10% was used for both the molecular weights, since PVA205 becomes highly viscous at higher concentrations, as discussed in section 4.5.

Three levels of applied voltage, 22, 26 and 30 KV, were chosen for the experiment. The highest voltage that could be obtained from the high voltage source installed in the laboratory was 30 KV. The lower limit was chosen was 22 KV, because it was not possible to electrospin the blends of PVA205 with SPC at voltages below 22 KV. Strong electrostatic forces are required while electrospinning viscous solutions, in order to overcome the viscoelastic force that resists jet extension (Reneker and Yarin, 2008).

Three levels of needle tip-collector distance, 15, 18 and 21 cm, were chosen for the experiment. The lower limit was chosen as 15 cm, since incomplete solvent evaporation leading to flat fibers, was observed at smaller distances. This is because the fluid jet travels over a shorter distance before getting deposited on the collector (Bhardwaj and Kundu, 2012). The upper limit was 21 cm in this experiment, due to limitation in accurately measuring small nanofiber diameters. According to the open literature, it was expected that the fiber diameter would decrease with an increase in the needle tip-collector distance (Bhardwaj and Kundu, 2012); (Chowdhury and Stylios, 2010); (Reneker and Yarin, 2008); (Zhang et al., 2005).

Electric field, given by the ratio of applied voltage and the needle tip-collector distance, was calculated for each combination of applied voltage and needle tip-collector distance. It was used as an independent variable initially instead of using the two parameters separately. This is

because applied voltage and the needle tip-collector distance are known to act together (as electric field) in affecting the fiber diameter (Yördem et al., 2008).

Observations from all combinations of the abovementioned parameters were collected in order to determine if there was interaction among them. An interaction exists if the effect of one independent variable on the dependent variable changes depending on the level of another independent variable. A main effect, on the other hand, is the effect of one of the independent variables on the dependent variable, ignoring the effects of all other independent variables. Before testing the main effects, it is first necessary to test if any interactions exist (Trochim, 2006). In the model, interactions between any two independent variables, C and D for instance, are represented as CxD. A similar convention is followed for the higher order interactions.

In the experiment detailed above, three-way interaction CxMxE and two-way interactions CxM, CxE, MxE were first tested for significance. All three-way and two-way interactions were found to be statistically insignificant. Therefore, all interaction terms were dropped from the model and the main effects were tested.

The three-way ANOVA (analysis of variance) model for this experiment is given by the following equation (Booth, 2012):

$$\mathbf{Y_{ijklm} = \mu + C_i + M_j + E_k + \varepsilon_{ijkl}}$$

Y_{ijklm} = m^{th} response at factor combination (i,j,k)

μ = overall mean or reference level

C_i= main effect of i^{th} level of factor C, i= 1, 2

M_j = main effect of j^{th} level of factor M, j= 1, 2

V_k = main effect of k^{th} level of factor V, k= 1, 2, 3..9 and

ε_{ijklm} = random error associated with l^{th} response at levels (i, j, k)

The standard assumption of the model is that ε_{ijkl}'s are a random sample from a normal distribution with mean 0 and variance σ^2.

The results obtained from running the three-way ANOVA model gave only molecular weight and concentration as significant parameters affecting the fiber diameters. The effect of electric field was observed to be insignificant. Since it had been observed qualitatively that the needle tip-collector distance had a significant effect on fiber morphology, the analysis the repeated keeping applied voltage and needle tip-collector distance as separate parameters. Hence, statistical analysis was repeated with concentration (C), molecular weight (M), applied voltage (V) and needle tip-collector distance (D) as independent parameters in the model. Four-way interaction CxMxVxD, three-way interactions CxMxD, CxMxV, CxDxV, MxDxV, and two-way interactions CxM, CxV, CxD, MxV, MxD, VxD, were first tested for significance. All four-way and three-way interactions were found to be statistically insignificant. Only one two-way interaction, CxD, was found significant, with a p-value of 0.0416. Therefore, all other two-way and higher order interactions were dropped from the model and the main effects were tested.

The four-way ANOVA (analysis of variance) model for this experiment is given by the following equation (Booth, 2012):

$$\mathbf{Y_{ijklm} = \mu + C_i + M_j + V_k + D_l + CD_{il} + \varepsilon_{ijklm}}$$

Y_{ijklm} = mth response at factor combination (i,j,k,l)

μ = overall mean or reference level

C_i= main effect of i^{th} level of factor C, i= 1, 2

M_j = main effect of j^{th} level of factor M, j= 1, 2

V_k = main effect of k^{th} level of factor V, k= 1, 2, 3

D_l= main effect of l^{th} level of factor D, l= 1, 2, 3

CD_{il} = interaction effect for combination (i, l) and

ε_{ijklm} = random error associated with mth response at levels (i, j, k, l)

The standard assumption of the model is that ε_{ijklm}'s are a random sample from a normal distribution with mean 0 and variance σ^2.

4.3.1. Results of ANOVA

The results obtained from running the four-way ANOVA model in *JMP* are summarized in Tables 4.4, 4.5 and 4.6. Table 4.4 presents the source, degrees of freedom associated with each source (DF), the sum of squares explained by each source, mean square given as sum of squares over DF and the F-ratio given by the F-test. The F-test is used to determine if the model is successful is explaining variations in the dependent variable (fiber diameter).

Table 4.4: Analysis of Variance

Source	**DF**	**Sum of Squares**	**Mean Square**	**F-Ratio**
Model	8	22820.91	2852.61	24.88
Error	27	3095.21	114.64	Prob > F
C.Total	35	25916.12		<0.0001*

The p-value < 0.0001 in Table 4.4 indicates that the model is successful in explaining a majority of the variation in fiber diameter, that is, at least one of the independent variables in the model has a significant effect on the fiber diameter.

The parameter estimates are given in Table 4.5. When these estimates are fitted in the model, the estimated average diameter for some combination of M, C, V and D, can be calculated.

Table 4.5: Parameter Estimates

Term	Estimate	Std. Error	t Ratio	Prob>|t|
Intercept	160.53	1.78	89.96	<0.0001*
Mol.wt [130]	-20.14	1.78	-11.29	<0.0001*
Concentration [10]	12.90	1.78	7.23	<0.0001*
Voltage [22]	1.32	2.52	0.52	0.6042
Voltage [26]	1.98	2.52	0.79	0.4381
Distance [15]	7.50	2.52	2.97	0.0061*
Distance [18]	-0.95	2.52	-0.38	0.7091
Distance [15]*Concentration [10]	-2.44	2.52	-0.97	0.3419
Distance [18]*Concentration [10]	-4.23	2.52	-1.68	0.1047

For example, using the parameter estimates obtained from *JMP*, the average diameter of a 10% SPC/PVA 130 blend electrospun at an applied voltage of 22 KV and a needle tip–collector distance of 15 cm can be estimated by fitting the corresponding parameter estimates in the ANOVA model.

Estimated Dia. = 160.53 - 20.14 + 12.90 + 1.32 + 7.50 - 2.44

Estimated Dia. = 159.67

Thus, the average diameter of a 10% SPC/PVA 130 blend electrospun at an applied voltage of 22 KV and a needle tip –collector distance of 15 cm, was estimated to be 159.67 nm by the ANOVA model.

Table 4.6: Effect Tests

Source	Nparm	DF	Sum of Squares	F Ratio	Prob > F
Mol.wt	1	1	14602.71	127.38	<0.0001*
Concentration	1	1	5994.63	52.29	<0.0001*
Voltage	2	2	199.81	0.8	0.4298
Distance	2	2	1201.41	5.24	0.0119*
Distance*Concentration	2	2	822.35	3.59	0.0416*

The effect of every independent variable and the interaction terms is given in Table 4.6. The table presents the source, the number of parameters associated with it (Nparm, (number of levels in the factor-1)), the corresponding degrees of freedom (number of levels in the factor-1), the sum of squares explained by each source, the F-ratio given by the F-test, and the p-value.

The effect of the independent variables and the interaction terms is given by their corresponding p-value. For instance, molecular weight has a p-value < 0.0001, which indicates that molecular weight has a significant effect on fiber diameter. The lower the p-value, the more significant the parameter is.

4.3.2. Effect of needle tip-collector distance (D) and solution concentration (C)

Since C and D have an interaction, the main effect of D is measured by comparing difference between its levels for the same value of C. For instance, the differences between 15, 18 and 21 cm (levels of needle tip-collector distance) were compared for the 12.5% concentration solutions, ignoring the effect of molecular weight and voltage. Similarly, the differences between 15, 18 and 21 cm were compared for 10% concentration solutions, ignoring the effect of molecular weight and voltage. Figure 4.11 illustrates graphically the interaction effect of concentration (C) and distance (D).

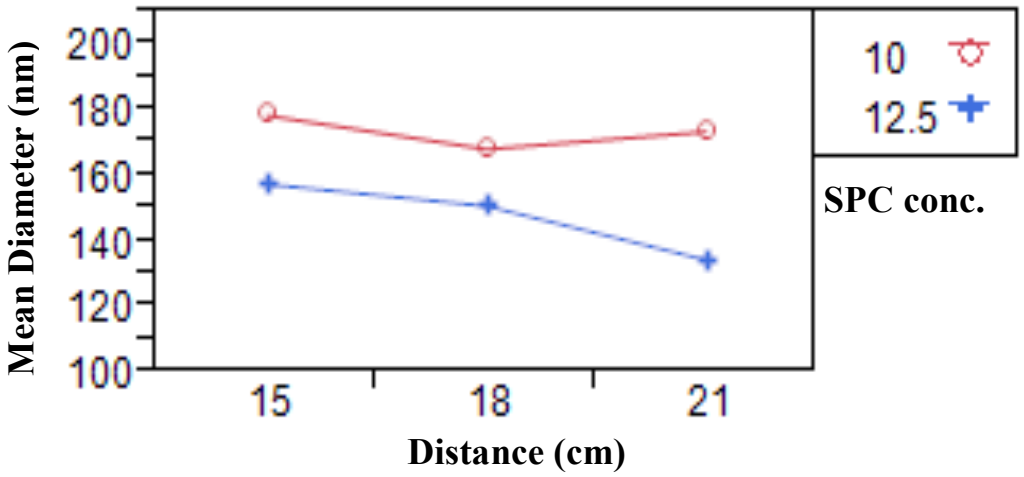

Figure 4.11: Interaction effect of concentration (C) and distance (D)

As evident from the graph in Figure 4.11, the effect of distance on fiber diameter is different for different concentrations of SPC in the blend. For the 12.5% blends of SPC, fiber diameter decreased as the needle tip-collector distance increased. This is because the fluid jet undergoes whipping motion, caused by bending instability over a larger distance. It is this region where the jet diameter reduces by several orders of magnitude (Reneker and Yarin, 2008). Moreover, at high concentrations of SPC, branching of the primary jet into secondary jets is commonly observed (Reneker and Yarin, 2008). This also causes a reduction in the average fiber diameter. The distribution of fiber diameter was analyzed using *JMP*. The 12.5% concentration solutions of SPC produce bimodal and trimodal distributions of fiber diameter, which is caused by branching. A bimodal distribution was also observed by Dietzel et al. at high concentrations of PEO (400,000 g/mol) in water (Dietzel et al., 2001). The appearance of a bimodal distribution is attributed to branching or splaying of the primary jet into more stable secondary jets. The secondary population of fibers were observed to have diameters about one third of those in the primary population (Dietzel et al., 2001).

Reneker and Yarin have also reported the formation of branches when the jet diameter was relatively large (Reneker and Yarin, 2008). This phenomenon was observed to occur more frequently in concentrated and viscous solutions, and at electric fields higher than the minimum field required for the production of a single jet (Reneker and Yarin, 2008).

The histograms in Figure 4.12 show distribution of fiber diameter (nm) of 12.5% SPC/10% PVA 205 (left) and 12.5% SPC/10% PVA 130 (right), both electrospun at a 15 cm needle tip-collector distance and 22 KV voltage. The top part of the histograms represents the quantiles, and the dots represent the outliers in the data.

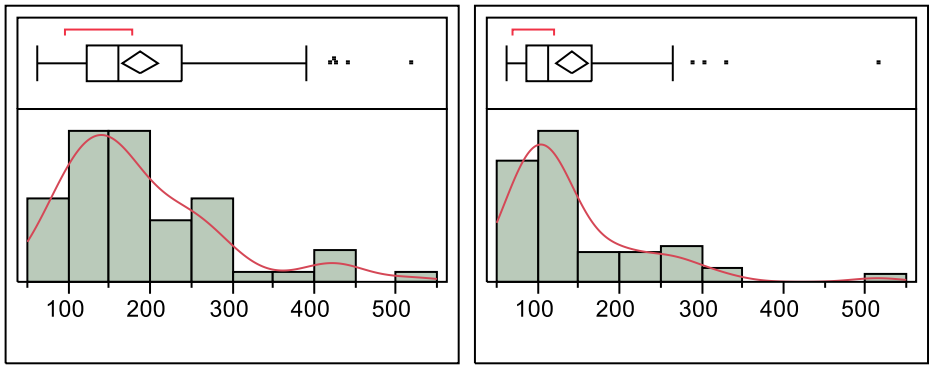

Figure 4.12: Distribution of fiber diameter (nm) of 12.5% SPC/10% PVA 205 (left) and 12.5% SPC/10% PVA 130 (right)

The histogram for the 12.5% SPC/10% PVA 205 blend seems to have 2 modes, one at approx. 150 nm and the other at 425 nm. The mean and percent coefficient of variation (CV) values of the distribution were 188.4 nm and 50.8% respectively. The 12.5% SPC/10% PVA 130 blend also showed a bimodal distribution, with modes at 100 and 250 nm. The mean and CV values of the distribution were 141.95 nm and 56.3% respectively. The results are in agreement with Dietzel's observation that the secondary population of fibers has diameters one third of those in the primary population (Dietzel et al., 2001). Figure 4.13 shows branching and splitting in a

12.5% SPC/10% PVA 205 blend. The solution was electrospun at 22 KV and a needle tip-collector distance of 18 cm. The mean and CV of the diameter distribution were 167.77 nm and 35.3% respectively.

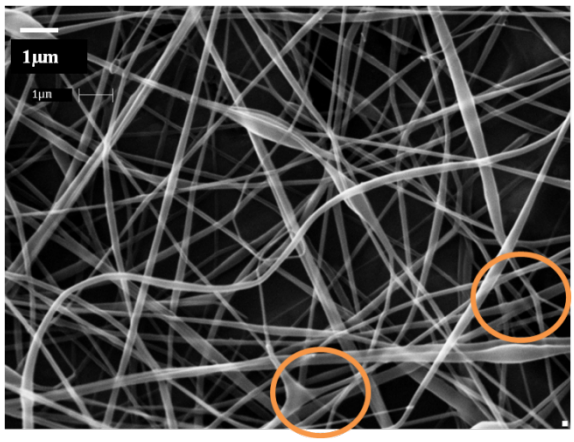

Figure 4.13: Branching and splitting in a 12.5% SPC/PVA 205 blend

The solutions of 10% SPC with PVA showed a reduction in fiber diameter as needle tip-collector distance increased from 15 cm to 18 cm, followed by an increment at 21 cm. The average diameter at 15 cm was 178.5 nm. It was reduced to 168.3 nm at 18 cm, and then increased to 173.6 nm at 21 cm. However, the diameter followed a downward trend with an increase in the needle tip-collector distance. This is because the 10% SPC/10% PVA 130 blend forms beaded fibers at 15 cm. At small distances, the jet cannot elongate, leaving beads and spindle-like fibers (Bhardwaj and Kundu, 2010). Moreover, for the 10% SPC/10% PVA 130 blend, the surface tension dominates over the viscoelastic force, favoring bead formation in the fibers. At larger distances, the jet elongates before getting deposited on the collector. Thus, the average diameter decreases. However, the electrostatic force is reduced with an increase in distance, which accounts for the slight increase in average diameter at 21 cm. The electrostatic force stretches the jet because of mutual repulsion between like charges on the jet surface, which leads to a reduction in jet diameter. Since the viscosity of the 10% SPC/10% PVA 130 solution is not

very high (1.13 Pa.s), changes in electrostatic force become a dominant factor in the determination of fiber diameter.

Figure 4.14 shows 10% SPC/10% PVA 130 solution electrospun at a needle tip-collector distance a) 15 cm b) 18 cm c) 21 cm. There is a reduction in beads as the needle tip-collector distance is increased progressively from 15 cm to 21 cm.

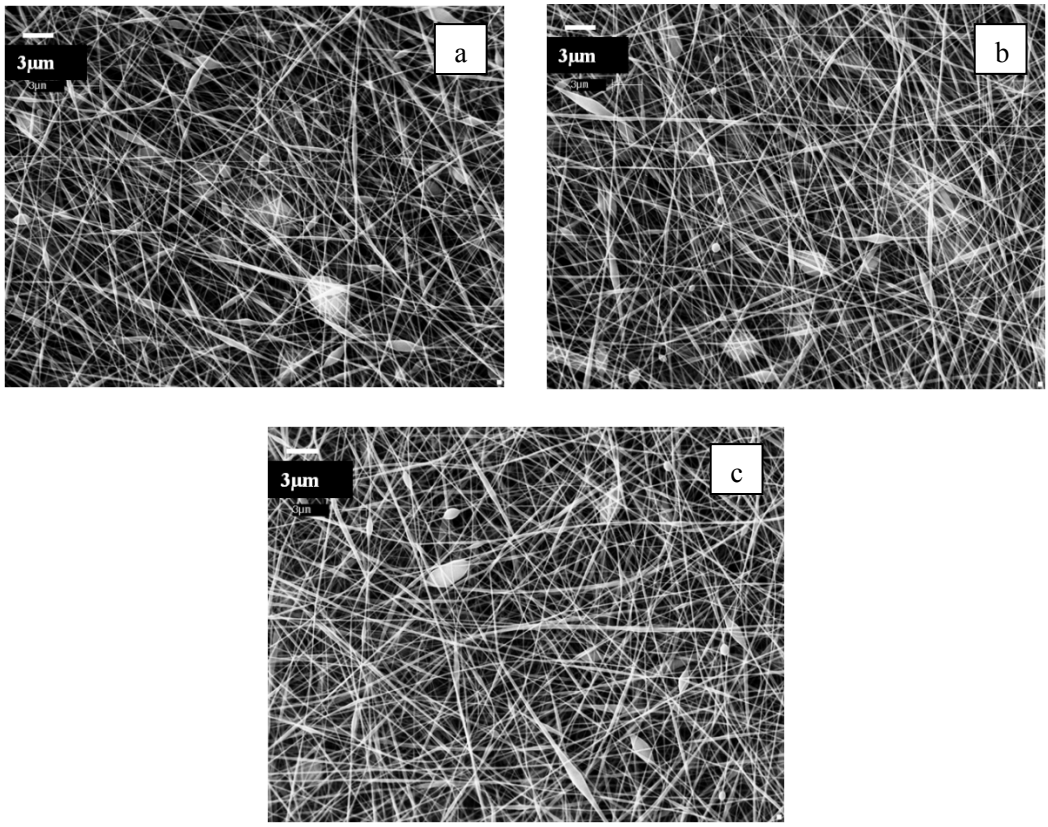

Figure 4.14: 10% SPC/10% PVA 130 solution electrospun at a needle tip-collector distance a) 15 cm b) 18 cm c) 21 cm

The 10% SPC/10% PVA 205 blend also forms more uniform fibers when the needle tip-collector distance is increased, especially at higher applied voltages. A high voltage is required to provide adequate electrostatic repulsion force to overcome the viscoelastic force in the electrospinning of viscous solutions. Figure 4.15 shows SEM micrographs of 10% SPC/10%

PVA 205 blends, electrospun at 15 cm (a), 18 cm (b) and 21 cm (c), keeping the voltage constant at 26 KV. It was observed that flat fibers were obtained at needle tip-collector distance of 15 cm. At 18 cm, large beads and spindle-like fibers were electrospun, whereas at 21 cm, the number and size of beads got reduced and uniform fibers were electrospun. The formation of flat fibers is due to insufficient solvent evaporation at small needle tip-collector distances. Koski et al. also observed formation of flat fibers of PVA as the molecular weight was increased (Koski et al., 2004).

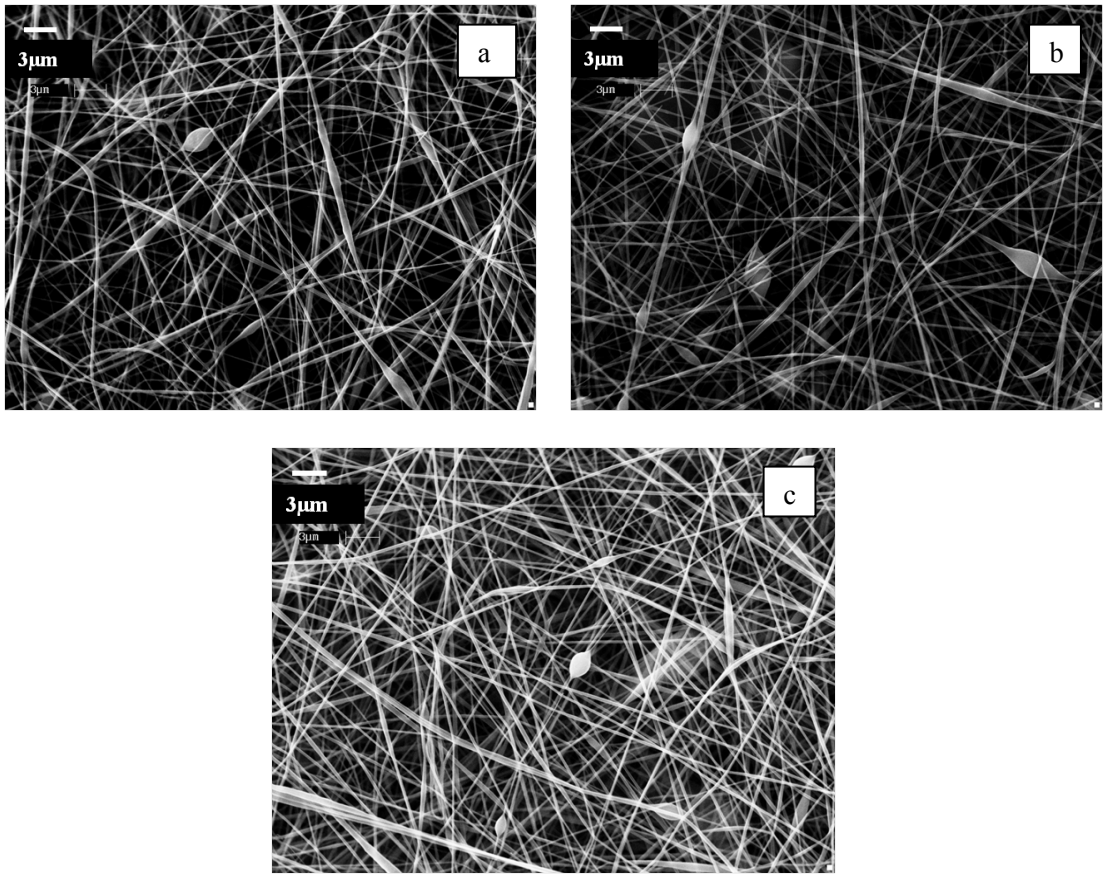

Figure 4.15: 10% SPC/10% PVA 205 blends, electrospun at needle tip-collector distances of 15 cm (a), 18 cm (b) and (c) 21 cm

As the concentration of SPC was increased from 10% to 12.5%, the distribution of fiber diameter became larger. This is because of the branching and other defects that are introduced at high

solution concentrations and viscosities (Reneker and Yarin, 2008). Figure 4.16 shows the distribution of fiber diameter of 10% SPC/10% PVA 205 (left) and 12.5% SPC/10% PVA 205 (right), both electrospun at 15 cm and 22 KV.

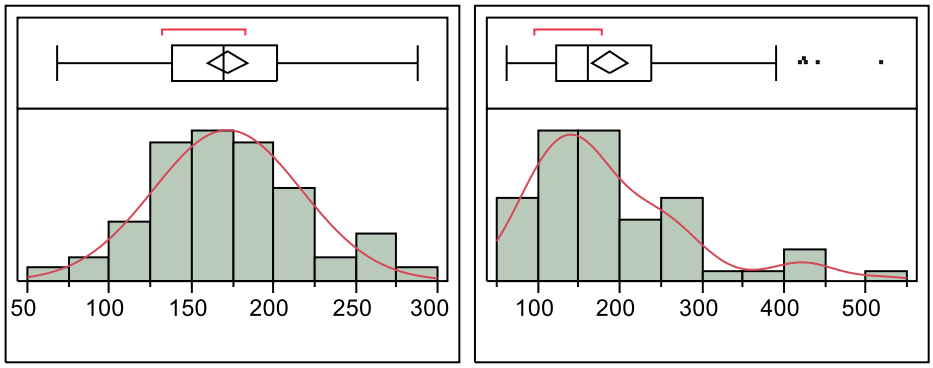

Figure 4.16: Distribution of fiber diameter (nm) of 10% SPC/10% PVA 205 (left) and 12.5% SPC/10% PVA 205 (right), both electrospun at 15 cm and 22 KV

The 10% SPC/10% PVA 205 blend resulted in a normal distribution, with mean fiber diameter of 171.8 nm and CV of 26.8 %. The 12.5% SPC/10% PVA 205 resulted in a bimodal distribution, with a mean of 188.4 nm and much higher CV of 50.7%.

4.3.3. Effect of molecular weight (M)

The main effect of molecular weight was found to be statistically significant with a p-value of < 0.0001. It was observed that the fiber diameter increased significantly when PVA molecular weight was increased from 130,000 g/mol to 205,000 g/mol, as shown graphically in Figure 4.17.

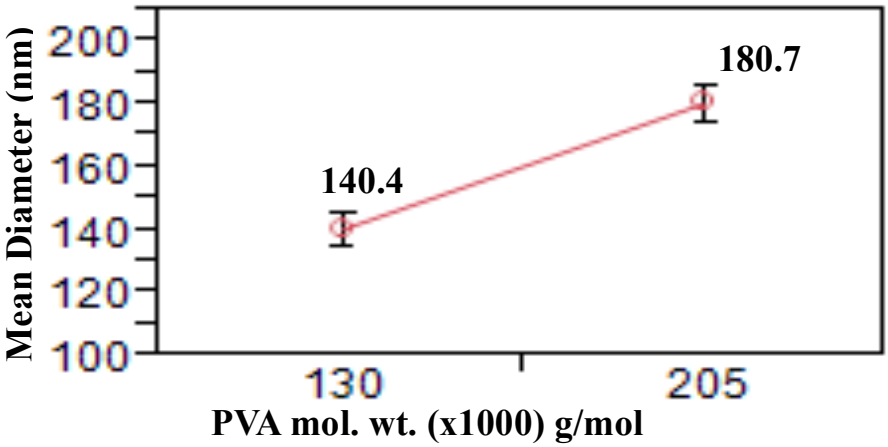

Figure 4.17: Effect of molecular weight of PVA on fiber diameter

The increase in diameter is due to increased chain entanglements at higher molecular weights, which increase the solution viscosity. The increased viscosity in turn increases the viscoelastic force, which resists jet elongation (Mit-uppatham, 2004). Moreover, at higher viscosities, the fluid jet follows a straight trajectory over a longer distance before undergoing bending instability, further increasing the diameter (Mit-uppatham, 2004). Therefore, the fiber diameter increases when PVA 205,000 g/mol is used instead of PVA 130,000 g/mol. Figure 4.18 shows SEM micrographs of fibers electrospun using 10% SPC/10% PVA 130 (a) and 10% SPC/10% PVA 205 (b), at a voltage of 22 KV and a needle tip-collector distance of 21 cm. It can be observed that there is a significant reduction in the number of beads when the molecular weight is increased. This is also explained by the fact that surface tension dominates at lower viscosities, leading to bead formation and spindle-like fibers as shown in red circles.

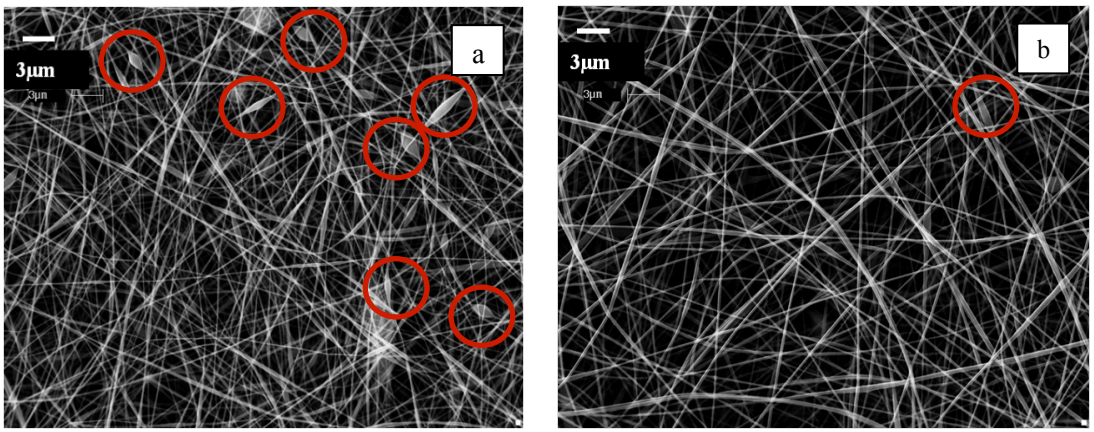

Figure 4.18: SEM micrographs of fibers electrospun using 10% SPC/10% PVA 130 (a) and 10% SPC/10% PVA 205 (b), at a voltage of 22 KV and a needle tip-collector distance of 21 cm

4.3.4. Effect of applied voltage (V)

Voltage had a p-value of 0.429, which is insignificant at a 5% level of significance. This is because two opposing forces are at play when the voltage is increased. Firstly, material coming out of the needle reaches the collector faster when voltage increases because of the higher potential bias. This increases the fiber diameter since the number of fibers getting deposited on the collector per unit times is not affected, but the material reaching the collector increases. However, at the same time, electrostatic repulsion between like charges on the jet surface increases. This favors jet stretching and a corresponding reduction in fiber diameter (Zhang et al., 2005). Hence, no clear trend can be inferred from the experiments in this study. Figure 4.19 illustrates graphically the effect of applied voltage on average fiber diameter.

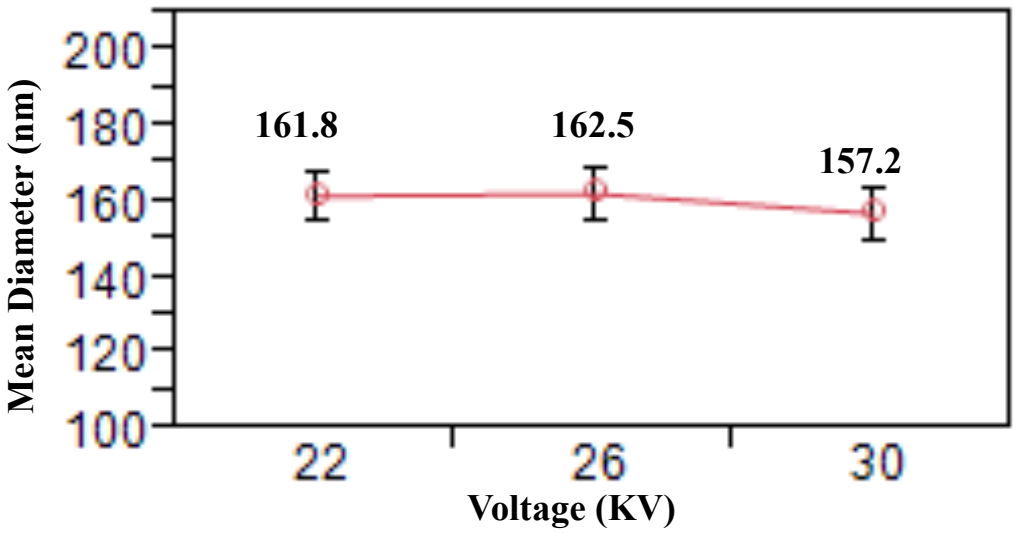

Figure 4.19: Effect of applied voltage on average fiber diameter

Because of the two opposing factors discussed above, researchers have reported both an increase as well as decrease in average fiber diameter with increase in electric field (Zhang et al., 2005); (Yördem et al., 2008). Electric field is calculated as a ratio of applied voltage to needle tip-collector distance. Zhang et al. have reported a slight increase in average fiber diameter with increasing applied electric field (Zhang et al., 2005). They have also reported a widening of the fiber diameter distribution with increasing applied voltage (Zhang et al., 2005). Hence, the effect of voltage has to be considered in conjunction with the needle tip-collector distance. Moreover, Yordem et al. have reported that the effect of voltage also varies with the solution concentration (Yördem et al., 2008). They observed that the applied voltage was an insignificant factor when the solution concentration was high. However, at low solution concentrations and needle tip-collector distances, voltage becomes an important parameter in controlling the fiber diameter. Similar results were reported by Baumgarten (Baumgarten, 1971) and Fennessey (Fennessey and Farris, 2004) for electrospun PAN, and Sukigara et al. (Sukigara et al., 2004) for electrospun

Bombyx silk fibers.

Figure 4.20 shows 10% SPC/10% PVA 205 electrospun at a needle tip-collector distance of 21 cm, applied voltages of (a) 22 KV, (b) 26 KV (b) and (c) 30 KV.

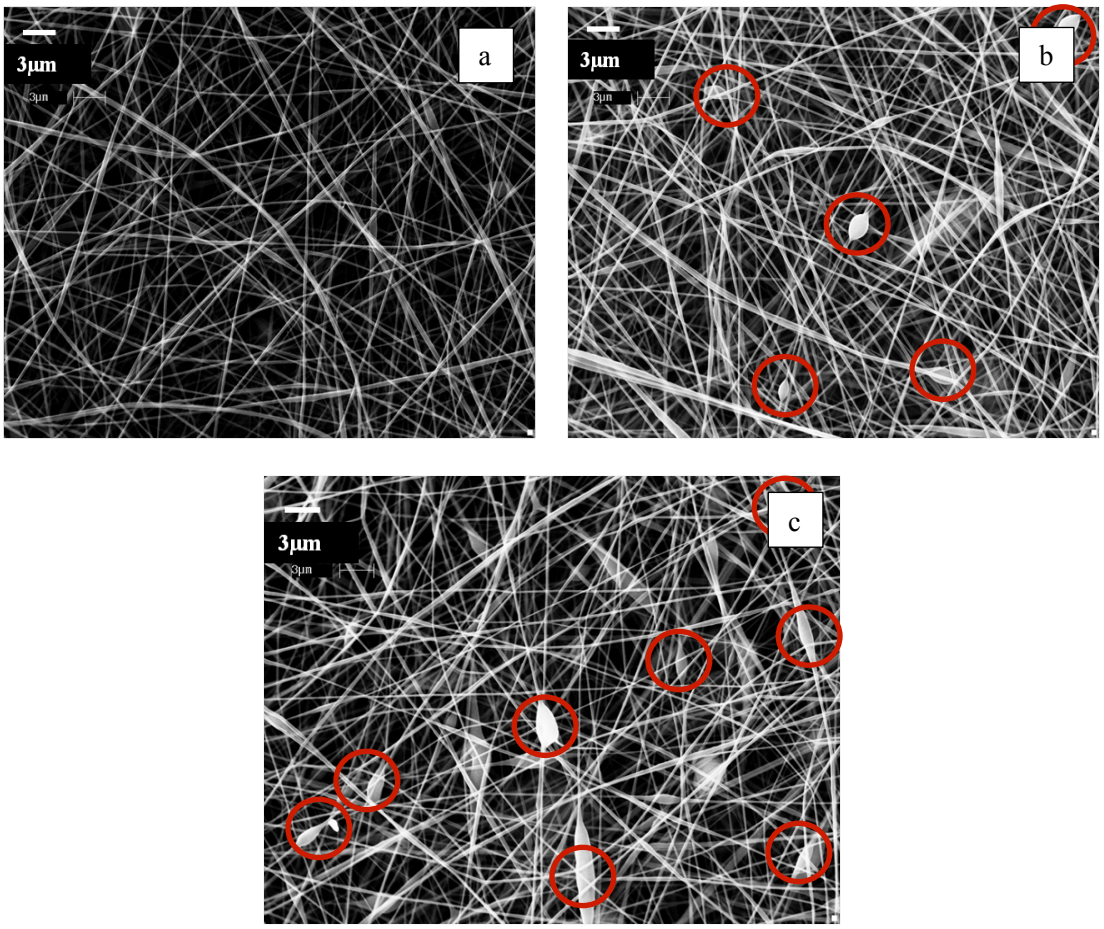

Figure 4.20: 10% SPC/10% PVA 205 electrospun at a needle tip-collector distance of 21 cm, applied voltages of (a) 22 KV, (b) 26 KV (b) and (c) 30 KV

A comparison of the nanofiber membranes at the three voltages shows that bead formation increased as the voltage is increased. Also, the distribution of fiber diameter became larger. This result is in agreement with Zhang's observation that the diameter distribution becomes wider at higher applied voltages (Zhang et al., 2005). The distributions of fiber diameter for the 10% SPC/10% PVA 205 blends electrospun at a needle tip-collector distance of 21 cm, and

voltages of 22 KV (left) and 30 KV (right) are shown in Figure 4.21. The increase in spread of the diameter distribution is attributed to increased jet instability. When the voltage is increased to a certain level, the shape of the pendant drop from which the jet originates, changes. This leads to jet instability (Chowdhury and Stylios, 2010).

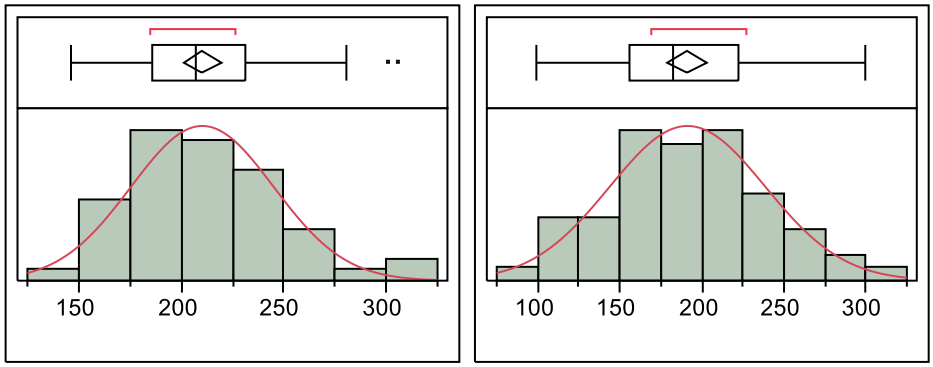

Figure 4.21: Distributions of fiber diameter for the 10% SPC/10% PVA 205 blends electrospun at a needle tip-collector distance of 21cm, and voltages of 22 KV (left) and 30 KV (right)

The 10% SPC/10% PVA 205 blend electrospun at 22 KV resulted in a normal distribution with mean fiber diameter of 210.29 nm and CV of 16.5%. The 10% SPC/10% PVA 205 blend electrospun at 30 KV also resulted in a normal distribution with mean fiber diameter of 191.28 nm and CV of 24.8%.

4.3.5. Effect of solution flow rate

Blends of SPC with PVA were electrospun at three flow rates of 15 µl/min, 20 µl/min and 30 µl/min, to determine the effect of flow rate on fiber diameter and fiber morphology. Figure 4.22 shows graphically the effect of solution flow rate on the average fiber diameter. The flow rate was found to have a statistically significant effect on fiber diameter, with a p-value of 0.025.

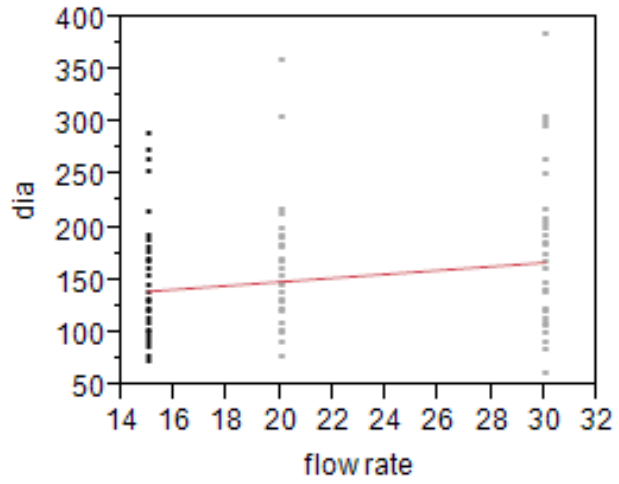

Figure 4.22: Effect of solution flow rate on the average fiber diameter

Figure 4.23 shows SEM of a 10% SPC/10% PVA 130 solution electrospun at an applied voltage of 22 KV, needle tip-collector distance of 15 cm and flow rates of (a) 15 µl/min, (b) 20 µl/min and (c) 30 µl/min.

From the figure, it can be seen that the nanofibers electrospun at flow rates of 15 and 30 µl/min have more defects, whereas nanofibers electrospun at 20 µl/min flow rate show uniform fiber formation. The solution electrospun at 30 µl/min formed somewhat flat fibers, which is due to incomplete solvent evaporation before being deposited on the collector. At high solution flow rates, incomplete solvent evaporation takes place if the rate at which material leave the needle tip exceeds the rate at which it reaches the collector. Hence, fibers become flat when they deposit on the collector in a wet state. On the other hand, at low solution flow rates, solvent evaporation starts taking place at the needle tip, which increases solution viscosity and leads to needle clogging (Bhardwaj and Kundu, 2010); (Chowdhury and Stylios, 2010). Hence, an optimal solution flow rate is needed to obtain uniform fibers.

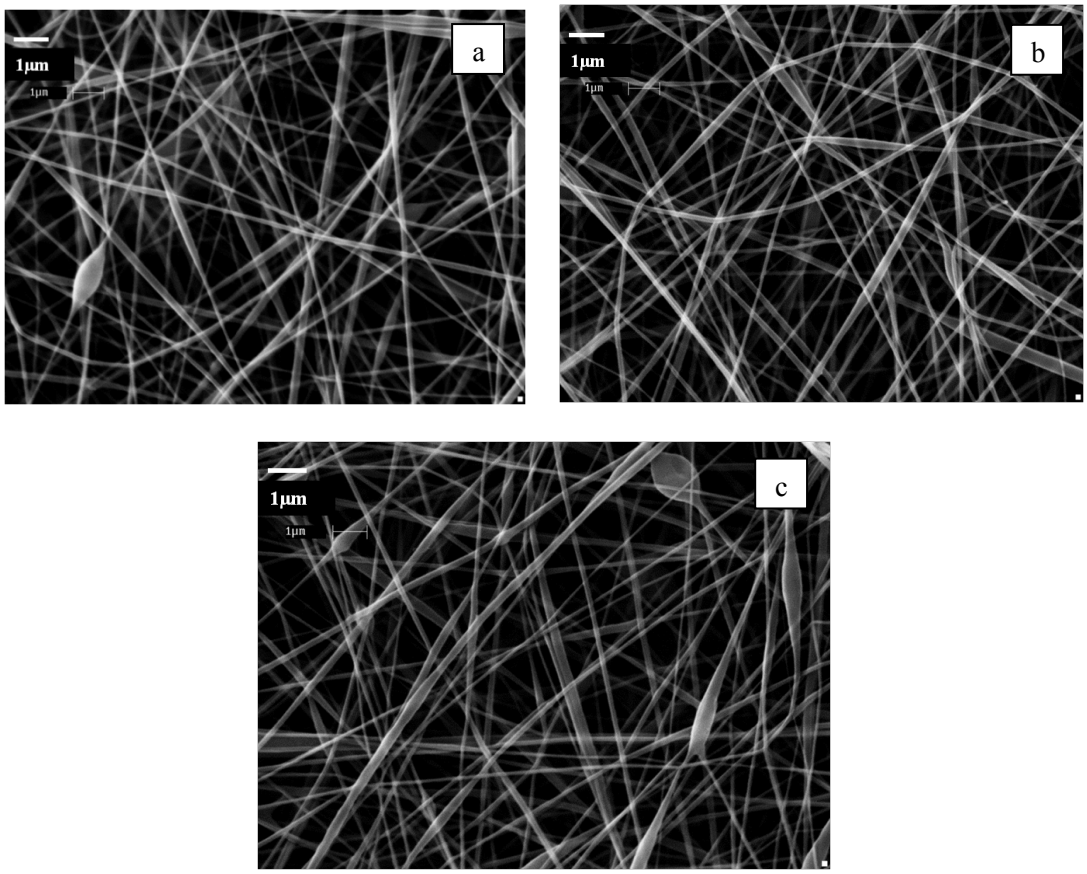

Figure 4.23: SEM of 10% SPC/10% PVA 130 solution electrospun at an applied voltage of 22 KV, needle tip-collector distance of 15 cm, and flow rates of (a) 15 µl/min, (b) 20 µl/min and (c) 30 µl/min

4.4. Measurement of solution viscosity

The viscosity measurements for 600,000 and 900,000 g/mol of PEO as a function of concentration are shown in Figure 4.24. PEO showed a shear thinning behavior over the range of concentrations tested for each molecular weight.

The viscosity decreases as a function of the shear rate (Rodriguez, 2003). A power law model was used to fit the data obtained from viscosity measurements on a Rheometer. According to power law, the shear stress (τ) and apparent viscosity (μ) are given by equations 4.1 and 4.2

(Rodriguez et al., 2003). The constant K is the flow consistency index and $\frac{\partial u}{\partial y}$ is the shear rate or the velocity gradient perpendicular to the plane of shear.

$$\tau = K\left(\frac{\partial u}{\partial y}\right)^{n} \tag{4.1}$$

$$\mu = K\left(\frac{\partial u}{\partial y}\right)^{n-1} \tag{4.2}$$

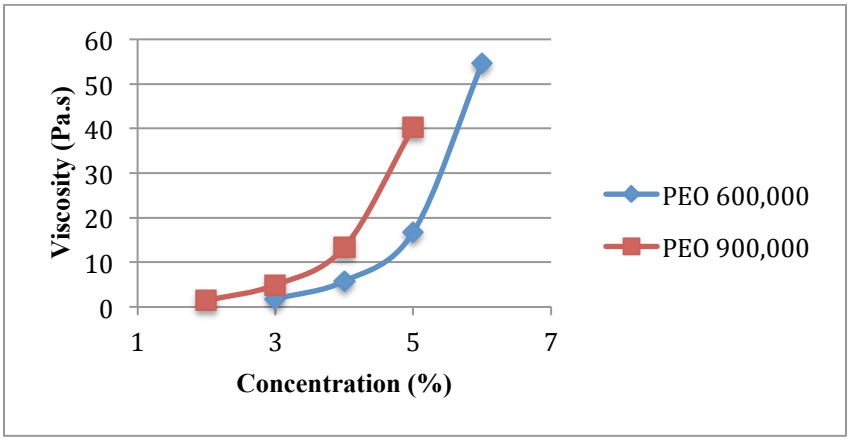

Figure 4.24: Viscosity of 600,000 and 900,000 g/mol of PEO as a function of concentration

Similarly, the viscosity of PVA 130 and PVA 205 was measured over a range of concentrations. PVA also shows shear thinning behavior. However, the lower concentrations have a slightly Newtonian behavior, that is, the viscosity stays almost constant over the range of shear rates tested. A comparison of the viscosities of PVA 130 and PVA 205 is shown graphically in Figure 4.25.

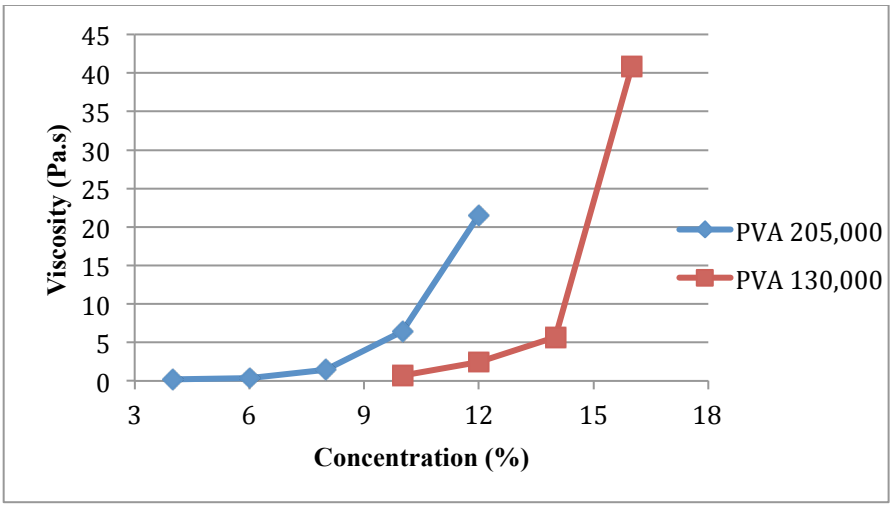

Figure 4.25: Comparison of the viscosities of PVA 130 and PVA 205

The viscosity of SPC/PVA blends, which were used for determining the effect of electrospinning parameters on fiber diameter, was also measured. The viscosity was measured in order to determine the range of viscosities that could give uniform fibers for the 60/40 SPC/PVA blends. The viscosities of the blends are given in Table 4.7.

Table 4.7: Viscosities of SPC/PVA blends

Blend type	Viscosity (Pa.s)
10% SPC/ 10% PVA 130	1.13
12.5% SPC/ 10% PVA 130	3.96
10% SPC/ 10% PVA 205	9.30
12.5% SPC/ 10% PVA205	27.72

It can be inferred from the viscosity data that SPC/PVA blends with viscosity in the range of 3 to 10 Pa.s can be electrospun to form uniform fibers. The 10% SPC/10% PVA 130, with a viscosity 1.13 Pa.s resulted in a number of beads primarily because of low solution viscosity. The upper electrospinnable limit of viscosity for SPC/PVA blends cannot be inferred from the viscosity data, since the 12.5% SPC/10% PVA 205 did not produce uniform nanofibers.

The viscosity range for uniform fiber formation during electrospinning varies from one polymer to another (Bhardwaj and Kundu, 2010). Researchers have reported maximum spinning

viscosities ranging from 1 to 215 Pa.s (Baumgarten, 1971); (Doshi and Reneker, 1995); (Deitzel et al., 2002); (Buchko et al., 1999). Fong et al. studied nanofiber formation at different viscosities of PEO, and found that a range of viscosity between 1 and 20 Pa.s to be suitable for production of uniform nanofibers by electrospinning (Fong et al., 1999).

The SEM micrographs of the four blends presented in Table 4.7 showed uniform fiber formation in the 10% SPC/10% PVA 205 blend followed by uniform fibers with some beads for the 10% SPC/10% PVA 130 blend. The 12.5% blends showed large number of beads, and flat fibers due to incomplete solvent evaporation for 12.5% SPC/10% PVA 205 blend. Figure 4.26 shows SEM micrographs of fiber electrospun from (a) 10% SPC/10% PVA 130 (b) 10% SPC/10% PVA 205 (c) 12.5% SPC/10% PVA 130 (d) 12.5% SPC/10% PVA205, electrospun at a voltage of 22 KV and a needle tip-collector distance of 15 cm. It can be seen from the SEM micrographs in Figure 4.26 that there was a significant increase in the number of beads at 12.5% concentration of SPC.

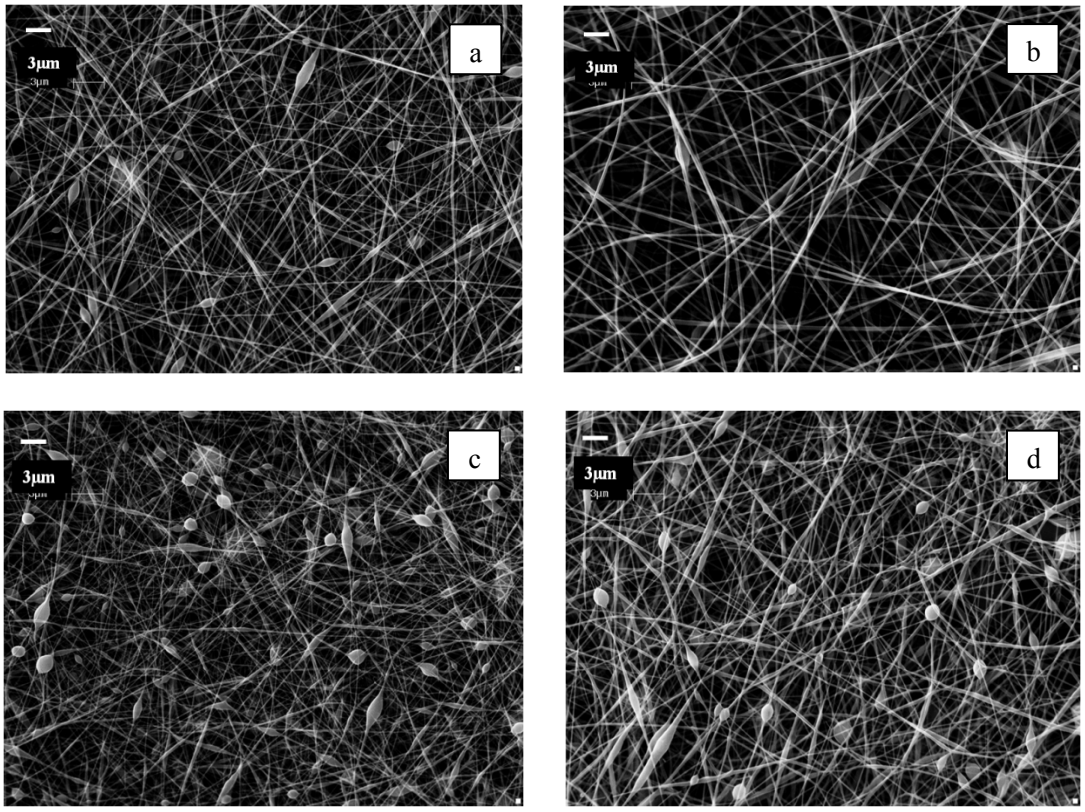

Figure 4.26: SEM micrographs of fiber electrospun from (a) 10% SPC/10% PVA 130 (b) 10% SPC/10% PVA 205 (c) 12.5% SPC/10% PVA 130 (d) 12.5% SPC/10% PVA 205, electrospun at a voltage of 22 KV and a needle tip-collector distance of 15 cm

The expected viscosity calculated from adding the viscosities of the constituents in the ratio of the blends, was compared with the actual viscosity obtained from rheometer measurements. Figure 4.27 shows the actual viscosity plotted against the expected value.

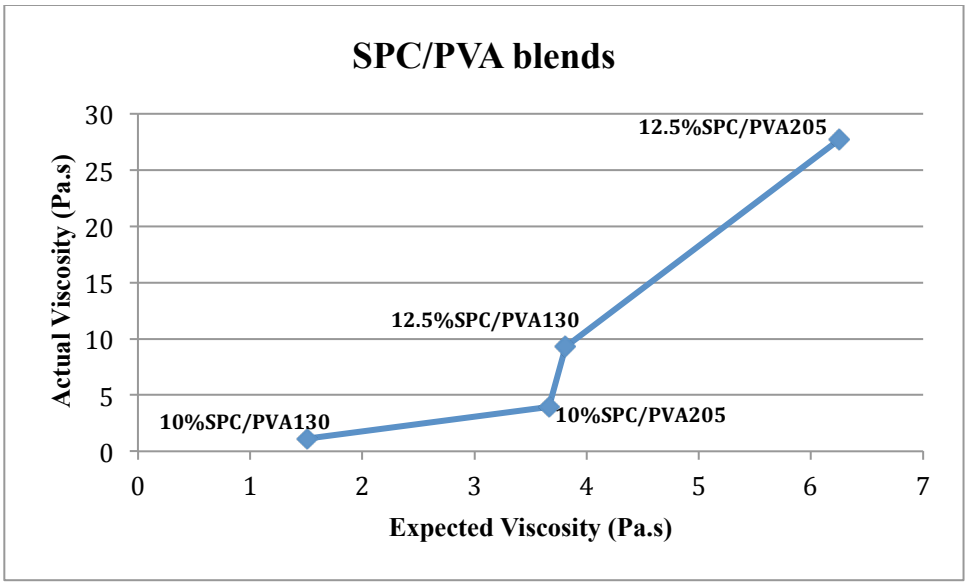

Figure 4.27: Actual viscosity plotted against the expected value

From the plot, it can be inferred that the actual viscosity values of the 12.5% blends of SPC were much higher than the expected values, resulting from significant hydrogen bonding that exists between PVA and SPC. Due to the increased hydrogen bonding, the solution surface tension also increases. Increased surface tension in the 12.5% blends of SPC could also be responsible for the extensive beading in both the blends (Fong et al., 1998).

4.5. Experiment with wire mesh and hot plate

It was observed that at high concentrations of SPC blend solutions, flat fibers were getting deposited on the collector because of incomplete solvent evaporation. Several researchers have observed similar behavior at high concentrations and molecular weights of polymer solutions (Reneker and Yarin, 2008); (Mit-uppatham et al., 2004). In order to increase the rate of drying of fluid jet during its flight, heat and air flow were used. The temperature inside the hood in which the electrospinning setup is installed, was raised to 30^0C by keeping a hot plate in the vicinity of the setup. The hot plate served the purpose of increasing ambient temperature, and also reduced the humidity in the hood, which was favorable for solvent evaporation. In

other experiments, a commercial hair dryer was used to supply hot air to the collector. A spun bonded fabric (pore size 50 μm) was taped to the wire mesh collector, to serve as a substrate for nanofiber deposition. A porous substrate was used in order to allow hot air blown from the other side of the wire mesh to pass through the fabric. The arrangement of the hot plate and hair dryer has been discussed earlier in section 3.7. The hot air was blown in a direction opposite to the path of the jet, to delay the deposition of nanofibers and allow solvent evaporation as well as to provide more time for drying up by slowing the deposition speed.

It was observed that these efforts were insufficient and the fibers were still wet while depositing on the wire mesh collector, as shown by the flat fibers in Figure 4.28 (a). Hence, the needle tip-collector distance was increased from 17 cm (a) to 22 cm (b).

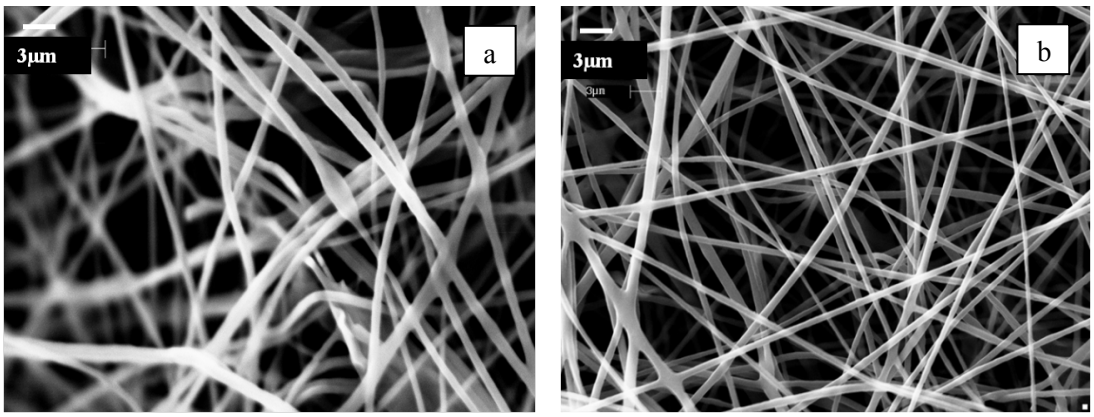

Figure 4.28: Nanofibers obtained from the wire mesh and hair dryer arrangement at needle tip-collector distance of (a) 17 cm (b) 22 cm

It can be observed from the flatness of the nanofibers in Figure 4.28 that the hot plate and dryer together were not enough to dry the nanofibers fully. The presence of flat fibers and their web-like appearance indicates that they had not dried up completely before depositing on the collector. At high concentrations of SPC/PEO, non-ionic bonds form between the two polymers, making the exit of water difficult from the jet surface. Moreover, the presence of long chains of

high molecular weight PEO makes the evaporation of solvent more difficult (Koski, 2004). At high concentrations, jet stretching is also limited because of which the jet surface area doesn't increase as significantly as in the case of lower concentrations. This also limits the evaporation of solvent.

Zeng et al. have also used a heater to increase the ambient temperature to 25^0C, and therefore increase solvent evaporation during electrospinning of poly(l-lactide) (PLLA) and poly(caprolactone) (PCL) solutions (Zeng et al., 2002). However, they obtained coiled and entangled nanofibers in the presence of a heater. They concluded that this morphology of nanofibers was due to air circulation inside the cabinet in the presence of a heater.

4.6. Strength of nanofiber membranes

Nanofiber membranes electrospun from blends of SF, SPC and SPI with PEO, were tested on Instron to measure their mechanical (tensile) properties. Membranes (gauge length 10 mm, width 5 mm) were attached to a paper window, which was mounted between the clamps of Instron. The paper window was used to facilitate the clamping of the membranes, and ensure accurate measurements of tensile strength and modulus.

The stress, strain and Young's modulus of the membranes electrospun from blends of SF, SPC and SPI with PEO, are presented in Table 4.8.

Table 4.8: Tensile properties of nanofiber membranes of soy with PEO

Nanofiber Membrane type	**Tensile Stress at maximum load (MPa) (CV%)**	**Tensile Strain at maximum load (%) (CV%)**	**Young's Modulus (MPa) (CV%)**
51/49 SF/PEO	9.3 (5.1)	103.9 (19.5)	20 (8.5)
51/49 SPC/PEO	6.2 (4.6)	72.2 (31.6)	27.8 (16.4)
70/30 SPC/PEO	6.3 (3.6)	8.7 (1.4)	166.3 (108.3)
51/49 SPI/PEO	10.1 (7.1)	99.6 (20.7)	30.9 (19.8)
70/30 SPI/PEO	6.5 (3.7)	8.1 (4.2)	182.5 (107.6)
4% Pure PEO	11.6 (18.6)	230.1 (48.5)	21.9 (25.9)

Figure 4.29 shows SEM micrographs of the 51/49 SF/PEO and SPC/PEO membranes and typical stress vs. strain plots are presented in Figure 4.30. Since PSF protein content and other properties were identical to SPC, PSF nanofiber membranes were not prepared for this test.

It was found that the tensile strength of the pure PEO nanofiber membrane was the highest, followed by the 51/49 membrane of SPI/PEO. Since SPI has the highest protein content, it is expected to have the largest tensile strength, followed by the SPC/PEO and SF/PEO nanofiber membranes. However, the nanofiber SF/PEO membrane was electrospun for 1.5 hours, while the 51/49 SPC/PEO nanofiber membrane was electrospun for 0.5 hr. SF/PEO was electrospun for longer time duration, since it is difficult to obtain a membrane from SF/PEO that could be peeled off for tensile testing. Hence, the number of fibers per unit area and the number of fiber-fiber crossovers is higher in the case of SF/PEO. Similarly, the high tensile strength of the pure PEO membrane can be attributed to strong cohesion due to fiber-fiber crossovers.

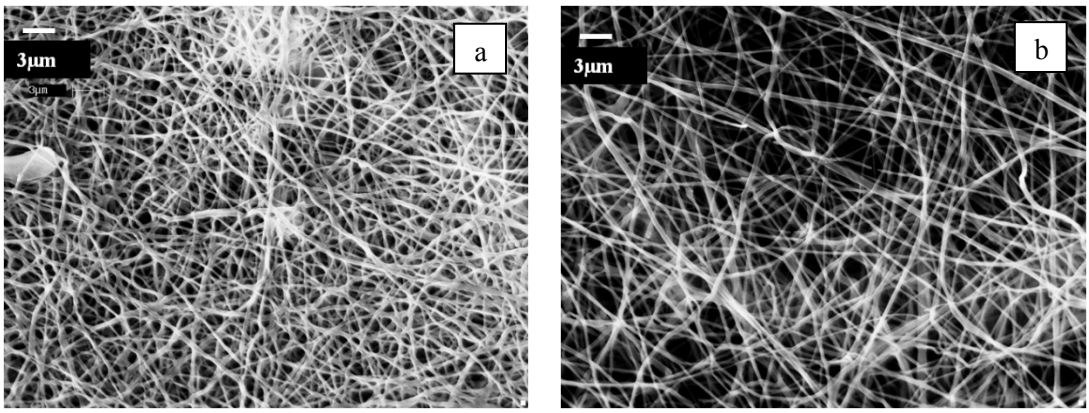

Figure 4.29: SEM micrographs of (a) 51/49 SF/PEO and (b) SPC/PEO nanofiber membranes

It is evident from the SEM micrographs in Figure 4.29 that the number of fibers per unit area and the fiber diameters was lesser in the SPC/PEO membranes than SF/PEO membranes.

The tensile strengths of the 70/30 membranes of SPI and SPC blends with PEO were lower than the respective 51/49 blends. However, the young's modulus values of the 70/30 membranes are

almost 6 times that of the 51/49 membranes. This is because the addition of PEO imparts stretch to the membranes, as indicated by the high strains at break of the pure PEO membranes. The membranes undergo strains up to 100-120% before breaking. The slopes of the initial linear region of the 70/30 membranes are steeper than the 51/49 membranes, as shown in Figure 4.30. Moreover, it was observed that the coefficients of variation (CV) of Young's modulus were high. This was expected because membranes with defects would have a much lower modulus than defect free membranes.

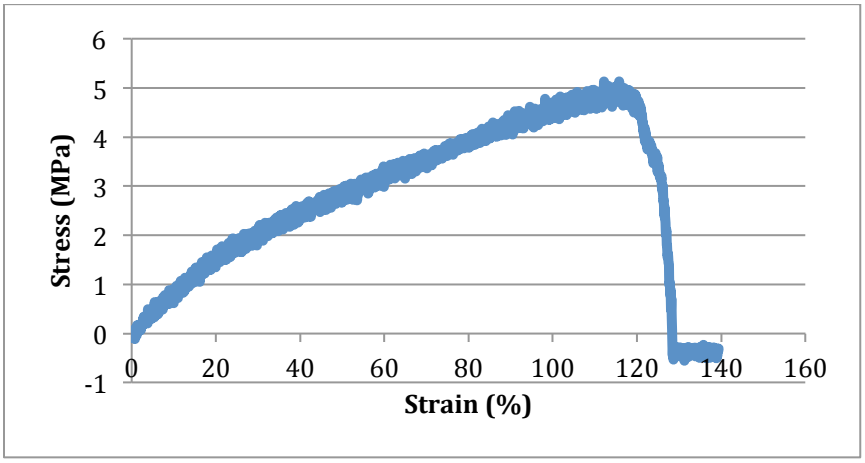

Figure 4.30: (a) Stress vs. strain plot of a nanofiber membrane electrospun from a 51/49 blend of SF/PEO

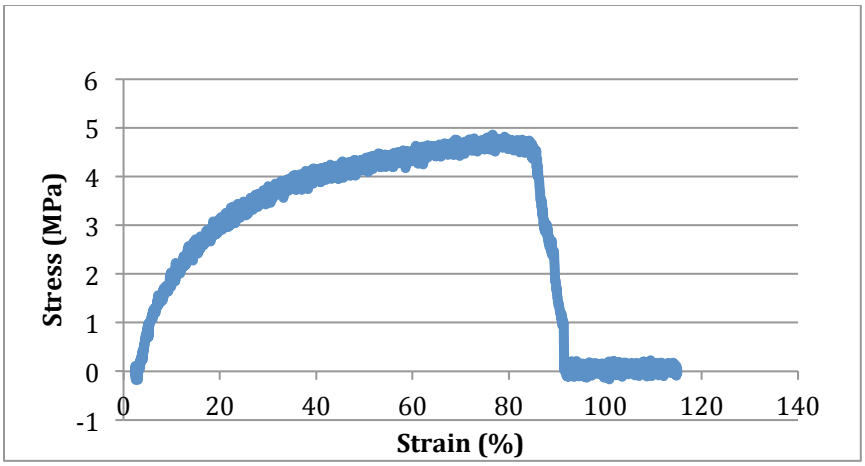

Figure 4.30: (b) Stress vs. strain plot of a nanofiber membrane electrospun from a 51/49 blend of SPC/PEO

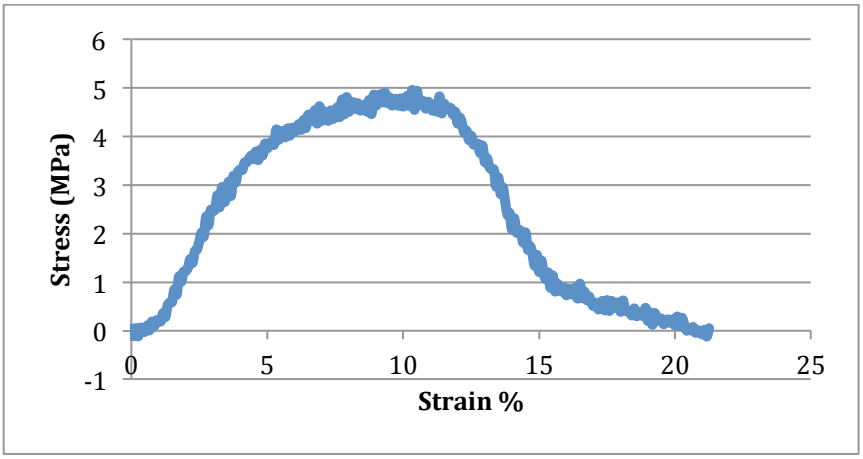

Figure 4.30: (c) Stress vs. strain plot of a nanofiber membrane electrospun from a 70/30 blend of SPC/PEO

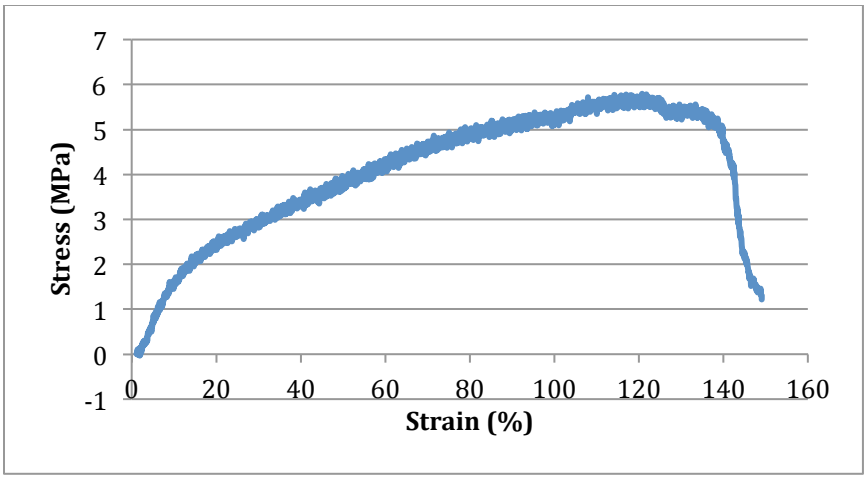

Figure 4.30: (d) Stress vs. strain plot of a nanofiber membrane electrospun from a 51/49 blend of SPI/PEO

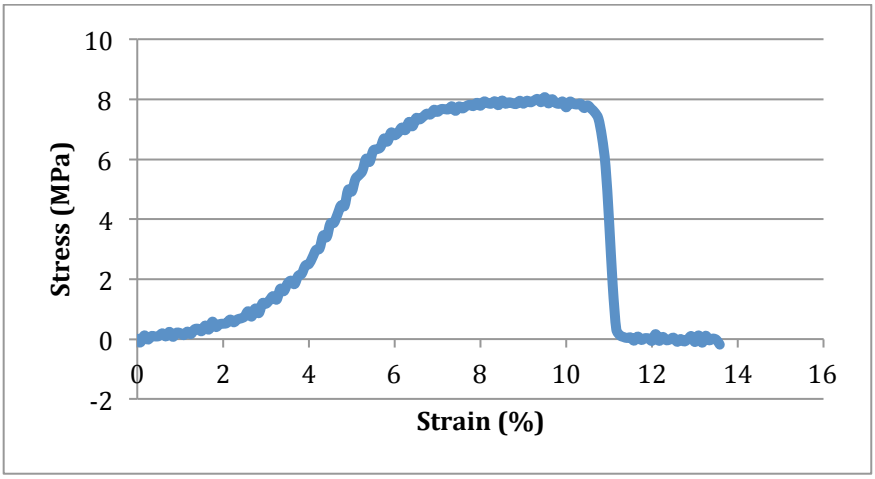

Figure 4.30: (e) Stress vs. strain plot of a nanofiber membrane electrospun from a 70/30 blend of SPI/PEO

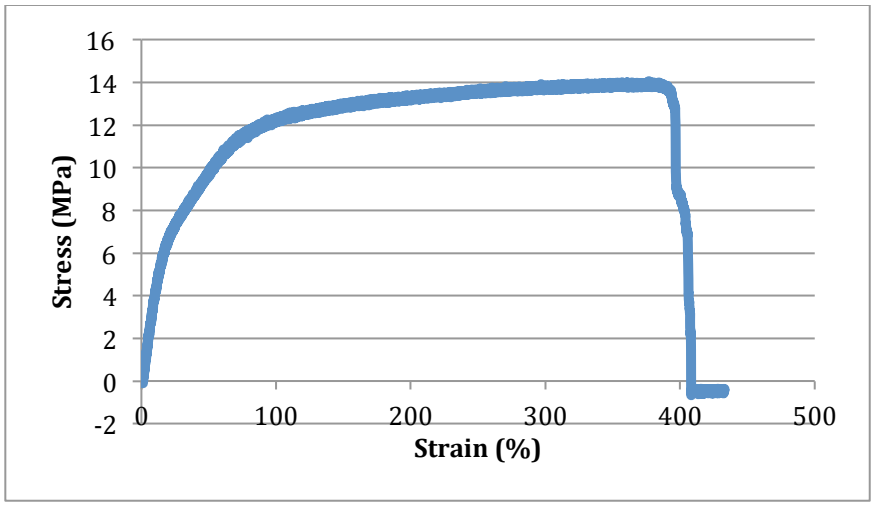

Figure 4.30: (f) Stress vs. strain plot of nanofiber membrane electrospun from pure PEO solution (4% concentration)

The mechanical properties of the electrospun membranes can be explained further by measuring the porosity of the membranes. The mean pore diameters of the membranes, estimated from the SEM images of the membranes using *ImageJ,* are given in Table 4.9.

Table 4.9: Mean pore diameters of electrospun membranes

Nanofiber membrane type	Mean pore diameter (µm)
51/49 SF/PEO	1.14
51/49 SPC/PEO	1.53
70/30 SPC/PEO	1.28
51/49 SPI/PEO	1.91
70/30 SPI/PEO	1.05
4% Pure PEO	.76

The low pore diameter of the pure PEO membrane gives a denser membrane and results in higher tensile strength. The estimated pore sizes of the electrospun membranes of soy protein/PEO blends were not very different from each other. Hence, differences in mechanical properties because of differences in pore size could be ignored for simplicity.

Huang et al. have reported the mechanical properties of electrospun gelatin nanofiber membranes (Huang et al., 2004). They performed the tension tests on Instron, and reported that the finest

nonfiber mats have the highest tensile modulus and ultimate tensile strength, due to strong cohesion between the fibers. They also observed poorer mechanical performance in nanofiber membranes that had beaded fibers, because the beads reduced the cohesion between the nanofibers in the membranes. The highest tensile modulus obtained by them was 123 MPa, with an ultimate strength of 3.4 MPa. In the present case the highest modulus and strength values of 182.5 MPa and 11.6 MPa, respectively, are comparable.

Cho et al. have studied the mechanical properties of electrospun SPI/PVA hybrid nanofibers. They reported that pure PVA nanofiber membranes showed the highest breaking force and elongation. As the SPI content in the membranes increased, both the breaking force and elongation decreased sharply (Cho et al., 2012).

Li and coworkers have electrospun poly (D, L-lactide-co-glycolide) (PLGA) nanofiber membranes and measured their mechanical properties (Li et al., 2002). They obtained a tensile modulus of 323.15 MPa. The ultimate tensile stress of the nanofiber membranes was 22.67 MPa and the ultimate strain was 95.8% (Li et al., 2002).

Other researchers have also reported the mechanical properties of individual electrospun nanofibers. Tan et al. conducted tensile tests of individual poly (e-caprolactone), PCL, electrospun nanofibers (Tan et al., 2005). When comparing the results to gravity-spun PCL fibers, they found that the modulus and maximal tensile stress of the electrospun nanofibers were observed to be high (Tan et al., 2005).

Zussman et al. studied the mechanical properties of a single Nylon 6,6 nanofibers obtained from electrospinning on to a rotating disk collector (Zussman et al., 2006). The tensile testing was performed on an atomic force microscope (AFM). They obtained a tensile strength of 110 MPa and Young's modulus 453 MPa for a fiber take-up velocity of 5 m/s of the rotating disk

collector. When the take-up velocity was increased, the tensile strength and Young's modulus also increased correspondingly. The increase in take up velocity was responsible for greater stretching and orientation of the nanofiber, resulting in better mechanical properties.

Inai et al. investigated the mechanical properties of as-spun poly (L-lactic acid) PLLA nanofibers (Inai et al., 2005). The tensile strength of these nanofibers was close to that of the melt-spun PLLA fibers. In contrast, the tensile modulus of these nanofibers was close to that of the melt-spun PLLA fibers. In contrast, the tensile modulus and the strain at break of the electrospun nanofibers were lower than those of the melt-spun fibers.

4.7. Composting Study

Composting technique was utilized to characterize the biodegradability of the nanofiber membranes electrospun from SPC/PVA and SPC/PEO. However, because of difficulty in preparing nanofiber membranes of sufficient weight for testing, films of both the solutions were used instead. SPC solution (12% concentration) was blended with PEO (5% concentration, molecular weight 600,000 g/mol) in a 70/30 proportion by weight. Similarly, SPC (12% concentration) was blended with PVA (14% concentration, molecular weight 130,000 g/mol) in the same proportion. These concentrations and molecular weights of each polymer were chosen because their blends gave uniform fibers on electrospinning. The film specimens were weighed after drying completely. They were placed inside porous nonwoven PP bags, and kept in the compost medium for up to 5 weeks. Every week, 2 specimens of each blend type were retrieved and the extent of degradation was analyzed. The loss in weight of the specimens was a measure of the extent of biodegradation.

The change in weight of the SPC/PVA and SPC/PEO specimens over 5 weeks of composting is summarized in Table 4.10.

Table 4.10: Change in weight of the SPC/PVA and SPC/PEO specimens over 5 weeks of composting

Composting time (in weeks)	**SPC/PVA (weight as a % of initial)**	**SPC/PEO (weight as % of initial)**
0 (Control)	100	100
1	100	97.9
2	98.3	97.1
3	99.6	98
4	97.7	98.2
5	99.4	96.1

As seen from Table 4.9, the degradation in both the specimen types was not significant after 5 weeks of composting. Both PEO and PVA are known to degrade slowly. However, soy protein is known to degrade fast (Cho et al., 2012). The SPC/PEO specimen showed greater degradation because a lower concentration (5%) of PEO was blended with SPC (12%), giving 85/15 ratio by weight. PVA, on the other hand, was used in 14% concentration, giving 67/33 ratio by weight. Assuming that only SPC degraded during the 5 weeks of composting, there was a 4.5% loss in weight of SPC in the SPC/PEO blend. Similarly, the maximum loss in SPC during the 5 weeks of composting was 3.5% for the SPC/PVA blend.

Cho et al. studied the biodegradability of SPI/PVA hybrid nanofiber mats (Cho et al., 2012). They observed that the pure PVA fiber mats lost only 3.7% of their original weight after 26 days of composting. A pure SPI resin, on the other hand, retained only 2.5% of its initial weight, showing much faster degradation. Hence, it was expected that SPC would degrade fast during the 5 weeks of composting. However, the data from change in weight of the specimens indicates that the SPC/PVA and SPC/PEO films have degraded at approximately the rate of PVA degradation. This could be possible if the soy protein in the film got covered by PVA or PEO during film formation. In such a scenario, the PVA or PEO would degrade first, followed by SPC.

Cho et al. have reported a 54% loss in weight of the SPI/PVA nanofiber membranes that contained 50% SPI (Cho et al., 2012). However, their composting specimens were the nanofiber membranes themselves. Therefore, the SPI present in the nanofibers with large surface area were exposed to the compost medium as compared to the films with limited surface area in the present case.

SEM micrographs of SPC/PEO specimens after (a) 0 weeks (b) 2 weeks and (c) 4 weeks (d) 5 weeks of composting are shown in Figure 4.31.

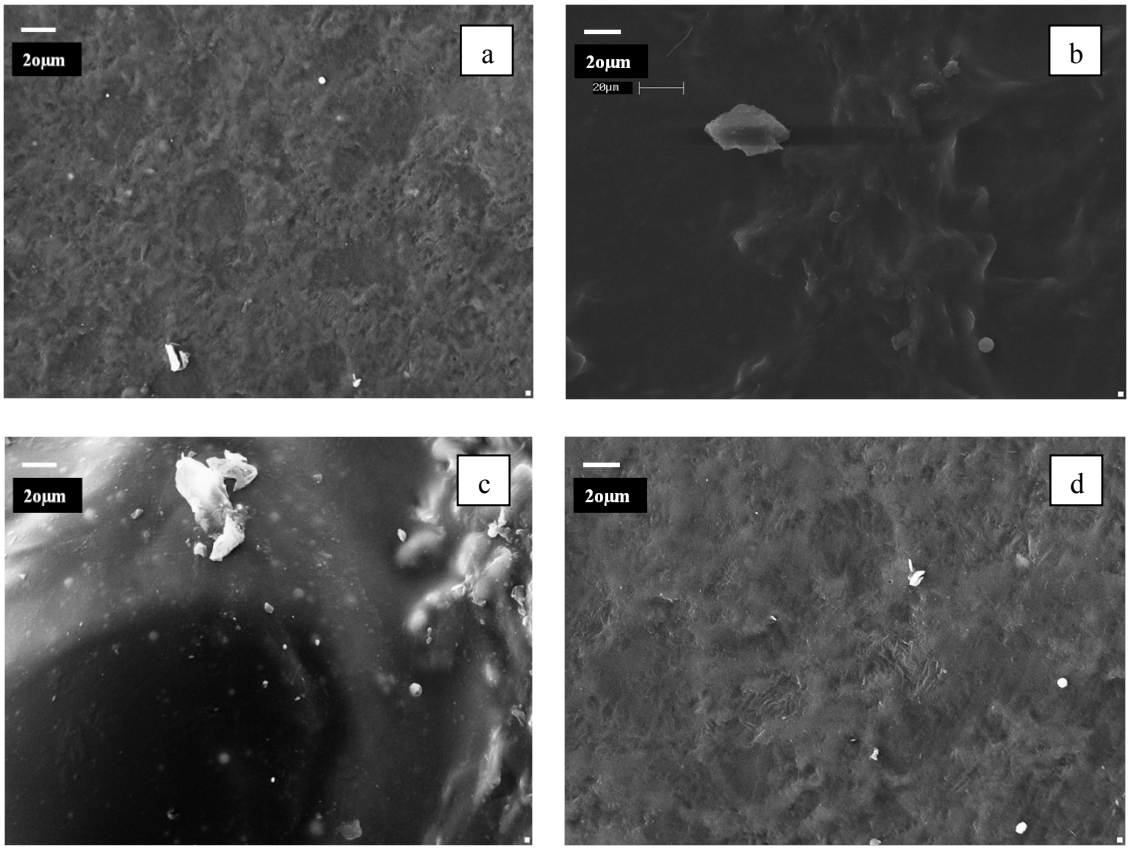

Figure 4.31: SEM micrographs of SPC/PEO specimens after (a) 0 weeks (b) 2 weeks and (c) 4 weeks (d) 5 weeks of composting

From the SEM micrographs, it can be seen that the SPC/PVA films don't show any significant degradation, which is consistent when the data on weight loss.

Hence, it could not be concluded from the composting study what the degradation rates of the SPC/PVA and SPC/PEO nanofiber membranes would be.

5. CONCLUSIONS

Commercially available soy protein was blended with PVA and PEO to form electrospun nanofibers membranes. The composition of electrospinning solution and process parameters were studied to determine their effect on the diameter and morphology of the nanofibers. Statistical analysis was performed to measure the significance of the solution and process parameters in controlling fiber diameter. The mechanical properties of the electrospun membranes were also characterized. Based on the results obtained in this research, following conclusions can be drawn:

1. The lab-scale filtration process, which uses the principle of minimum protein solubility at its isoelectric point, can be utilized to remove soluble sugars from SF. The protein content in the purified soy flour (PSF) was close to 66%, which is similar to the protein content of SPC.
2. The filtration process gave the highest protein content when the solution pH was 4. Microfiber based fabrics, with an average pore size of 7 μm, were used as filters. They offer the advantage of repeated use as opposed to filter paper, which is for one time use only.
3. It was difficult to electrospin solutions of 100% SPI, SPC and PSF. However, when blended with PVA or PEO, uniform nanofibers were obtained from electrospinning.
4. It was easier to electrospin SPI, followed by SPC and PSF, because of the higher protein content in SPI. This is because protein consists of long chains of amino acids, whereas carbohydrates (in SF and SPC) consist of small molecules, which cannot be electrospun.
5. The mean diameter and distribution of electrospun nanofibers can be controlled by varying the solution composition, process parameters and ambient conditions. The

solution related parameters consist of polymer molecular weight, concentration, viscosity, surface tension and conductivity. The process parameters include applied voltage, needle tip-collector distance, solution flow rate, needle gauge and collector type. The ambient conditions consist of temperature, humidity and the presence of airflow.

6. Molecular weight was found to have a significant effect of fiber diameter. The fiber diameter increased with an increase in molecular weight of PVA or PEO. This was due to the increased chain entanglements at high molecular weights, and the fluid jet following a straight trajectory over a longer distance before undergoing whipping motion. Statistical analysis confirmed that molecular weight had a significant effect on fiber diameter, with a p-value less than 0.0001.
7. An increase in solution concentration was found to decrease the average fiber diameter significantly. The decrease in diameter was due to formation of large beads, and branching of thick fibers into secondary fibers with diameters about $1/3^{rd}$ those of the primary fibers. In the statistical analysis, concentration was also found to have a p-value less than 0.0001.
8. An increase in the needle tip-collector distance was found to decrease the average fiber diameter for the high concentration blend, and increase it for the low concentration blend. The increase in diameter in the 10% SPC/ 10%PVA blends was because of uniform fiber formation when needle tip-collector distance was increased. The decrease in diameter in the 12.5% SPC/10% PVA blends was due to whipping motion of the fluid jet over a longer distance, which resulted in reduction in fiber diameter. Moreover, branching of the primary fibers into secondary fibers was observed, which also brought down the average diameter.

9. Voltage was not a significant parameter in this study, with a p-value of 0.4298. This was because of two opposing factors; increase in electrostatic repulsion force and increase in material drawn from the needle.
10. An increase in solution flow rate was also found to increase the fiber diameter. This was because more material was drawn from the needle per unit time.
11. Viscosity measurements showed that both PVA and PEO solutions and their blends with SPC had a shear thinning behavior. The viscosity decreased with an increase in the shear rate. Viscosity measurements of SPC/PVA blends also gave larger than expected values for the 12.5% blends of PVA, which might be responsible for bead formation during electrospinning. Blends with viscosities in the range of 3 to 10 Pa.s were found to give uniform nanofibers.
12. The addition of anionic surfactant was useful in increasing protein solubility at high concentrations. It was possible to electrospin up to 15% concentration of SPC with PEO when SPC was prepared in 1% SDS solution.
13. The blend of SPI with PEO (51/49 by wt.) was found to have a tensile strength of 10.11 MPa, which was higher than the corresponding SPC/PEO and SF/PEO blends. The tensile strength of the 51/49 (by wt.) blend of SF/PEO was higher than the SPC/PEO blend, because it had a larger number of fibers per unit area. The larger number of fibers per unit area implied greater fiber-fiber crossovers, and hence stronger cohesion between the fibers in the membrane.
14. The Young's moduli of the 70/30 (by wt.) membranes of SPI/PEO and SPC/PEO were 6 to 8 times than those of the 51/49 blends. This is because the addition of PEO imparted greater stretch to the membranes, resulting in fracture strains up to 100-120% for the

51/49 blends.

15. The biodegradation of SPC/PVA and SPC/PEO films for the duration of 5 weeks was not significant. Shielding of SPC by PVA/PEO could be responsible for the slow degradation.

In this thesis, it is concluded that SPI, SPC, and purified SF can be successfully electrospun when blended with PVA or PEO. Uniform nanofibers with average diameters in the range of 100 to 500 nm can be electrospun from these blends. The small diameters of nanofibers make them suitable for applications that require small pore sizes, such as filtration. Also, the use of biodegradable materials makes disposal of these membranes easy and environment friendly.

6. REFERENCES

http://rsbweb.nih.gov/ij/.

http://www.t3portal.org/T3_Portal_v1/!SSL!/WebHelp/ales_vancura/proteins.htm

http://en.wikipedia.org/wiki/Sodium_dodecyl_sulfate

http://en.wikipedia.org/wiki/Triton_X-100

http://en.wikipedia.org/wiki/Polysorbate_80

A. Koski, K. Yim, S. Shivkumar. "Effect of molecular weight on fibrous PVA produced by electrospinning." *Materials Letters* 58 (2003): 493-497.

A.H. Brandenburg, C.L. Weller, R.F. Testin. "Edible Films and Coatings from Soy Protein." *Journal of Food Science* 58 (2006): 1086–1089.

A.-C. V.-Lugo, L.-T. Lim. "Electrospinning of Soy Protein Isolate Nanofibers." *Journal of Biobased materials and Bioenergy* 2 (2008): 223-230.

A.-C. V.-Lugo, L.-T. Lim. "Controlled release of allyl isothiocyanate using soyprotein and poly(lactic acid) electrospun fibers ." *Food Research International* 42 (2009): 933–940.

A. Frenot, I. S. Chronakis. "Polymer nanofibers assembled by electrospinning." *Current opinion in Colloid and Interface Science* 8 (2003): 64–75.

B. Briscoe, P. Luckham, S. Zhu. "The effects of hydrogen bonding upon the viscosity of aqueous poly(vinyl alcohol) solutions." *Polymer* 41, no. 10 (2000): 3851–3860.

C. Kriegel, K. M. Kit, D. J. Mc Clements, J. Weiss. "Electrospinning of chitosan–poly(ethylene oxide) blend nanofibers in the presence of micellar surfactant solutions ." *Polymer* 50 (2009): 189–200.

C. Shao, H.-Y. Kim, J. Gong, B. Ding, D.-R. Lee, S.-J. Park. "Fiber mats of poly (vinyl alcohol)/silica composite via electrospinning." *Materials Letters* 57 (2003): 1579–1584.

C. E. Ophardt. *Denaturation of Proteins*. 2003. http://www.elmhurst.edu/~chm/vchembook/568denaturation.html.

C. Mit-uppatham, M. Nithitanakul, P. Supaphol. "Ultrafine Electrospun Polyamide-6 Fibers: Effect of Solution Conditions on Morphology and Average Fiber Diameter." *Macromolecular Chemistry and Physics* 205 (2004).

C. Burger, B. S. Hsiao, B. Chu. "Nanofibrous materials and their applications." *Annual Review of Materials Research* 36 (2006): 333-368.

C. J. Buchko, L. C. Chen, Y. Shen, D. C. Martin. "Processing and microstructural characterization of porous biocompatible protein polymer thin films." *Polymer* 40 (1999): 7397–7407.

C. Zhang, X. Yuan, L. Wu, Y. Han, J. Sheng. "Study on morphology of electrospun poly(vinyl alcohol) mats." *European Polymer Journal* 41 (2005): 423–432.

D. Cho, A. N. Netravalib, Y. L. Joo. "Mechanical properties and biodegradability of electrospun soy protein Isolate/PVA hybrid nanofibers." *Polymer Degradation and Stability* 97 (2012): 747–754.

D. H. Reneker, Iksoo Chun. "Nanometre diameter fibres of polymer, produced by electrospinning." *Nanotechnology* 7 (1996): 216–223.

D. H. Reneker, A. L. Yarin. "Electrospinning jets and polymer nanofibers." *Polymer* 49 (2008): 2387-2425.

D. J. Mc Clements. *Analysis of Proteins.* Amherst, 2007.

D. Li, Y. Xia. "Electrospinning of Nanofibers: Reinventing the Wheel?" *Advanced Materials* 16 (2004): 1151–1170.

E. W. Lusas, K. C. Rhee. "Soybean protein processing and utilization." In *Practical Handbook of Soybean Processing and Utilization*, by D.R. Erickson, 117–160. AOCS Press, 1995.

E. Zussman, A. Theron, A. L. Yarin. "Formation of nanofiber crossbars in electrospinning ." *Applied Physics Letters* 82 (2003): 973-975.

E. Zussman, M. Burman, A.L. Yarin, R. Khalfin, Y. Cohen. "Tensile deformation of Electrospun Nylon-6,6 Nanofibers." *Journal of Polymer Science Part B: Polymer Physics Vol 44*, 2006: 1482-1489.

E.P.S. Tan, S.Y. Ng, C.T. Lim. "Tensile testing of a single ultrafine polymeric fiber." *Biomaterials 26*, 2005: 1453.

F. Rodriguez, C. Cohen, C. K. Ober, L. A. Archer. *Principles of Polymer Systems.* 2003.

G. A. Denavi, M. Pe´rez-Mateos, M. C. An˜o´n, P. Montero, A. N. Mauri, M. C. Go´mez-Guille´n. "Structural and functional properties of soy protein isolate and cod gelatin blend films." *Food Hydrocolloids* 23 (2009): 2094–2101.

G. C. Rutledge, S. B. Warner, S. C. Ugbolue. *Electrostatic Spinning and Properties of Ultrafine fibers.* National Textile Center Annual Report, 2004.

G. Robertson. "Active and intelligent packaging." In *Food Packaging*, by G. Robertson. Boca

Raton: CRC Press, 2006.

H. Fong, I. Chun, D.H. Reneker. "Beadednanofibersformed during electrospinning." *Polymer* 40 (1999): 4585–4592.

H. Liu, Y.-L. Hsieh. "Ultrafine fibrous cellulose membranes from electrospinning of cellulose acetate." *Journal of Polymer Science Part B: Polymer Physics* 40 (2002): 2119–2129.

H. Fong, D. H. Reneker. "Elastomeric Nanofibers of Styrene–Butadiene–Styrene Triblock Copolymer." *Journal of Polymer Science: Part B: Polymer Physics* 37 (1999): 3488 –3493.

H. Homayoni, S. A. Hosseini Ravandi, M. Valizadeh. "Electrospinning of chitosan nanofibers: Processing optimization." *Carbohydrate Polymers* 77 (2009): 656–661.

H.-J. Jin, S. V. Fridrikh, G. C. Rutledge, D. L. Kaplan. "Electrospinning Bombyx mori Silk with Poly(ethylene oxide)." *Biomacromolecules*, 2002: 1233-1239.

H. S. Kim, K. Kim, H. J. Jin, I.-J. Chin. "Morphological Characterization of Electrospun Nano-Fibrous Membranes of Biodegradable Poly(L-lactide) and Poly(lactide-co-glycolide)." *Macromolecular Symposia* 224 (2005): 145–154.

J. Lannutti, D. Reneker, T. Ma, D. Tomasko, D. Farson. "Electrospinning for tissue engineering scaffolds." *Materials Science and Engineering C* 27 (2007): 504–509.

J. M Deitzel, J. Kleinmeyer, D. Harris, N. C BeckTan. "The effect of processing variables on the morphology of electrospun nanofibers and textiles." *Polymer* 42 (2001): 261–272.

J. M. Deitzel, W. Kosik, S. H. McKnight, N. C. Beck Tan, J. M. DeSimone, S. Crette. "Electrospinning of polymer nanofibers with specific surface chemistry." *Polymer* 43 (2002): 1025–1029.

J. M. Deitzel, J. D. Kleinmeyer, J. K. Hirvonen, N. C. Beck Tan. "Controlled deposition of electrospun poly(ethylene oxide) fibers." *Polymer* 42 (2001): 8163–8170.

J. M. Deitzel, J. Kleinmeyer, D. Harris, N. C. Beck Tan. "The effect of processing variables on the morphology of electrospun nanofibers and textiles." *Polymer* 42 (2001): 261–272.

J. Doshi, D. H. Reneker. "Electrospinning Process and Applications of Electrospun Fibers." *Journal of Electrostatics* 35 (1995): 151-160.

J.-H. He, Y.-Q. Wan, J.-Y. Yu. "Scaling law in electrospinning: relationship between electric current and solution flow rate." *Polymer* 46 (2005): 2799–2801.

J. Booth. "Statistical Methods II Lecture notes." 2012. http://www.bscb.cornell.edu/~booth/courses/btry6020_website/handouts/week6-handout.pdf.

J. Zeng, X. Chen, X. Xu, Q. Liang, X. Bian, L. Yang, X. Jing. "Ultrafine Fibers Electrospun from Biodegradable Polymers." *Journal of Applied Polymer Science* 89 (2003): 1085–1092.

J. G. Endres. *Soy Protein Products: Characteristics, Nutritional Aspects, and Utilization.* The American Oil Chemists Society, 2001.

J. T. Kim and A. N. Netravali. "Mechanical, Thermal, and Interfacial Properties of Green Composites with Ramie Fiber and Soy Resins." *Journal of Agruvultural and Food Chemistry* 58 (2010): 5400–5407.

K. H. Lee, H. Y. Kim, M. S. Khil, Y. M. Ra, D. R. Lee. "Characterization of nano-structured poly(ε-caprolactone) nonwoven mats via electrospinning." *Polymer* 44 (2003): 1287–1294.

K. Liu. *Soybeans, technology, and utilization.* New York: Chapman & Hall, 1997.

K. Nagapudi, W. T. Brinkman, J. E. Leisen, L. Huang, R. A. McMillan, R. P. Apkarian, V. P. Conticello, E. L. Chaikof. "Photomediated Solid-State Cross-Linking of an Elastin−Mimetic Recombinant Protein Polymer." *Macromolecules* 35 (2002): 1730–1737.

L. K. Kielce. *Calculation of protein isoelectric point.* 2012. http://isoelectric.ovh.org/.

M. Jones. "The interaction of sodium dodecyl sulfate with polyethylene oxide." *Journal of Colloid and Interface Science* 23 (1967): 36-42.

M. Krumova, D. López, R. Benavente, C. Mijangos, J. M. Pereña. "Effect of crosslinking on the mechanical and thermal properties of poly(vinyl alcohol)." *Polymer* 41 (2000): 9265–9272.

M. E. Watson, T. L. Galliher. "Comparison of Dumas and Kjeldahl methods with automatic analyzers on agricultural samples under routine rapid analysis conditions." *Communications in Soil Science and Plant Analysis* 32 (2001): 2007-2019.

M.M. Demir, I. Yilgor, E. Yilgor, B. Erman. "Electrospinning of polyurethane fibers." *Polymer* 43 (2002): 3303-3309.

M. I. Gjerde, W. Nerdal, H. Høiland. "Interactions between Poly(Ethylene Oxide) and Sodium Dodecyl Sulfate as Studied by NMR, Conductivity, and Viscosity at 283.1–298.1 K." *Journal of Colloid and Interface Science* 197 (1998): 191–197.

M. T. Hunley, T. E. Long. "Electrospinning functional nanoscale fibers: a perspective for the future." *Polymer International* 57 (2008): 385–389.

M. Li, M. J. Mondrinos, M. R. Gandhi, F. K. Ko, A. S. Weiss, P. I. Lelkes. "Electrospun protein fibers as matrices for tissue engineering." *Biomaterials* 26 (2005): 5999–6008.

M. Chowdhury, G. Stylios. "Effect of experimental parameters on the morphology of electrospun Nylon 6 fibres." *International Journal of Basic & Applied Sciences* 10 (2010): 116-131.

M. M. Hohman, M. Shin, G. Rutledge, M. P. Brenner. "Electrospinning and electrically forced jets. II. Applications." *Physics of Fluids* 13 (2001): 2221-2236.

M.-S. Khil, S. R. Bhattarai, H.-Y. Kim, S.-Z. Kim, K.-H. Lee. "Novel fabricated matrix via electrospinning for tissue engineering." *Journal of Biomedical Materials Research Part B: Applied Biomaterials* 72B (2005): 117–124.

N. Cao, Y. Fu, J. He. "Preparation and physical properties of soyprotein isolate and gelatin composite films." *Food Hydrocolloids* 21 (2007): 1153–1162.

N. Bhardwaj, S. C. Kundu. "Electrospinning: A fascinating fiber fabrication technique." *Biotechnology Advances* 28 (2010): 325-347.

National diagnostics. *Buffer Additives-Surfactants.* 2012. https://www.nationaldiagnostics.com/electrophoresis/article/buffer-additives-surfactants.

O.S. Yördem, M. Papila, Y. Z. Menceloğlu. "Effects of electrospinningparameters on polyacrylonitrile nanofiber diameter: An investigation by responsesurfacemethodology." *Materials and Design* 29 (2008): 34-44.

P. Gupta, C. Elkins, T. E. Long, G. L. Wilkes. "Electrospinning of linear homopolymers of poly(methyl methacrylate): exploring relationships between fiber formation, viscosity, molecular weight and concentration in a good solvent ." *Polymer* 46 (2005): 4799–4810.

P. D. Dalton, D. Klee, M. Möller. "Electrospinning with dualcollectionrings." *Polymer* 46 (2005): 611-614.

P. K. Baumgarten. "Electrostatic spinning of acrylic microfibers." *Journal of Colloid and Interface Science* 36 (1971): 71–79.

P. Supaphol, C. Mit-Uppatham, M. Nithitanakul. "Ultrafine Electrospun Polyamide-6 Fibers: Effect of Emitting Electrode Polarity on Morphology and Average Fiber Diameter ." *Journal of Polymer Science Part B: Polymer Physics* 43 (2005): 3699–3712.

P. Lodha, A. N. Netravali. "Effect of soy protein isolate resin modifications on their biodegradation in a compost medium ." *Polymer Degradation and Stability* 87 (2005): 465-477.

Q. P. Pham, U. Sharma, A. G. Mikos. "Electrospinning of Polymeric Nanofibers for Tissue Engineering Applications: A Review ." *Tissue Engineering* 12 (2006): 1197-1211.

R.M. Hodge, G. H. Edward, G. P. Simon. "Water absorption and states of water in semicrystalline poly(vinyl alcohol) films." *Polymer* 37 (1996): 1371–1376.

R. Jaeger, M. M. Bergshoef, C. Martin i Batlle, H. Schlinherr, G. J. Vancso. "Electrospinning of ultra-thin polymer fibers." *Macromol. Symp.* 127 (1998): 141-150.

R. Inai, M. Kotaki, S. Ramakrishna. "Structure and properties of electrospun PLLA single nanofibers." *Nanotechnology volume 16*, 2005: 208-213.

S. Sukigara, M. Gandhi, J. Ayutsede, M. Micklus, F. Ko. "Regeneration of Bombyxmori silk by electrospinning. Part 2. Process optimization and empirical modeling using response surface methodology." *Polymer* 45 (2004): 3701–3708.

S. N. Khan. *Electrospinning Polymer Nanofibers - Electrical and Optical Characterization.* Ohio University: Proquest, 2007.

S. Ramakrishna. *An Introduction to Electrospinning And Nanofibers.* World Scientific, 2005.

S. Ramakrishna, K. Fujihara, W.-E. Teo, T. Yong, Z. Ma, and R. Ramaseshan. "Electrospun nanofibers: solving global issues." *Materials today* 9 (2006): 40-50.

S. V. Fridrikh, J. H. Yu, M. P. Brenner and G. C. Rutledge. "Controlling the fiber diameter during electrospinning." *Phys. Rev. Lett.* 90 (2003).

S-H. Tan, R. Inai, M. Kotaki, S. Ramakrishna. "Systematic parameter study for ultra-fine fiber fabrication via electrospinning process ." *Polymer* 46 (2005): 6128–6134.

S. F. Fennessey, R. J. Farris. "Fabrication of aligned and molecularly oriented electrospun polyacrylonitrile nanofibers and the mechanical behavior of their twisted yarns." *Polymer* 45 (2004): 4217–4225.

S. Koombhongse, W. Liu, D. H. Reneker. "Flat Polymer Ribbons and other shapes by electrospinning." *Journal of Polymer Science Part B: Polymer Physics* 39 (2001): 2598–2606.

S. L. Shenoy, W. D. Bates, H. L. Frisch, G. E. Wnek. "Role of chain entanglements on fiber formation during electrospinning of polymer solutions: good solvent, non-specific polymer-polymer interaction limit." *Polymer* 46 (2005): 3372-3384.

S. Thandavamoorthy, G. S. Bhat, R. W. Tock, S. Parameswaran, S. S. Ramkumar. "Electrospinning of nanofibers." *Journal of Applied Polymer Science* 96 (2005): 557–569.

T. E. Creighton. *Proteins: structures and molecular properties.* Macmillan, 1993.

T. Lin, H. Wang, H. Wang and X. Wang. "The charge effect of cationic surfactants on the elimination of fibre beads in the electrospinning of polystyrene." *Nanotechnology* 15 (2004): 1375–1381.

T. J. Sill, H. A. Von Recum. "Electrospinning: Applications in drug delivery and tissue engineering." *Biomaterials* 29 (2008): 1989-2006.

V.Ya. Shkadov, A.A. Shutov "Drop and Bubble Deformation in an Electric Field." *Fluid Dynamics* 37 (2002): 713-724.

W. Cai, R. B. Gupta. "Hydrogels." In *Kirk-Othmer Encyclopedia of Chemical Technology*. John Wiley & Sons, Inc., 2002.

W.-E. Teo, R. Inai and S. Ramakrishna. "Technological advances in electrospinning of nanofibers." *Science and Technology of Advanced Materials* (IOP Science) 12 (2011).

W.-J. Li, C. T. Laurencin, E. J. Caterson, R. S. Tuan, F. K. Ko. "Electrospun nanofibrous structure: A novel scaffold for tissue engineering ." *Journal of Biomedical Materials Research Part A* 60 (2002): 613–621.

W. K. Son, J. H. Youk, T. S. Lee, W. H. Park. "Effect of pH on electrospinning of poly(vinyl alcohol)." *Materials Letters* 59 (2005): 1571–1575.

W. M. K. Trochim. *Factorial Designs.* 2006. http://www.socialresearchmethods.net/kb/expfact.php.

X.-H. Qin, E.-L. Yang, N. Li, S.-Y. Wang. "Effect of Different Salts on Electrospinning of Polyacrylonitrile (PAN) Polymer Solution ." *Journal of Applied Polymer Science* 103 (2007): 3865–3870.

X. Zong, K. Kim, D. Fang, S. Ran, B. S. Hsiao, B. Chu. "Structure and process relationship of electrospun bioabsorbable nanofiber membranes." *Polymer* 43 (2002): 4403–4412.

Y. C. Ahn, S. K. Park, G. T. Kim, Y. J. Hwang, C. G. Lee, H. S. Shin, J. K. Lee. "Development of high effciency nanofilters made of nanofibers." *Current Applied Physics* 6 (2006): 1030–1035.

Y. K. Luu, K. Kim, B. S. Hsiao, B. Chu, M. Hadjiargyrou. "Development of a nanostructured DNA delivery scaffold via electrospinning of PLGA and PLA-PEG block copolymers." *Journal of controlled release* 89 (2003): 341–353.

Y. M. Shin, M. M. Hohman, M. P. Brenner, G. C. Rutledge. "Experimental characterization of electrospinning: the electrically forced jet and instabilities." *Polymer* 42 (2001): 9955–9967.

Y. T.-P. Ly, L.A. Johnson, J. Jane. "Soy Protein as Biopolymer." In *Biopolymers from Renewable Resources*, by David Kaplan. Springer, 1998.

Z. Sun, J. M. Deitzel1, J. Knopf, X. Chen, J. W. Gillespie Jr. "The effect of solvent dielectric properties on the collection of oriented electrospun fibers." *Journal of Applied Polymer Science* 125 (2012): 2585–2594.

Z. Berg. "Technology of production of edible flours and protein products from soybeans." *FAO Agric. Serv. Bull.*, 1992.

Z.-M. Huang, Y.-Z. Zhang, M. Kotaki, S. Ramakrishna. "A review on polymer nanofibers by electrospinning and their applications in nanocomposites." *Composites Science and Technology* 63 (2003): 2223–2253.